**Supporting Information**

# Unprecedented roll-off ratio in high-performing red TADF OLED emitters featuring 2,3-Indole-annulated naphthalene imide and auxiliary donors.

Magdalena Grzelak,[‡,a,d] Dharmendra Kumar,[‡,b] Michał Andrzej Kochman,[‡,b] Maja Morawiak,[a] Gabriela Wiosna-Sałyga,[b] Adam Kubas,*[c] Przemysław Data,*[b] and Marcin Lindner*[a]

## Content:

## S1 Materials and methods

All reagents and solvents were purchased from commercial sources and were used as received unless otherwise noted, i.e. 4-bromo-1,8-naphthalic anhydride, and 3,6-di-tert-butylcarbazole (Ambeed), 2-nitrophenylboronic acid, 9,9-dimethyl-9,10-dihydroacridine, phenoxazine from Angene, N-bromosuccinimide (Chemat), tetra-N-butylammonium bromide (Fluka), phenothiazine (Fluorochem), 1-bromobutane, 9-anthraceneboronic acid, 4-cyanophenylboronic acid, $Pd(PPh_3)_4$, $Pd(PtBu_3)_2$, NaO*t*Bu, 2,4,6-trimethylaniline, triphenylphosphine, *o*-DCB, and DMF from Aldrich, KOH, $CH_3COOH$, DCM, toluene, ethanol, acetone, hexane, $K_2CO_3$, $Na_2SO_4$ from POCH. Reagent-grade solvents ($CH_2Cl_2$, hexane) were distilled prior to use. For water-sensitive reactions, solvents were dried using Mbraun Solvent Purification System. Transformations with moisture and oxygen-sensitive compounds were performed under argon using the Schlenk line.

The reaction progress was monitored by thin layer chromatography (TLC), performed on aluminium foil plates covered with Silica gel 60 F254 (Merck). Products purification was done utilizing column chromatography with Kieselgel 60 (Merck). The identity and purity of prepared compounds were confirmed by $^1H$ NMR and $^{13}C$ NMR spectroscopy as well as by MS spectrometry (*via* EI-MS) and IR spectroscopy. NMR spectra were measured on Bruker 400 MHz, Bruker 500 MHz, Bruker 600 MHz or Varian 600 MHz instruments with the TMS as the internal standard. Chemical shifts for $^1H$ NMR are expressed in parts per million (ppm) relative to tetramethylsilane (δ 0.00 ppm), $CDCl_3$ (δ 7.26 ppm) or DMSO-$d_6$ (δ 2.50 ppm). Chemical shifts for $^{13}C$ NMR are expressed in ppm relative to $CDCl_3$ (δ 77.16 ppm) or DMSO-$d_6$ (δ 39.52 ppm). Data are reported as follows: chemical shift, multiplicity (s = singlet, d = doublet, dd = doublet of doublets, t = triplet, m = multiplet), coupling constant (Hz), and integration. EI mass spectra were obtained on Waters AutoSpec Premier Spectrometer. IR spectra were recorded on JASCO FTIR 6200 and Shimadzu IRTracer-100 FTIR spectrometers.

## S2 Synthetic procedures

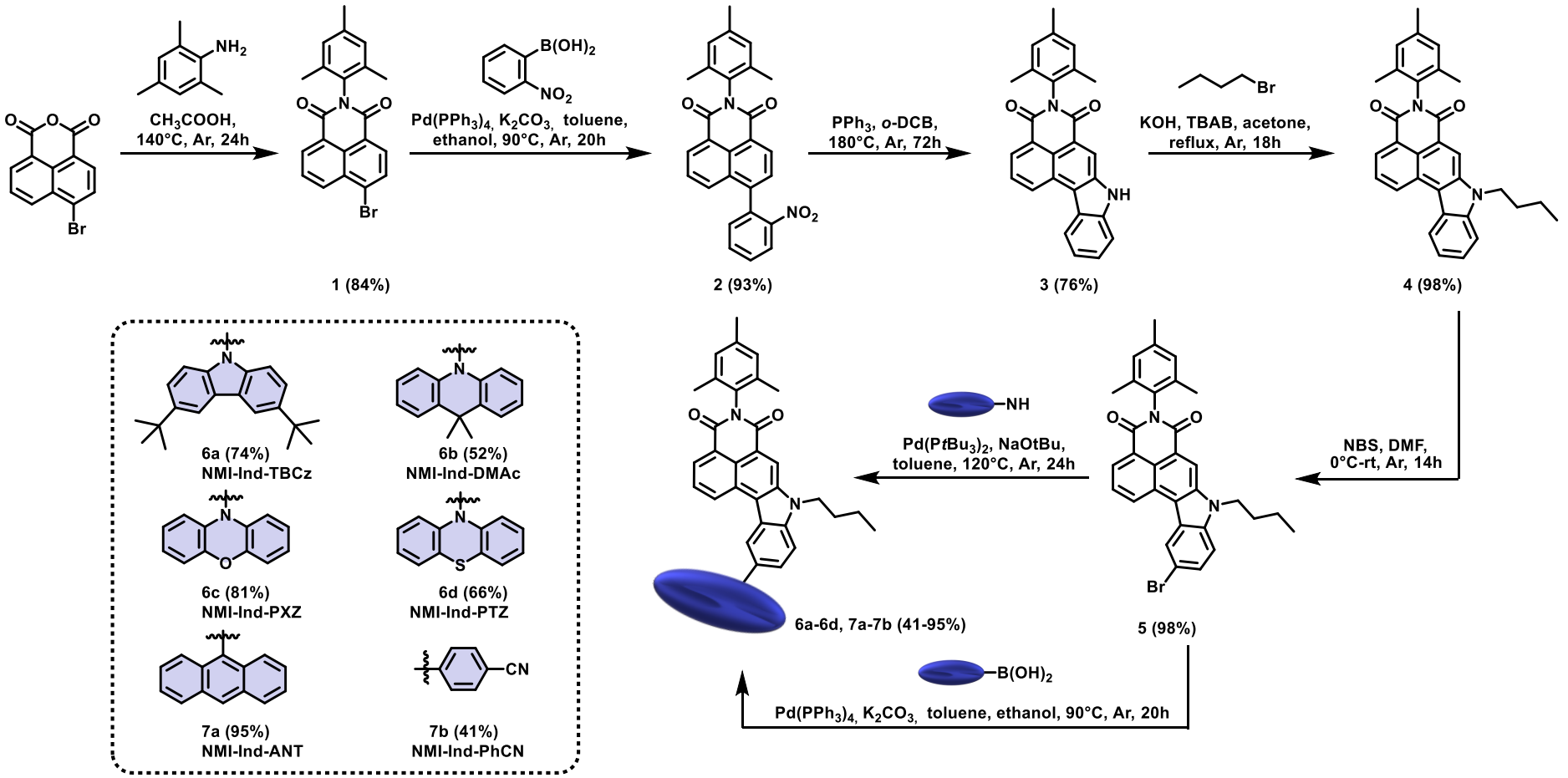


**Scheme S1. The synthetic path towards "dyes 6a-d and and 7a-7b**

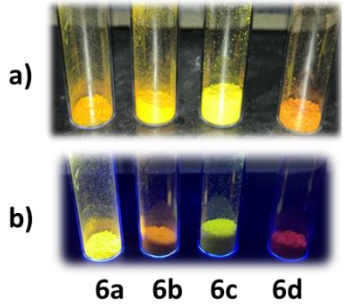


**Figure 1.** Compounds **6a-6d** a) under visible light, b) under UV light, λ 254nm.

**6-bromo-2-mesityl-benzo[de]isoquinoline-1,3-dione (1):**

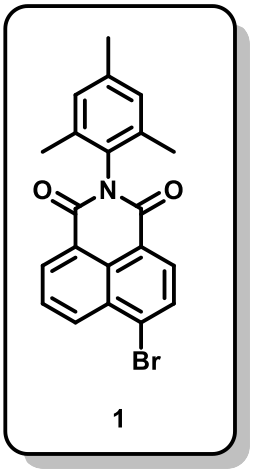

1

4-Bromo-1,8-naphthalic anhydride (3 g, 10.83 mmol) was added to a pressure tube equipped with a magnetic stir bar and dissolved in $CH_3COOH$ (40 mL) under argon. To this solution, 2,4,6-trimethylaniline (3eq.; 4.56 mL, 32.49 mmol) was added, and the mixture was vigorously purged by Ar for 10 minutes and closed. The reaction mixture was stirred overnight at 140°C. After this time, the solution was cooled and poured into ice water to form a precipitate, followed by filtration. The crude product was purified by column chromatography separation on silica gel (DCM/hexane 5:1) to form a white solid product (3.6 g, 84%). Purification is also possible without column chromatography through crystallization from hot acetic acid (3.24 g, 76%).

**$^1$H NMR (400 MHz, $CDCl_3$)** δ 8.72 (dd, *J* = 7.3, 1.1 Hz, 1H), 8.66 (dd, *J* = 8.5, 1.2 Hz, 1H), 8.48 (d, *J* = 7.9 Hz, 1H), 8.09 (d, *J* = 7.9 Hz, 1H), 7.90 (dd, *J* = 8.5, 7.3 Hz, 1H), 7.03 (s, 2H), 2.36 (s, 3H), 2.09 (s, 6H).

**$^{13}$C NMR (126 MHz, $CDCl_3$)** δ 163.19, 163.16, 138.81, 135.19, 133.78, 132.64, 131.80, 131.33, 131.05, 130.82, 129.82, 129.56, 128.31, 123.36, 122.47, 21.33, 17.91.

**HRMS (EI)** calcd for $C_{21}H_{16}BrNO_2$ 393.0364, found 393.0359.

**IR (KBr)** ν ($cm^{-1}$): 3361, 3081, 3027, 2973, 2950, 2916, 2857, 1192, 1892, 1876, 1708, 1688, 1668, 1606, 1588, 1567, 1505, 1482, 1459, 1402, 1394, 1360, 1343, 1327, 1304, 1241, 1191, 1132, 1118, 1039, 967, 950, 902, 880, 847, 814, 783, 746, 732, 704, 563, 553, 497, 472, 436, 422.

**2-mesityl-6-(2-nitrophenyl)-1H-benzo[de]isoquinoline-1,3-dione (2):**

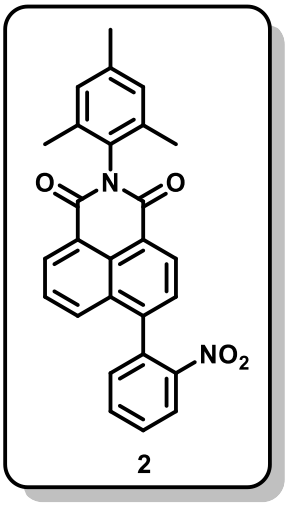

2

Compound (**1**) (2.5 g, 6.34 mmol) and 2-nitrophenylboronic acid (1.2 eq.; 1.26 g, 7.61 mmol) were placed in a two-neck round-bottom flask equipped with a magnetic stirring bar and a reflux condenser and degassed. Under argon, toluene (37.5 mL) and ethanol (26 mL) were added, and the solution was purged with argon for 10 minutes. Next, $K_2CO_3$ (19.4 mL of 2M aq. base solution) and $Pd(PPh_3)_4$ (10%, 732 mg, 0.63 mmol) were added. The reactor was placed in an oil bath and stirred for 20h at 90°C. After cooling, the mixture was extracted three times with DCM, dried over anhydrous $Na_2SO_4$ and filtered. After evaporation of solvents, the crude mixture was purified by column chromatography separation on silica gel (DCM/hexane 2:1), affording (**2**) (2.58 g, 93%) as a beige solid. Purification is also possible without column chromatography, by filtration of the mixture after dryness over $Na_2SO_4$ through the pad (silica gel, celite), evaporation of the solvent, precipitation in cold hexane and filtration of the obtained product (1.99 g, 72%).

**$^1$H NMR (400 MHz, $CDCl_3$)** δ 8.72 – 8.66 (m, 2H), 8.24 (dd, *J* = 8.1, 1.3 Hz, 1H), 7.82 (ddd, *J* = 13.6, 8.0, 1.3 Hz, 2H), 7.76 – 7.69 (m, 2H), 7.66 (d, *J* = 7.5 Hz, 1H), 7.51 (dd, *J* = 7.5, 1.5 Hz, 1H), 7.05 (d, *J* = 6.8 Hz, 2H), 2.37 (s, 3H), 2.16 (s, 3H), 2.12 (s, 3H).

**$^{13}$C NMR (126 MHz, $CDCl_3$)** δ 163.62, 163.39, 149.17, 142.93, 138.70, 135.45, 135.14, 133.83, 133.45, 132.73, 131.93, 131.55, 131.25, 131.21, 130.42, 130.03, 129.61, 129.47, 129.04, 127.63, 127.11, 125.05, 123.36, 122.97, 21.34, 18.09, 17.95.

**HRMS (EI)** calcd $C_{27}H_{20}N_2O_4$ 436.1423, found 436.1411.

**IR (KBr)** ν ($cm^{-1}$): 3066, 3026, 2918, 2858, 1707, 1663, 1590, 1527, 14,83, 1462, 1437, 1402, 1360, 1306, 1238, 1191, 1131, 1092, 1030, 967, 908, 888, 851, 817, 786, 756, 706, 685, 649, 563, 542, 519, 495, 473, 418.

**5-mesitylisoquinolino[4,5-bc]carbazole-4,6-dione (3):**

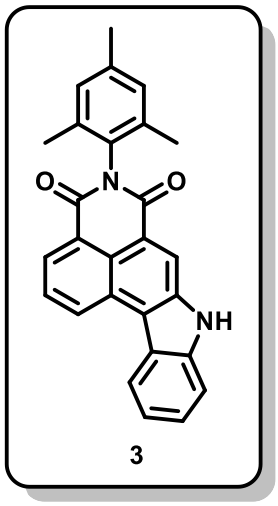

3

Compound (**2**) (2.6 g, 5.96 mmol) and $PPh_3$ (3eq.; 4.69 g, 17.87 mmol) were placed in a pressure tube equipped with a magnetic stir bar and degassed. 1,2-Dichlorobenzene (40 mL) was added, and the mixture was purged with argon for 10 minutes. The reaction was placed in an oil bath and heated for 72h at 180°C. After the solution was cooled to room temperature, the solvent was evaporated, and the crude mixture was purified by column chromatography on silica gel (DCM/acetone 98:2) to afford (**3**) as a yellow solid (1.82 g, 76%).

**$^1$H NMR (400 MHz, DMSO-$d_6$)** δ 12.36 (s, 1H), 9.37 (dd, *J* = 8.4, 1.2 Hz, 1H), 8.83 (s, 1H), 8.81 (d, *J* = 8.5 Hz, 1H), 8.51 (dd, *J* = 7.4, 1.0 Hz, 1H), 8.07 (t, 1H), 7.81 (d, *J* = 8.2 Hz, 1H), 7.62 (t, *J* = 7.2 Hz, 1H), 7.45 (t, *J* = 7.1 Hz, 1H), 7.06 (s, 2H), 2.34 (s, 3H), 2.02 (s, 6H).

**$^{13}$C NMR (126 MHz, DMSO-$d_6$)** δ 163.42, 163.24, 140.53, 137.44, 136.58, 135.03, 131.84, 129.97, 128.76, 127.70, 127.62, 127.12, 126.93, 123.64, 122.83, 122.58, 121.79, 120.76, 119.42, 119.12, 118.97, 112.56, 20.61, 17.35.

**HRMS (EI)** calcd for $C_{27}H_{20}N_2O_2$ 404.1525, found 404.1511.

**IR (KBr)** ν ($cm^{-1}$): 3333, 3053, 2950, 2912, 2912, 1695, 1651, 1618, 1589, 1574, 1540, 1493, 1463, 1448, 1400, 1381, 1365, 1346, 1323, 1303, 1274, 1240, 1206, 1183, 1164, 1121, 1093, 1078, 1033, 976, 893, 870, 856, 813, 780, 739, 692, 623, 564, 554, 523, 484, 464, 417.

**8-butyl-5-mesitylisoquinolino[4,5-bc]carbazole-4,6-dione (4):**

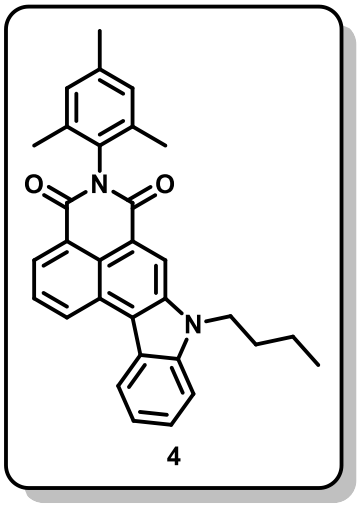

4

Compound (**3**) (1.25 g, 3.09 mmol) was placed in a glass reactor equipped with a magnetic stir bar and reflux condenser and dissolved with acetone (30 mL) under Ar. Then KOH (3eq.; 0.52 g, 9.27 mmol ), TBAB (10%, 100 mg, 0.309 mmol, and bromobutane (1.2eq.; 0.4 mL, 3.7 mmol) were added. The reactor was placed in an oil bath and refluxed for 18h. After completion of the reaction, the reaction mixture was cooled to room temperature, the solvent was evaporated, and the residue was extracted with DCM, dried over anhydrous $Na_2SO_4$, filtered, and the solvent was evaporated. The crude mixture was purified by column chromatography on silica gel (DCM as eluent) to get (1.4 g, 98%) of (**4**) as a yellow solid.

**$^1$H NMR (400 MHz, $CDCl_3$)** δ 9.20 (dd, *J* = 8.4, 1.2 Hz, 1H), 8.91 (s, 1H), 8.66 (t, 2H), 7.97 (t, 1H), 7.69 – 7.63 (m, 2H), 7.51 – 7.46 (m, 1H), 7.06 (s, 2H), 4.59 (t, *J* = 7.3 Hz, 2H), 2.38 (s, 3H), 2.15 (s, 6H), 2.01 – 1.92 (m, 2H), 1.50 – 1.41 (m, 2H), 0.98 (t, *J* = 7.4 Hz, 3H).

**$^{13}$C NMR (151 MHz, $CDCl_3$)** δ 164.41, 164.32, 141.28, 138.50, 137.46, 135.32, 131.68, 129.64, 129.49, 128.49, 128.00, 127.46, 127.04, 124.61, 123.51, 123.18, 122.56, 121.04, 120.34, 120.15, 116.90, 110.40, 43.53, 31.84, 21.36, 20.67, 18.01, 13.95.

**HRMS (EI)** calcd for $C_{31}H_{28}N_2O_2$ 460.2151, found 460.2131.

**IR (KBr)** ν ($cm^{-1}$): 3052, 2955, 2927, 2869, 1703, 1663, 1613, 1584, 1531, 1485, 1462, 1440, 1405, 1347, 1334, 1306, 1279, 1244, 1207, 1188, 1166, 1153, 1091, 1041, 977, 889, 849, 832, 810, 779, 746, 690, 672, 598, 564, 526, 495, 467, 421.

**11-bromo-8-butyl-5-mesitylisoquinolino[4,5-bc]carbazole-4,6-dione (5):**

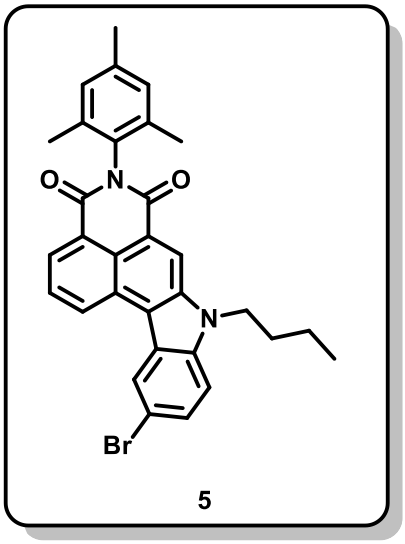

5

Compound (**4**) (500 mg, 1.09 mmol) was placed in a glass reactor equipped with a magnetic stir bar, then degassed and dissolved with DMF (10 mL) under Ar. The solution was placed in a cooling bath at 0°C, and then a solution of NBS (193.2 mg, 1.09 mmol) in DMF (6 mL) was slowly added dropwise. The mixture was kept at 0°C for an hour, then allowed to warm to room temperature and stirred overnight (additional 13h). After completion of the reaction, the solvent was evaporated, the residue was extracted with DCM, dried over anhydrous $Na_2SO_4$, filtered through the pad (silica gel and celite), and the solvent was evaporated to get (**5**) (574 mg, 98%) as a yellow solid.

**$^1$H NMR (500 MHz, $CDCl_3$)** δ 9.08 (dd, *J* = 8.4, 1.1 Hz, 1H), 8.88 (s, 1H), 8.78 (d, *J* = 1.8 Hz, 1H), 8.66 (dd, *J* = 7.3, 1.1 Hz, 1H), 8.00 (dd, *J* = 8.3, 7.3 Hz, 1H), 7.72 (dd, *J* = 8.8, 1.8 Hz, 1H), 7.54 (d, *J* = 8.7 Hz, 1H), 7.06 (s, 2H), 4.56 (t, *J* = 7.3 Hz, 2H), 2.38 (s, 3H), 2.15 (s, 6H), 1.99 – 1.90 (m, 2H), 1.47 – 1.39 (m, 2H), 0.97 (t, *J* = 7.4 Hz, 3H).

**$^{13}$C NMR (126 MHz, $CDCl_3$)** δ 164.20, 164.14, 139.80, 138.58, 137.88, 135.29, 131.56, 129.76, 129.51, 129.34, 128.36, 128.27, 127.86, 125.63, 124.67, 124.05, 123.61, 120.96, 119.19, 116.88, 114.03, 111.76, 43.71, 31.80, 21.36, 20.63, 18.00, 13.92.

**HRMS (EI)** calcd for $C_{31}H_{27}BrN_2O_2$ 538.1256, found 538.1281.

**IR (KBr)** ν ($cm^{-1}$): 2953, 2926, 2869, 1703, 1663, 1612, 1581, 1531, 1485, 1463, 1437, 1404, 1347, 1301, 1244, 1207, 1184, 1150, 1090, 1065, 1040, 947, 889, 843, 822, 799, 776, 752, 699, 679, 665, 566, 526, 498, 423.

**General procedure of Buchwald-Hartwig coupling (6a-6d):**

Compound (**5**) (120 mg, 0.22 mmol) and amine (1.2 eq.; 0.264 mmol) (for (**6a**) 73,8 mg of 3,6-di-tert-butylcarbazole; for (**6b**) 55.3 mg of 9,9-dimethyl-9,10-dihydroacridine; for (**6c**) 48.4 mg of phenoxazine; for (**6d**) 52.6 mg of phenothiazine) were placed in a pressure tube equipped with a magnetic stir bar and degassed. The mixture was dissolved in 3 mL of anhydrous toluene and purged with argon for 10 minutes, and NaOtBu (1.2 eq.; 25.4 mg, 0.264 mmol) and $Pd(P\mathit{t}Bu_3)_2$ (10%, 11.3 mg, 0.022 mmol) were added. After overnight heating at 120°C, the solution was cooled to room temperature, and the solvent was evaporated. The crude mixture was extracted with DCM, dried over anhydrous $Na_2SO_4$, filtered, evaporated and purified by column chromatography (silica gel, DCM as eluent) to afford (**6a**-**6d**) with various yields.

**8-butyl-11-(3,6-di-tert-butyl-9H-carbazol-9-yl)-5-mesitylisoquinolino[4,5-bc]carbazole-4,6-dione (6a):**

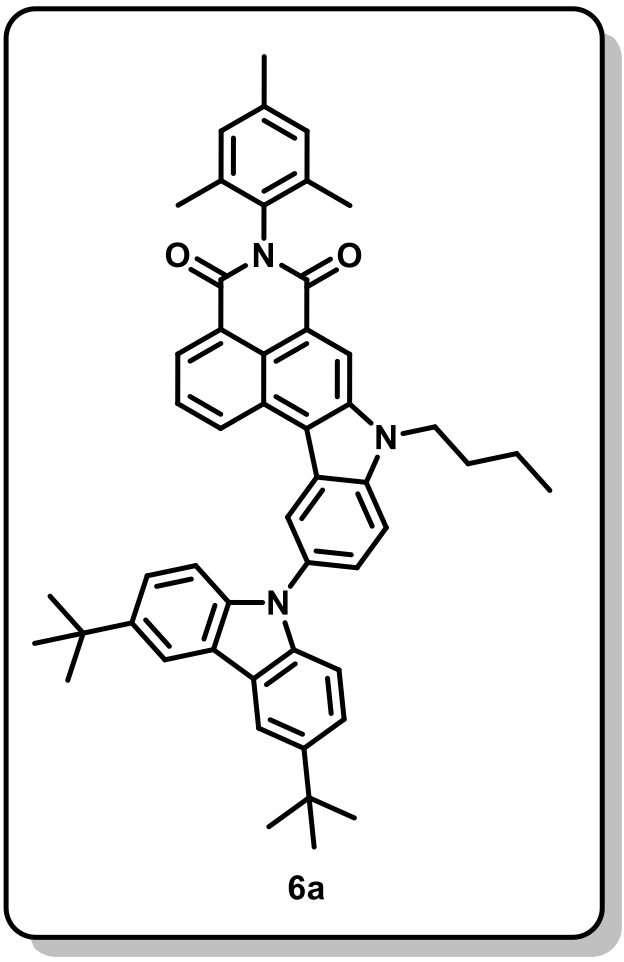


**6a**

Orange solid (121 mg, 74%).

**$^{1}$H NMR (400 MHz, $CDCl_3$)** δ 9.02 (dd, *J* = 8.5, 1.1 Hz, 1H), 8.96 (s, 1H), 8.80 (d, *J* = 1.8 Hz, 1H), 8.63 (dd, *J* = 7.4, 1.1 Hz, 1H), 8.23 (d, *J* = 1.3 Hz, 2H), 7.89 (dd, *J* = 8.4, 7.3 Hz, 1H), 7.85 (d, *J* = 8.7 Hz, 1H), 7.79 (dd, *J* = 8.7, 1.8 Hz, 1H), 7.50 (dd, *J* = 8.6, 1.9 Hz, 2H), 7.38 (dd, *J* = 8.7, 0.6 Hz, 2H), 7.07 (s, 2H), 4.68 (t, *J* = 7.4 Hz, 2H), 2.39 (s, 3H), 2.16 (s, 6H), 2.10 – 2.01 (m, 2H), 1.59 – 1.54 (m, 2H), 1.51 (s, 18H), 1.05 (t, *J* = 7.4 Hz, 3H).

**$^{13}$C NMR (126 MHz, $CDCl_3$)** δ 164.32, 164.20, 142.99, 140.41, 140.14, 138.58, 138.24, 135.31, 131.61, 131.49, 129.52, 129.44, 128.44, 128.22, 127.83, 126.62, 124.67, 123.85, 123.56, 123.39, 123.27, 121.90, 120.79, 120.03, 116.98, 116.55, 111.41, 109.15, 43.88, 34.95, 32.22, 31.98, 27.07, 21.37, 20.75, 18.01, 13.99.

**HRMS (EI)** calcd for $C_{51}H_{51}N_3O_2$ 737.3981, found 737.3950.

**IR (KBr)** ν ($cm^{-1}$): 3046, 2954, 2952, 2863, 1707, 1655, 1613, 1585, 1532, 1487, 1441, 1405, 1346, 1315, 1294, 1206, 1182, 1147, 1089, 1034, 1011, 940, 919, 895, 876, 849, 839, 807, 778, 743, 695, 681, 656, 613, 578, 563, 528, 499, 469, 424.

**8-butyl-11-(9,9-dimethylacridin-10(9H)-yl)-5-mesitylisoquinolino[4,5-bc]carbazole-4,6-dione (6b):**

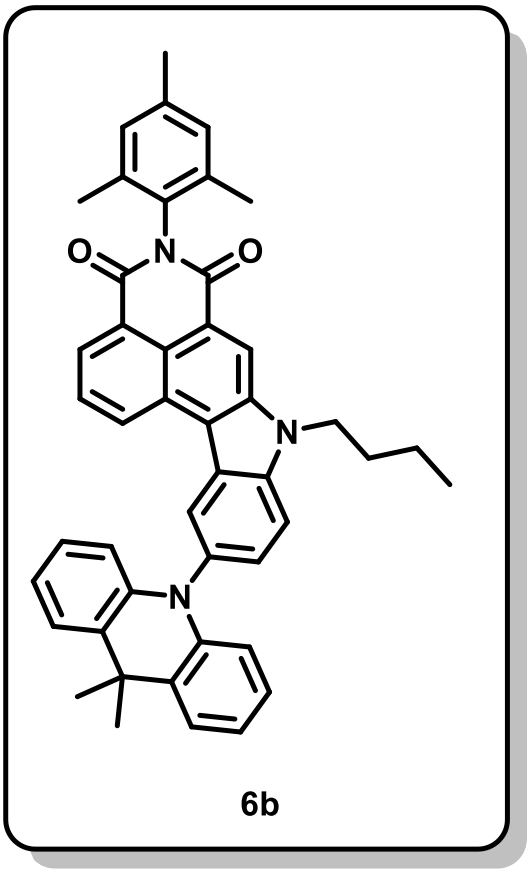


**6b**

Yellow solid, (77 mg, 52%).

**$^1$H NMR (500 MHz, $CDCl_3$)** δ 9.03 (dd, *J* = 8.5, 1.1 Hz, 1H), 8.96 (s, 1H), 8.65 – 8.61 (m, 2H), 7.92 – 7.86 (m, 2H), 7.58 (dd, *J* = 8.7, 1.8 Hz, 1H), 7.55 – 7.51 (m, 2H), 7.07 (s, 2H), 6.99 – 6.92 (m, 4H), 6.37 – 6.32 (m, 2H), 4.66 (t, *J* = 7.4 Hz, 2H), 2.38 (s, 3H), 2.16 (s, 6H), 2.10 – 2.03 (m, 2H), 1.80 (s, 6H), 1.60 – 1.55 (m, 2H), 1.06 (t, *J* = 7.4 Hz, 3H).

**$^{13}$C NMR (126 MHz, $CDCl_3$)** δ 164.34, 164.18, 141.65, 140.49, 138.58, 138.12, 135.31, 134.33, 131.60, 130.16, 130.04, 129.69, 129.52, 128.36, 128.30, 127.75, 126.57, 125.94, 125.68, 124.68, 124.23, 123.50, 120.76, 120.14, 116.97, 114.33, 112.64, 43.91, 36.22, 31.97, 31.94, 21.36, 20.77, 17.99, 14.00.

**HRMS (EI)** calcd for $C_{46}H_{41}N_3O_2$ 667.3199, found 667.2118.

**IR (KBr)** ν ($cm^{-1}$): 3059, 3030, 2952, 2925, 2867, 2726, 1992, 1794, 1703, 1664, 1614, 1583, 1531, 1498, 1470, 1442, 1405, 1379, 1345, 1322,1292, 1269, 1246, 1208, 1183, 1164, 1149, 1112, 1089, 1043, 1011, 954, 926, 887, 849, 833, 780, 745, 695, 683, 652, 612, 595, 566, 545, 528, 497, 440, 426, 416, 405.

**8-butyl-5-mesityl-11-(10H-phenoxazin-10-yl)isoquinolino[4,5-bc]carbazole-4,6-dione (6c):**

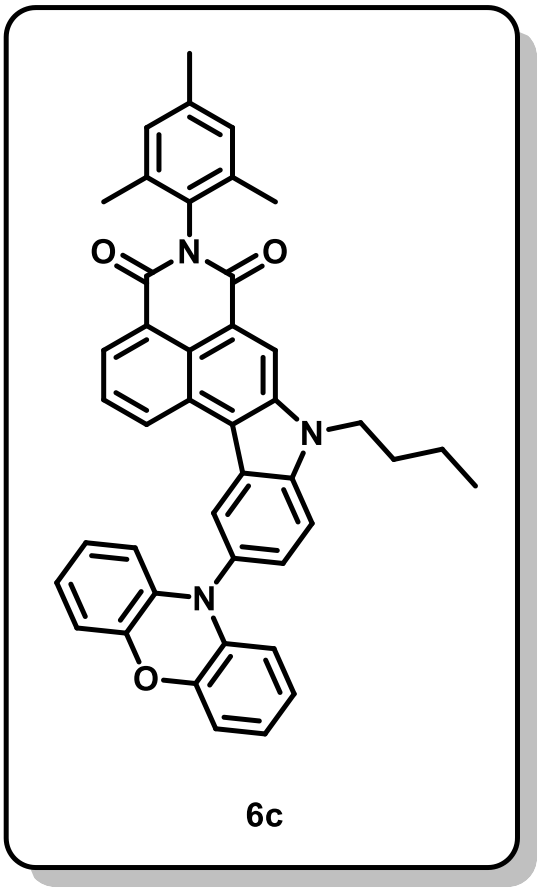


**6c**

Yellow solid, (115 mg, 81%).

**$^1$H NMR (600 MHz, $CDCl_3$)** δ 9.07 (dd, *J* = 8.4, 1.1 Hz, 1H), 8.94 (s, 1H), 8.67 – 8.63 (m, 2H), 7.94 (dd, *J* = 8.3, 7.3 Hz, 1H), 7.87 (d, *J* = 8.7 Hz, 1H), 7.59 (dd, *J* = 8.7, 1.9 Hz, 1H), 7.07 (s, 2H), 6.76 (dd, *J* = 7.9, 1.5 Hz, 2H), 6.68 (td, *J* = 7.6, 1.5 Hz, 2H), 6.59 (td, *J* = 8.0, 7.4, 1.5 Hz, 2H), 5.99 (dd, *J* = 8.0, 1.4 Hz, 2H), 4.64 (t, *J* = 7.4 Hz, 2H), 2.38 (s, 3H), 2.15 (s, 6H), 2.06 – 2.00 (m, 2H), 1.54 – 1.50 (m, 2H), 1.04 (t, *J* = 7.4 Hz, 3H).

**$^{13}$C NMR (151 MHz, $CDCl3_3$)** δ 164.28, 164.15, 144.20, 140.55, 138.61, 138.14, 135.29, 135.24, 131.93, 131.56, 129.63, 129.53, 129.36, 128.37, 128.32, 127.86, 125.74, 124.68, 124.29, 123.53, 123.44, 121.53, 120.90, 119.99, 116.95, 115.64, 113.53, 112.90, 43.88, 31.93, 21.36, 20.74, 17.99, 13.98.

**HRMS (EI)** calcd for $C_{43}H_{35}N_3O_3$ 641.2678, found 641.2649.

**IR (KBr)** ν ($cm^{-1}$): 2952, 2918, 2872, 1708, 1669, 1616, 1585, 1531, 1486, 1462, 1438, 1404, 1370, 1341, 1295, 1270, 1246, 1205, 1183, 1144, 1091, 1041, 917, 889, 854, 809, 779, 738, 681, 639, 616, 595, 562, 499.

**8-butyl-5-mesityl-11-(10H-phenothiazin-10-yl)isoquinolino[4,5-bc]carbazole-4,6-dione (6d):**

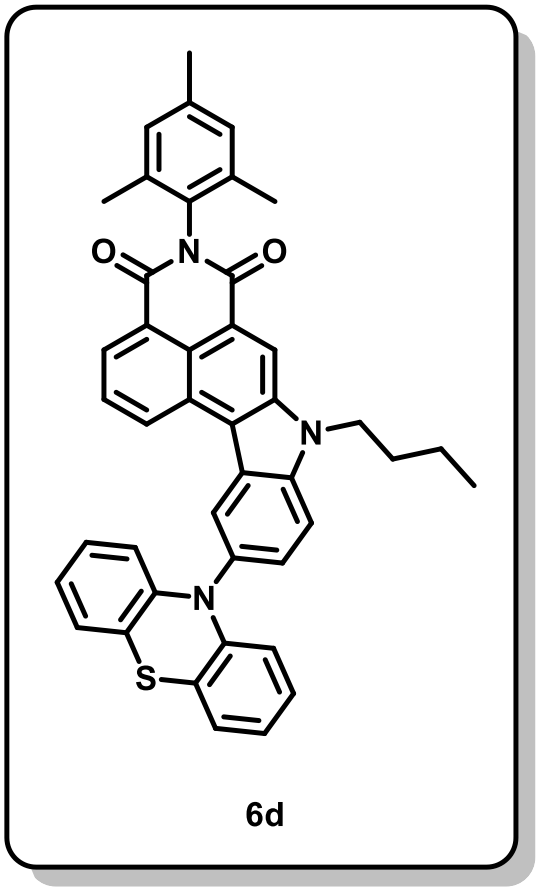


**6d**

Orange solid, (96 mg, 66%).

**$^1$H NMR (600 MHz, $CDCl_3$)** δ 9.09 (dd, *J* = 8.5, 1.2 Hz, 1H), 8.95 (s, 1H), 8.71 (d, *J* = 1.9 Hz, 1H), 8.64 (dd, *J* = 7.3, 1.1 Hz, 1H), 7.94 (dd, *J* = 8.4, 7.3 Hz, 1H), 7.89 (d, *J* = 8.6 Hz, 1H), 7.67 (dd, *J* = 8.7, 1.9 Hz, 1H), 7.09 – 7.06 (m, 4H), 6.85 – 6.81 (m, 4H), 6.28 – 6.24 (m, 2H), 4.66 (t, *J* = 7.5 Hz, 2H), 2.38 (s, 3H), 2.15 (s, 6H), 2.09 – 2.02 (m, 2H), 1.59 – 1.55 (m, 2H), 1.05 (t, *J* = 7.4 Hz, 3H).

**$^{13}$C NMR (126 MHz, $CDCl_3$)** δ 164.30, 164.15, 145.10, 140.46, 138.59, 138.15, 135.30, 133.87, 131.58, 130.17, 129.68, 129.52, 128.37, 128.33, 127.84, 127.02, 126.90, 125.84, 124.69, 124.23, 123.53, 122.60, 120.88, 120.15, 119.87, 116.94, 115.96, 112.28, 43.91, 31.96, 21.36, 20.76, 17.99, 13.99.

**HRMS (EI)** calcd for $C_{43}H_{35}N_3O_2S$ 657.2450, found 657.2422.

**IR (KBr)** ν ($cm^{-1}$): 3060, 2952, 2921, 2858, 1705, 1664, 1614, 1583, 1531, 1460, 1441, 1405, 1370, 1346, 1303, 1244, 1207, 1188, 1148, 1126, 1090, 1041, 949, 920, 889, 849, 809, 779, 744, 695, 682, 641, 628, 697, 564, 529, 498, 473, 437.

**General procedure of Suzuki-Miyaura coupling (7a-7b):**

Compound (**5**) (65 mg, 0.12 mmol) and 9-anthraceneboronic acid (32 mg, 0.144 mmol) or 4-cyanophenylboronic acid (22 mg, 0.144 mmol) were placed in a two-neck round-bottom flask equipped with a magnetic stirring bar and a reflux condenser and degassed. Under argon, toluene (2 mL) and ethanol (1 mL) were added, and the solution was purged with argon for 10 minutes. Next, $K_2CO_3$ (0.4 mL of 2M aq. base solution) and $Pd(PPh_3)_4$ (13.9 mg, 0.012 mmol) were added. The reactor was placed in an oil bath and stirred for 20h at 90°C. After cooling, the mixture was extracted three times with DCM, dried over anhydrous $Na_2SO_4$ and filtered. After evaporation of solvents, the crude mixture was purified by column chromatography separation on silica gel (eluent: DCM for **7a**, and DCM/hexane 9:1 for **7b**).

**11-(anthracen-9-yl)-8-butyl-5-mesitylisoquinolino[4,5-bc]carbazole-4,6-dione (7a):**

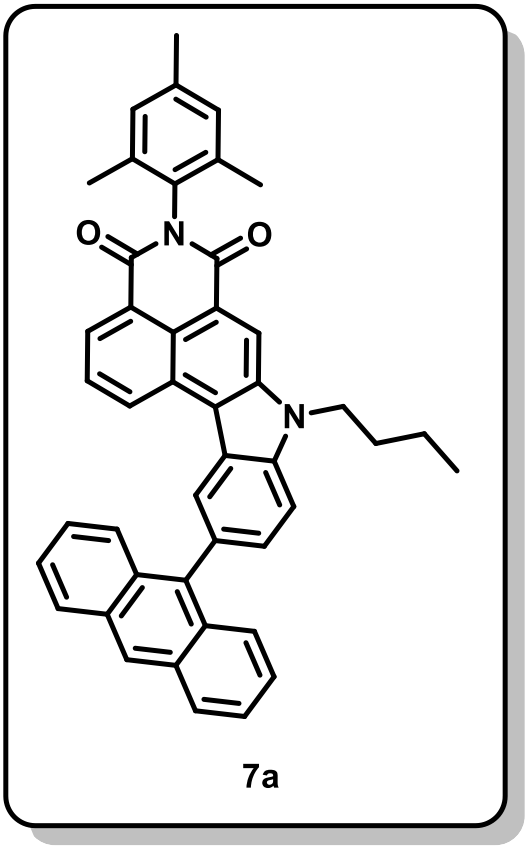


Yellow solid, (73 mg, 95%).

**$^1$H NMR (500 MHz, $CDCl_3$)** δ 9.03 (d, *J* = 8.5 Hz, 1H), 8.99 (s, 1H), 8.72 (s, 1H), 8.59 (d, *J* = 7.6 Hz, 2H), 8.13 (d, *J* = 8.5 Hz, 2H), 7.87 (d, *J* = 8.4 Hz, 1H), 7.79 (dd, *J* = 15.7, 8.2 Hz, 3H), 7.73 (d, *J* = 8.3 Hz, 1H), 7.50 (t, 2H), 7.36 (t, 1H), 7.07 (s, 2H), 4.71 (t, *J* = 7.4 Hz, 2H), 2.38 (s, 3H), 2.17 (s, 6H), 2.14 – 2.03 (m, 2H), 1.64 – 1.55 (m, 2H), 1.08 (t, *J* = 7.3 Hz, 3H), 0.89 (t, *J* = 6.7 Hz, 2H).

**$^{13}$C NMR (126 MHz, $CDCl_3$)** δ 164.45, 164.28, 140.73, 138.53, 137.96, 137.27, 135.32, 131.67, 131.63, 131.53, 131.08, 130.39, 129.80, 129.51, 128.64, 128.49, 128.08, 127.50, 127.11, 126.95, 125.68, 125.61, 125.34, 124.66, 123.44, 122.76, 120.36, 120.29, 116.96, 110.26, 43.82, 32.02, 21.36, 20.81, 18.00, 14.04.

**HRMS (EI)** calcd for $C_{45}H_{36}N_2O_2$ 636.2777 , found 636.2770.

**IR (KBr)** ν ($cm^{-1}$): 3046, 2955, 2924, 2860, 1704, 1663, 1612, 1584, 1531, 1482, 1460, 1349, 1404, 1349, 1320, 1204, 1246, 1208, 1186, 1156, 1112, 1090, 1039, 935, 890, 849, 809, 757, 698, 651, 608, 570, 528, 499, 466, 434.

**4-(8-butyl-5-mesityl-4,6-dioxo-4,5,6,8-tetrahydroisoquinolino[4,5-bc]carbazol-11-yl)benzonitrile (7b):**

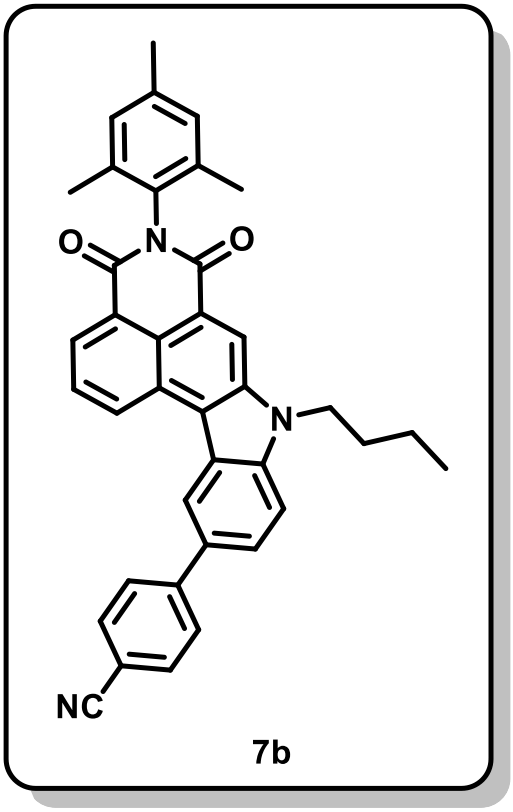


Yellow solid, (28 mg, 41%).

**$^1$H NMR (400 MHz, $CDCl_3$)** δ 9.21 (d, *J* = 7.3 Hz, 1H), 8.93 (s, 1H), 8.84 (s, 0H), 8.68 (d, *J* = 7.4 Hz, 1H), 8.01 (t, 1H), 7.92 – 7.80 (m, 5H), 7.76 (d, *J* = 8.7 Hz, 1H), 7.06 (s, 2H), 4.62 (t, *J* = 7.3 Hz, 2H), 2.38 (s, 3H), 2.16 (s, 6H), 2.06 – 1.94 (m, 2H), 1.53 – 1.43 (m, 2H), 1.00 (t, *J* = 7.4 Hz, 3H).

**$^{13}$C NMR (126 MHz, $CDCl_3$)** δ 164.23, 164.15, 146.40, 141.25, 138.59, 138.15, 135.28, 132.93, 132.51, 131.56, 129.51, 129.44, 128.48, 128.28, 128.24, 127.79, 126.45, 124.77, 123.67, 123.23, 121.95, 120.80, 120.26, 119.19, 116.93, 111.02, 110.70, 43.75, 31.88, 21.35, 20.67, 18.00, 13.94.

**HRMS (EI)** calcd for $C_{38}H_{31}N_3O_2$ 561.2416, found 561.2421.

**IR (KBr)** ν ($cm^{-1}$): 2961, 2926, 2860, 2223, 1888, 1763, 1707, 1664, 1604, 1582, 1530, 1464, 1441, 1405, 1365, 1347, 1319, 1285, 1262, 1240, 1205, 1159, 1090, 1027, 950, 919, 901, 889, 845, 834, 800, 775, 744, 730, 698, 646, 609, 576, 552, 528, 511, 491, 467, 424.

## S3 NMR, HRMS and IR spectra of synthesized compounds

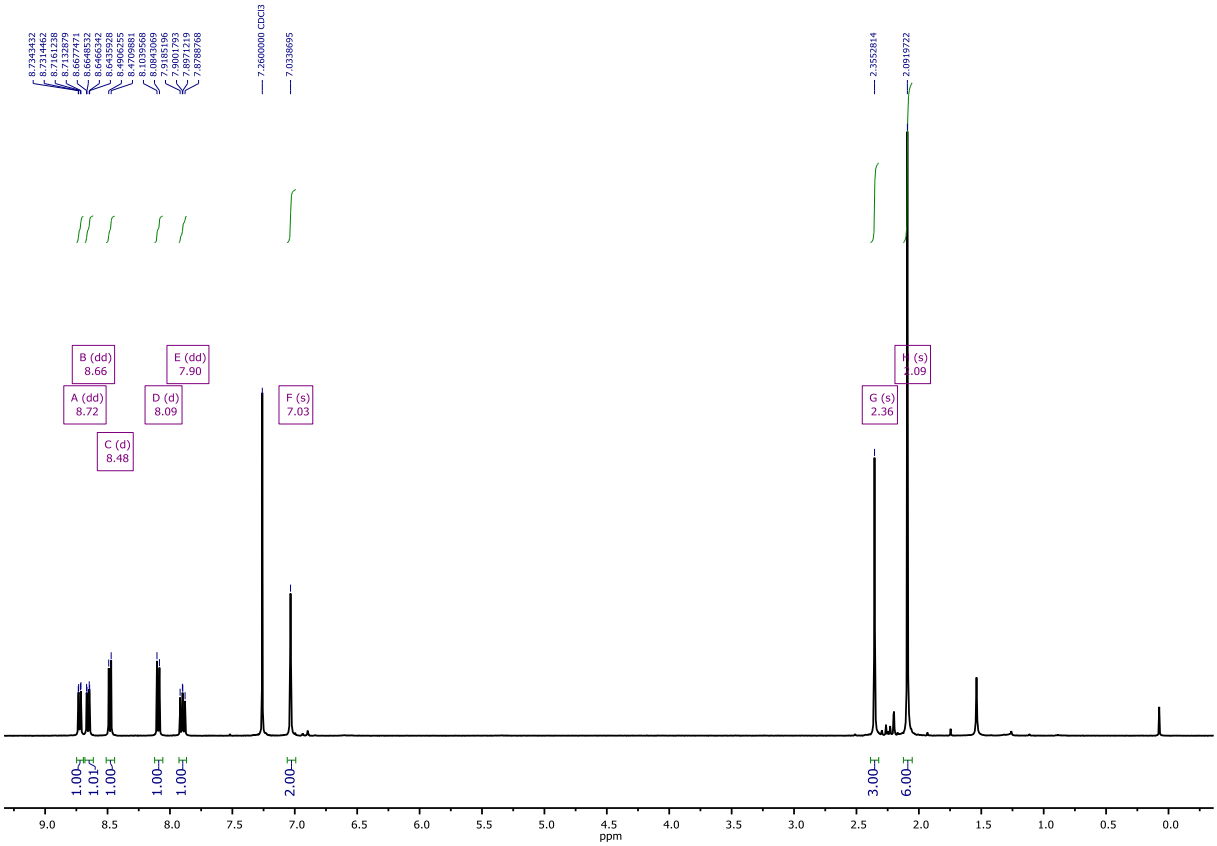


**Figure 2.** $^{1}$H NMR spectrum of (**1**) (400 MHz, $CDCl_3$).

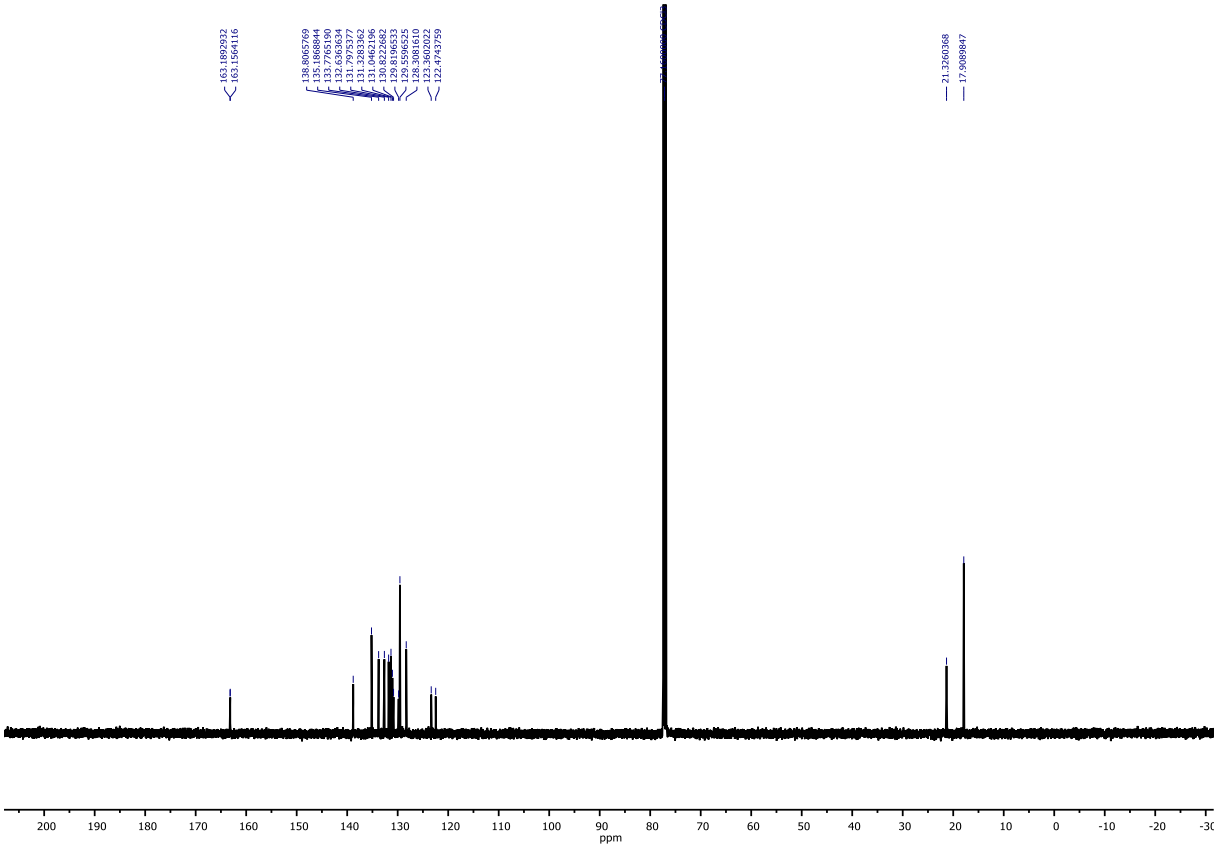


**Figure 3.** $^{13}$ C NMR spectrum of (**1**) (126 MHz, $CDCl_3$).

**Single Mass Analysis**
Tolerance = 20.0 PPM / DBE: min = -1.5, max = 80.0
Selected filters: None

Monoisotopic Mass, Odd and Even Electron Ions
22 formula(e) evaluated with 1 results within limits (up to 50 closest results for each mass)
Elements Used:
C: 0-100 H: 0-200 N: 0-2 O: 2-2 Br: 1-2

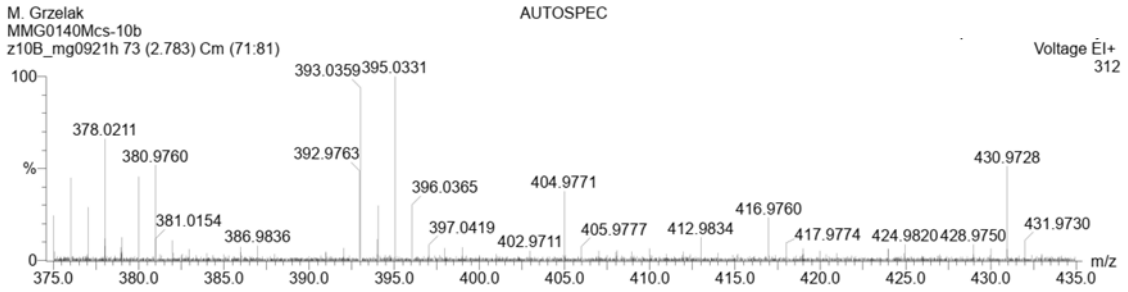


| | | | | | | |
|---|---|---|---|---|---|---|
| Minimum: | | | | -1.5 | | |
| Maximum: | | 5.0 | 20.0 | 80.0 | | |
| Mass | Calc. Mass | mDa | PPM | DBE | i-FIT | Formula |
| 393.0359 | 393.0364 | -0.5 | -1.3 | 14.0 | 2.4 | C21 H16 N O2 Br |

**Figure 4.** HRMS (EI) spectrum of (**1**).

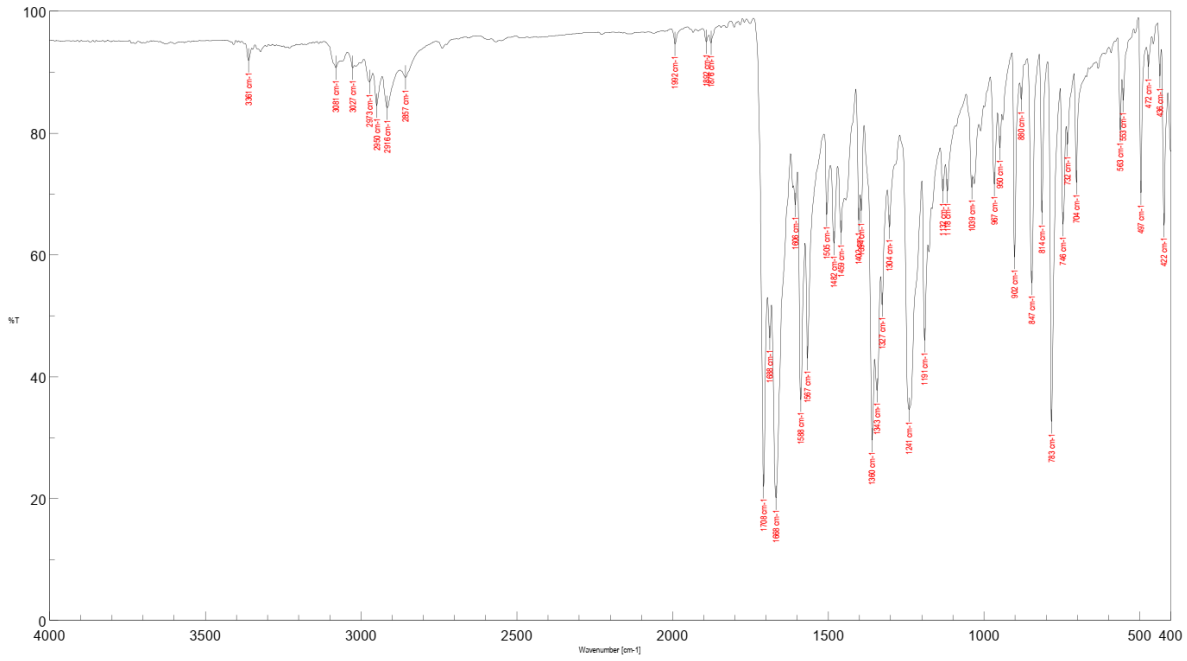


**Figure 5.** IR spectrum of (**1**) in KBr.

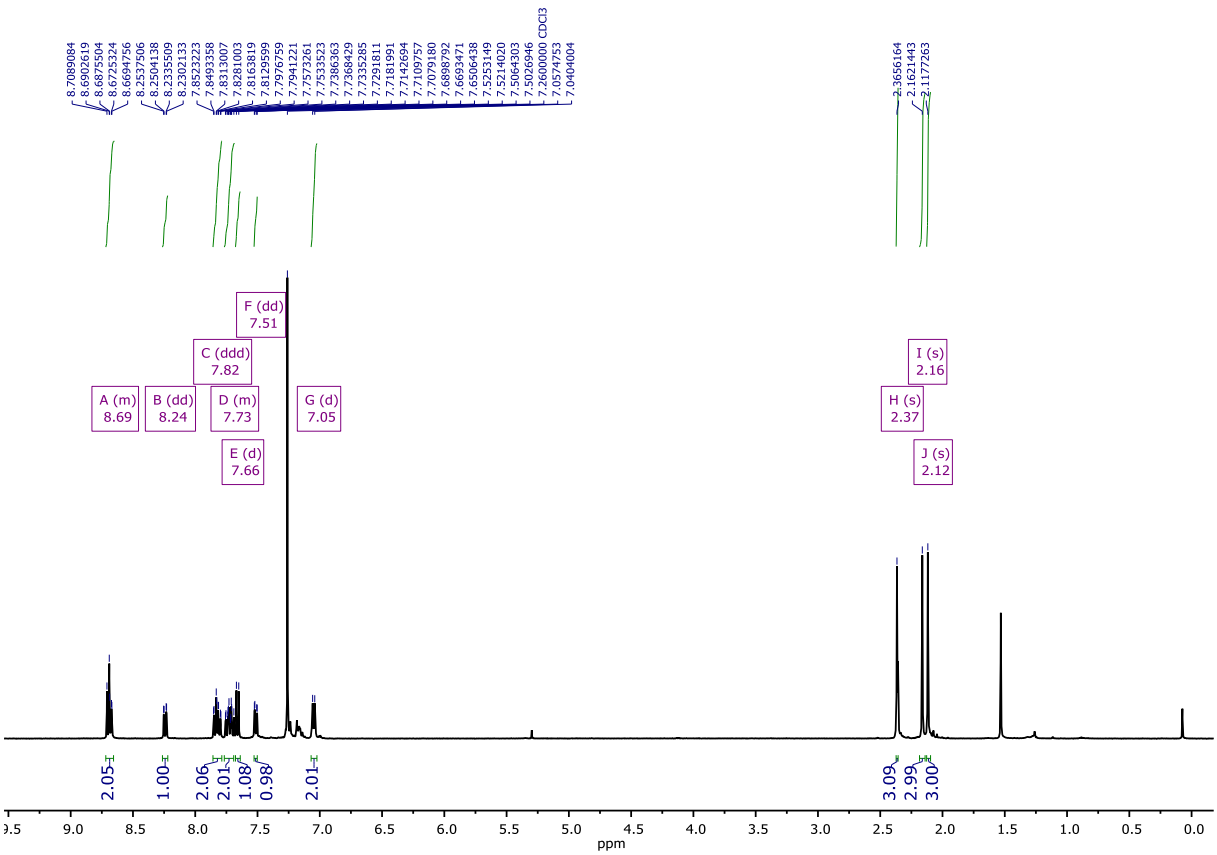


**Figure 6.** $^{1}H$ NMR spectrum of (**2**) (400 MHz, $CDCl_3$).

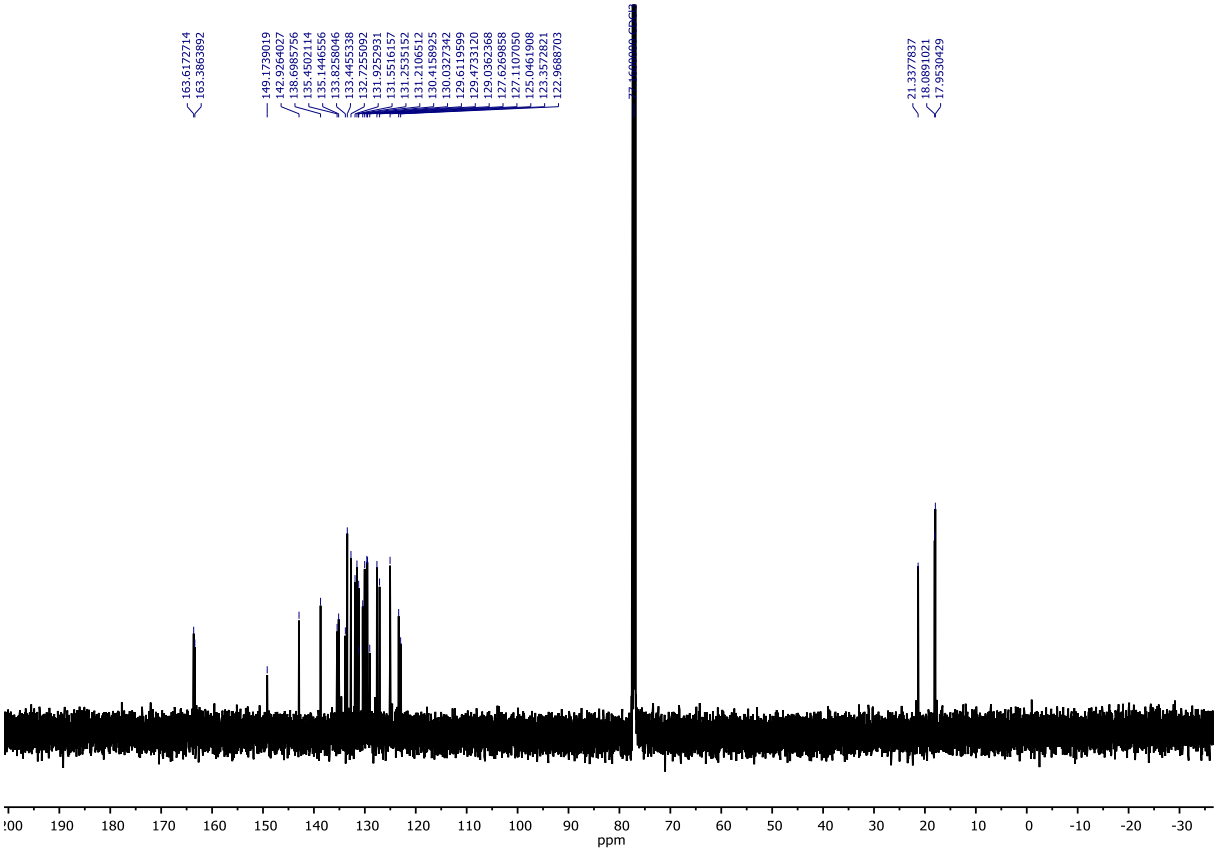


**Figure 7.** $^{13}C$ NMR spectrum of (**2**) (126 MHz, $CDCl_3$).

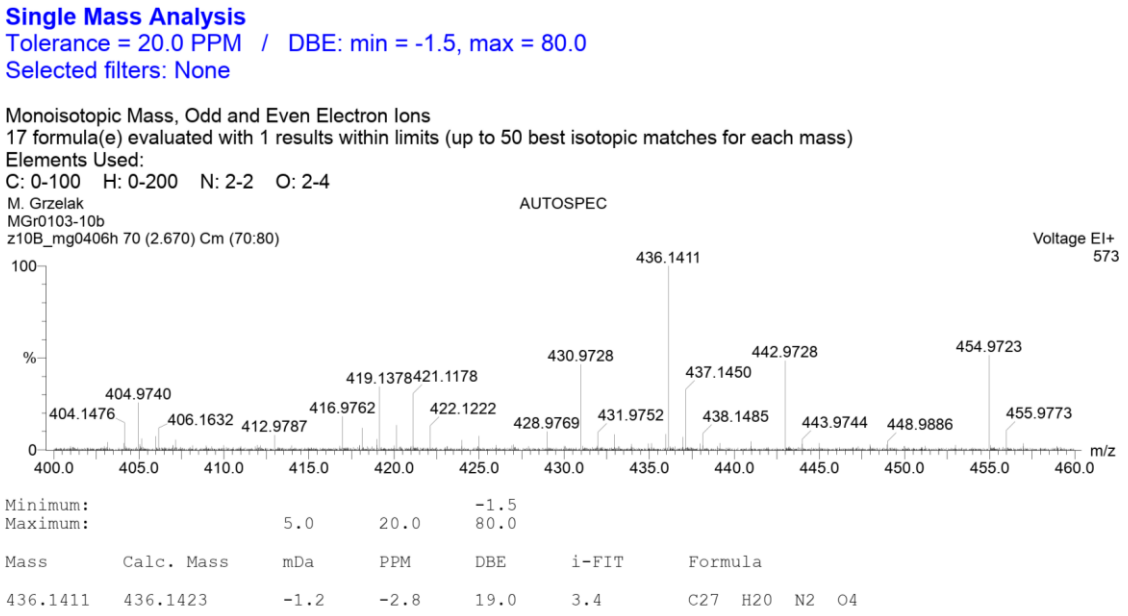


**Figure 8.** HRMS (EI) spectrum of (**2**).

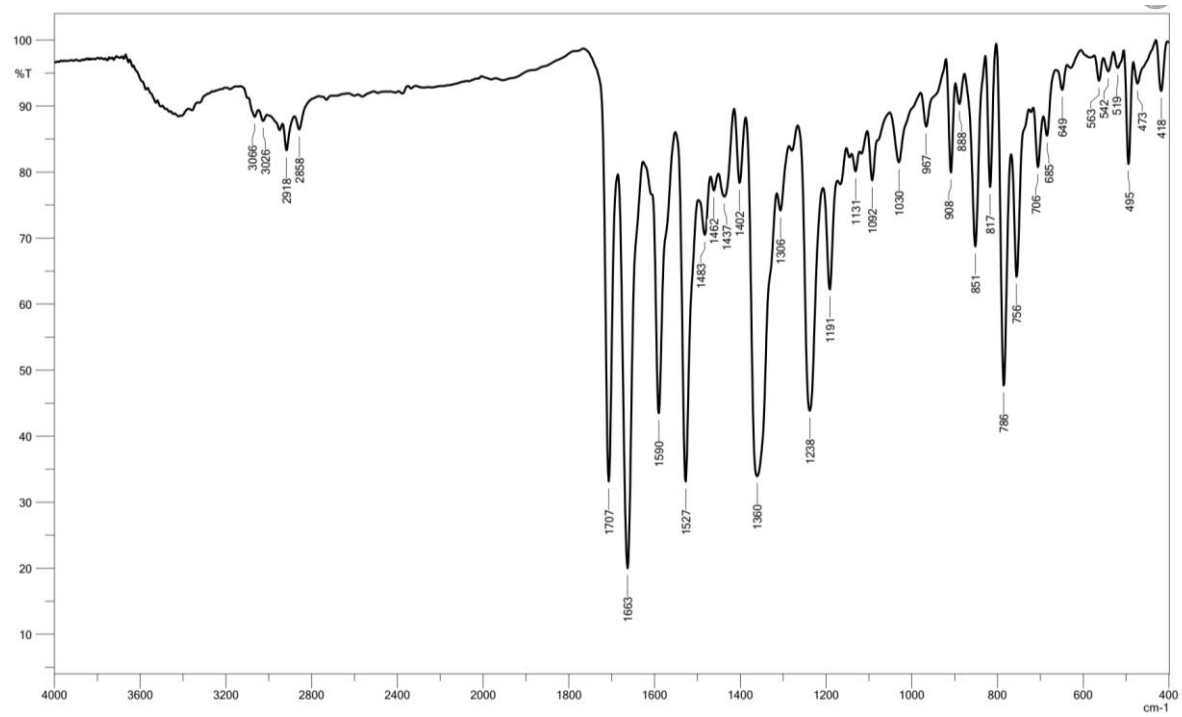


**Figure 9.** IR spectrum of (**2**) in KBr.

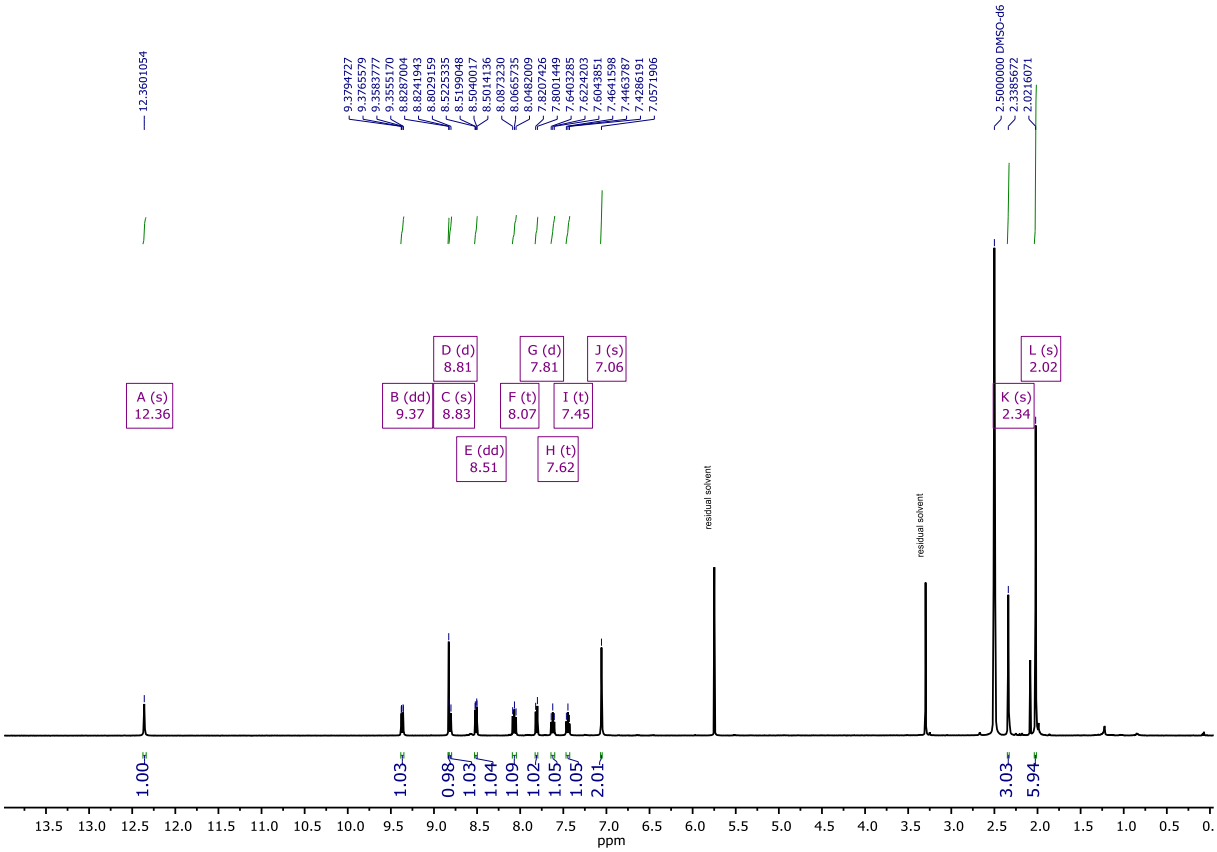


**Figure 10.** $^{1}$H NMR spectrum of (**3**) (400 MHz, DMSO-$d_6$).

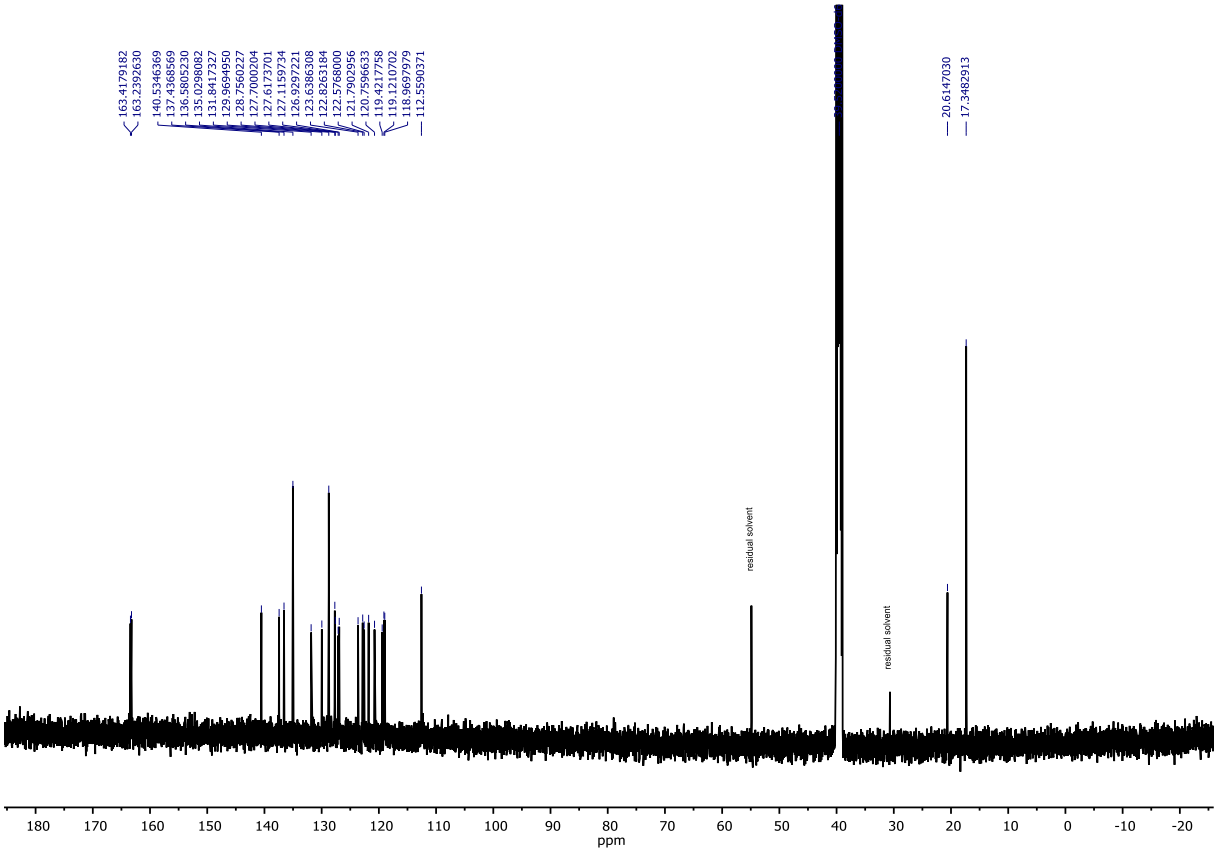


**Figure 11.** $^{13}$C NMR spectrum of (**3**) (126 MHz, DMSO-$_{d6}$).

**Single Mass Analysis**
Tolerance = 20.0 PPM / DBE: min = -1.5, max = 80.0
Selected filters: None

Monoisotopic Mass, Odd and Even Electron Ions
10 formula(e) evaluated with 1 results within limits (up to 50 best isotopic matches for each mass)
Elements Used:
C: 0-100 H: 0-200 N: 2-2 O: 2-3

M. Grzelak
MGr0107-10b
z10B_mg0404h 112 (4.272) Cm (100:120)

AUTOSPEC

Voltage EI+
236

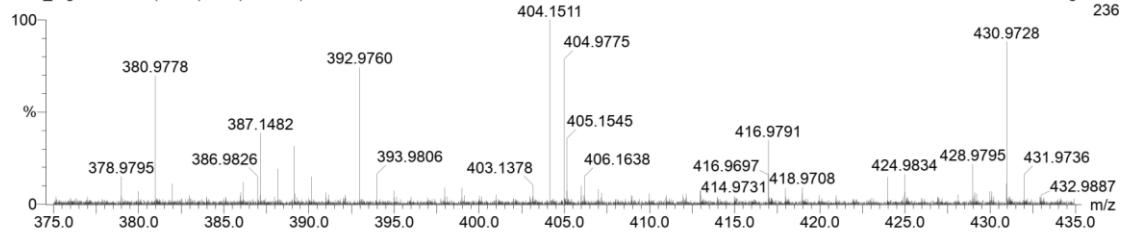


| | | | | | | |
|---|---|---|---|---|---|---|
| Minimum: | | | | -1.5 | | |
| Maximum: | | 5.0 | 20.0 | 80.0 | | |
| Mass | Calc. Mass | mDa | PPM | DBE | i-FIT | Formula |
| 404.1511 | 404.1525 | -1.4 | -3.5 | 19.0 | 7.8 | C27 H20 N2 O2 |

**Figure 12.** HRMS (EI) spectrum of (**3**).

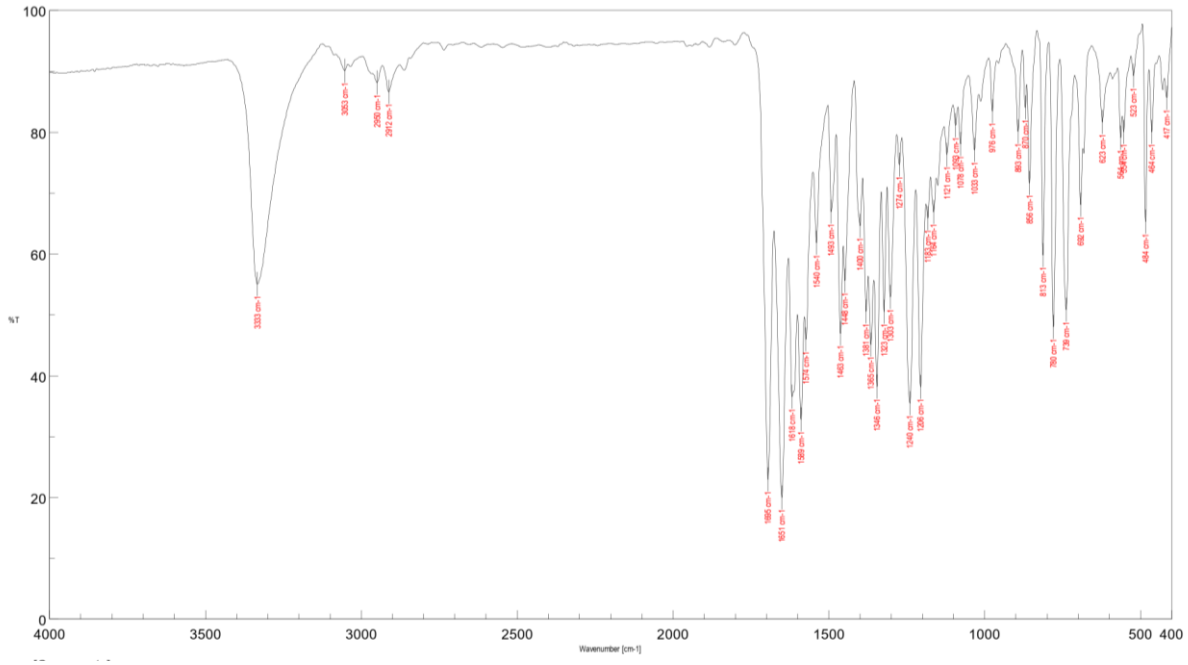


**Figure 13.** IR spectrum of (**3**) in KBr.

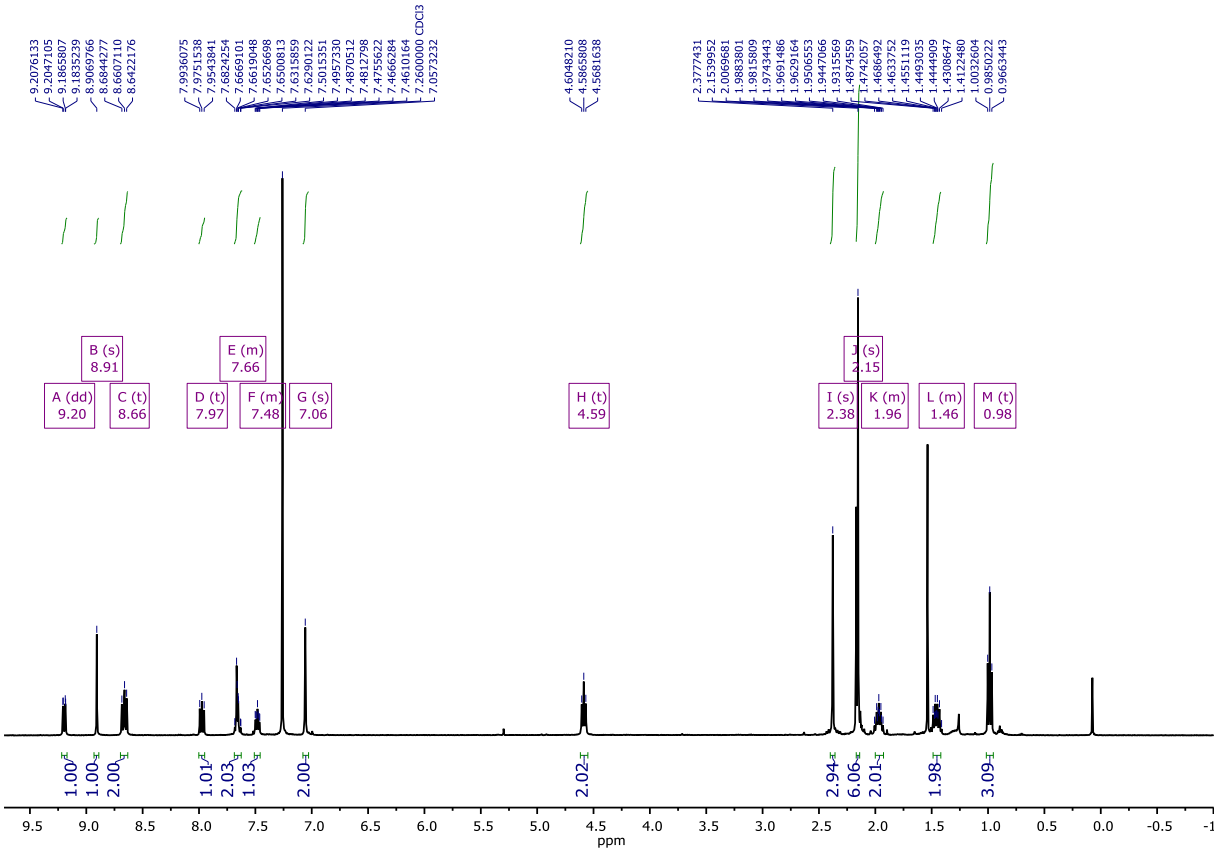


**Figure 14.** $^{1}$H NMR spectrum of (**4**) (400 MHz, $CDCl_3$).

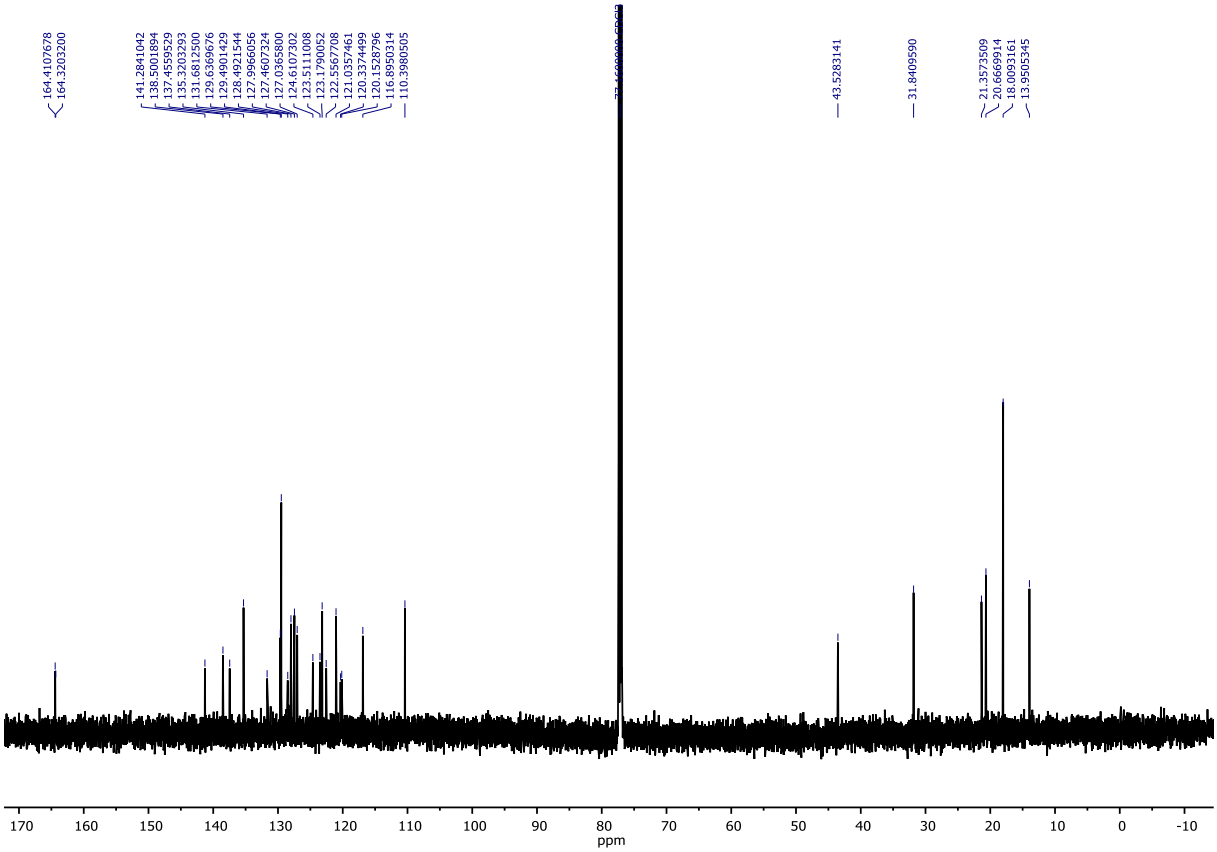


**Figure 15.** $^{13}$C NMR spectrum of (**4**) (151 MHz, $CDCl_3$).

**Single Mass Analysis**
Tolerance = 20.0 PPM / DBE: min = -1.5, max = 80.0
Selected filters: None

Monoisotopic Mass, Odd and Even Electron Ions
18 formula(e) evaluated with 1 results within limits (up to 50 closest results for each mass)
Elements Used:
C: 0-100 H: 0-200 N: 0-2 O: 2-2

M. Grzelak
MMG0139-10b
z10B_mg0922h 108 (4.118) Cm (108:137)

AUTOSPEC

Voltage EI+
152

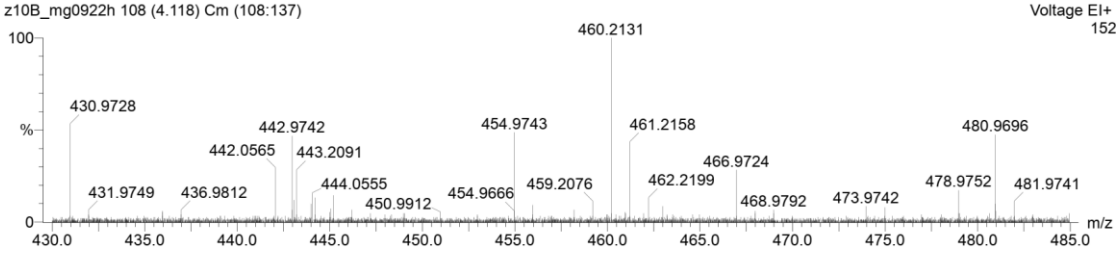


| | | | | | | |
|---|---|---|---|---|---|---|
| Minimum: | | | | -1.5 | | |
| Maximum: | | 5.0 | 20.0 | 80.0 | | |
| Mass | Calc. Mass | mDa | PPM | DBE | i-FIT | Formula |
| 460.2131 | 460.2151 | -2.0 | -4.3 | 19.0 | 3.0 | C31 H28 N2 O2 |

**Figure 16.** HRMS (EI) spectrum of (**4**).

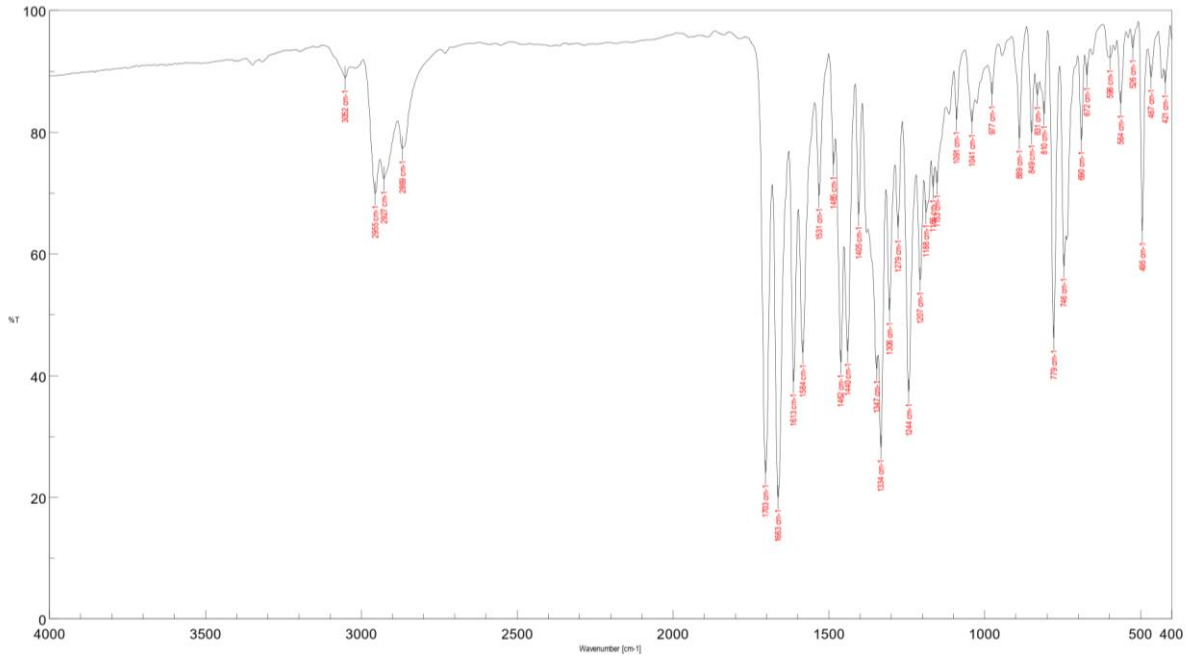


**Figure 17.** IR spectrum of (**4**) in KBr.

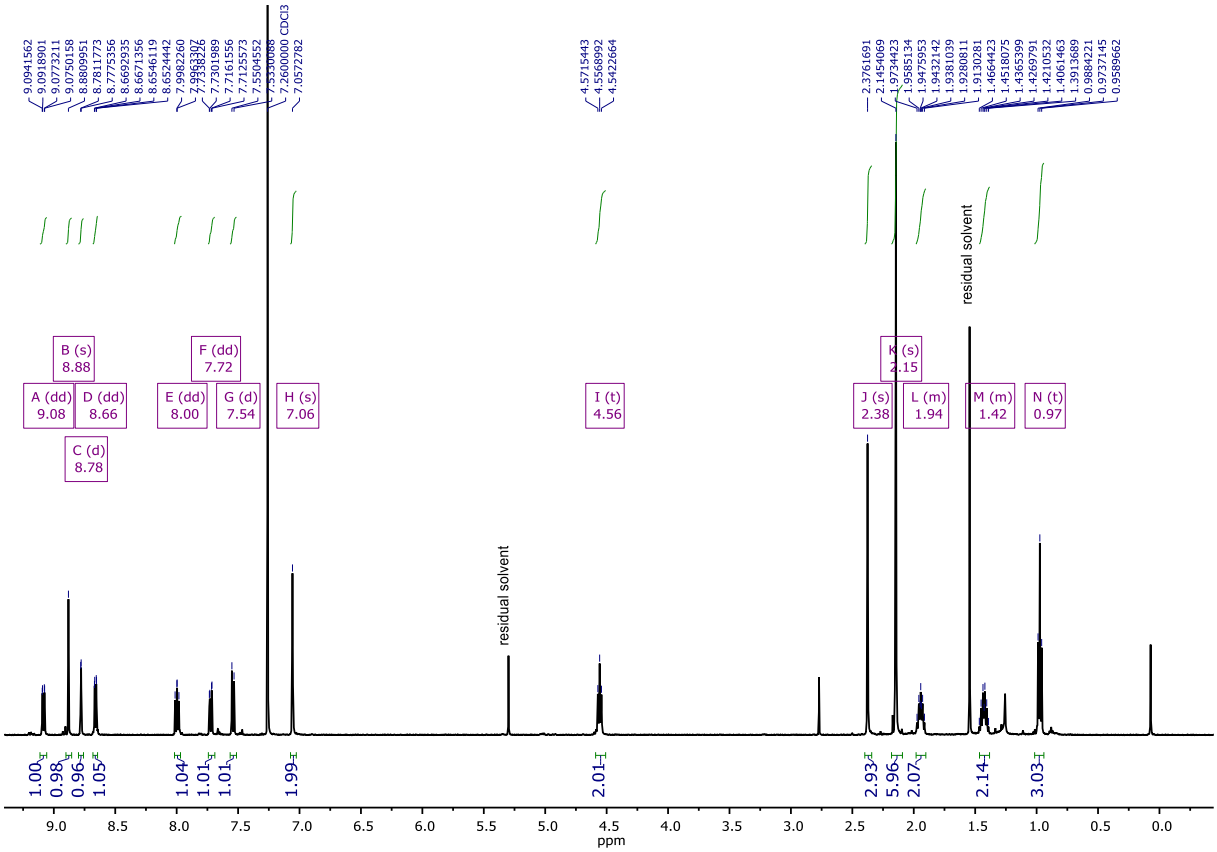


**Figure 18.** $^{1}$H NMR spectrum of (**5**) (500 MHz, $CDCl_3$).

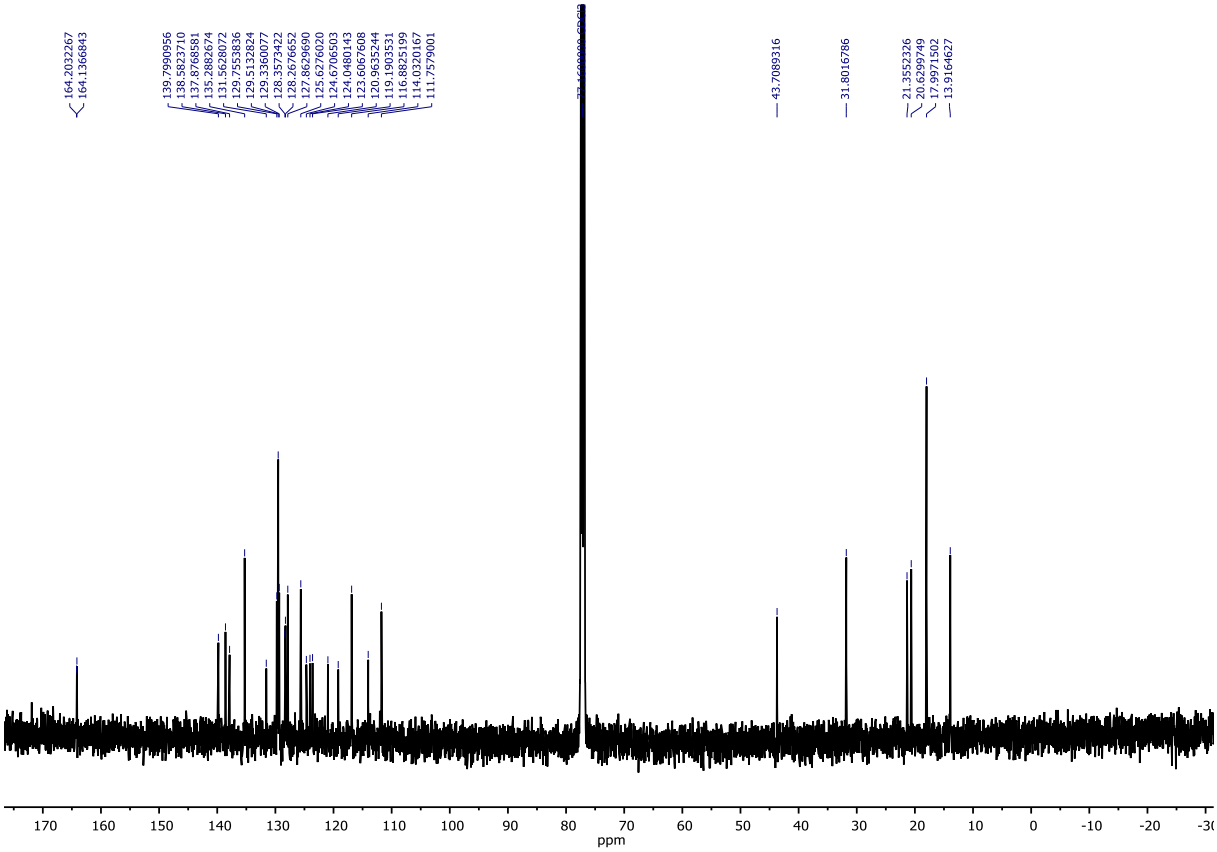


**Figure 19.** $^{13}$C NMR spectrum of (**5**) (126 MHz, $CDCl_3$).

**Single Mass Analysis**
Tolerance = 20.0 PPM / DBE: min = -1.5, max = 80.0
Selected filters: None

Monoisotopic Mass, Odd and Even Electron Ions
6 formula(e) evaluated with 1 results within limits (up to 50 closest results for each mass)
Elements Used:
C: 0-100 H: 0-200 N: 2-2 O: 2-2 Br: 1-1

M. Grzelak
MMG0138-10b
z10B_mg0923h 71 (2.707) Cm (71:79)

AUTOSPEC

Voltage EI+
238

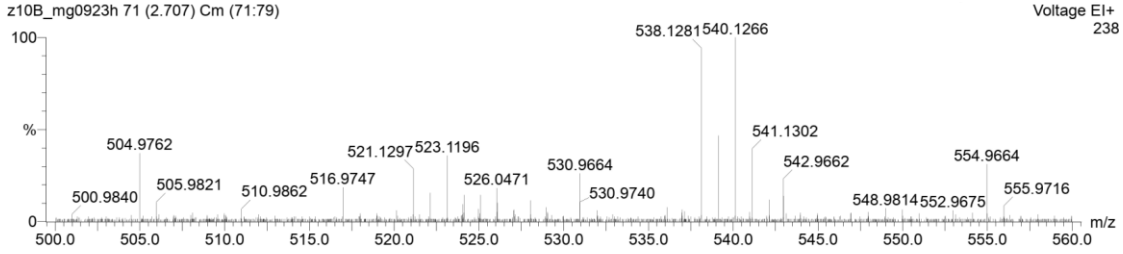


| | | | | | | |
|---|---|---|---|---|---|---|
| Minimum: | | | | -1.5 | | |
| Maximum: | | 5.0 | 20.0 | 80.0 | | |
| Mass | Calc. Mass | mDa | PPM | DBE | i-FIT | Formula |
| 538.1281 | 538.1256 | 2.5 | 4.6 | 19.0 | 3.7 | C31 H27 N2 O2 Br |

**Figure 20.** HRMS (EI) spectrum of (**5**).

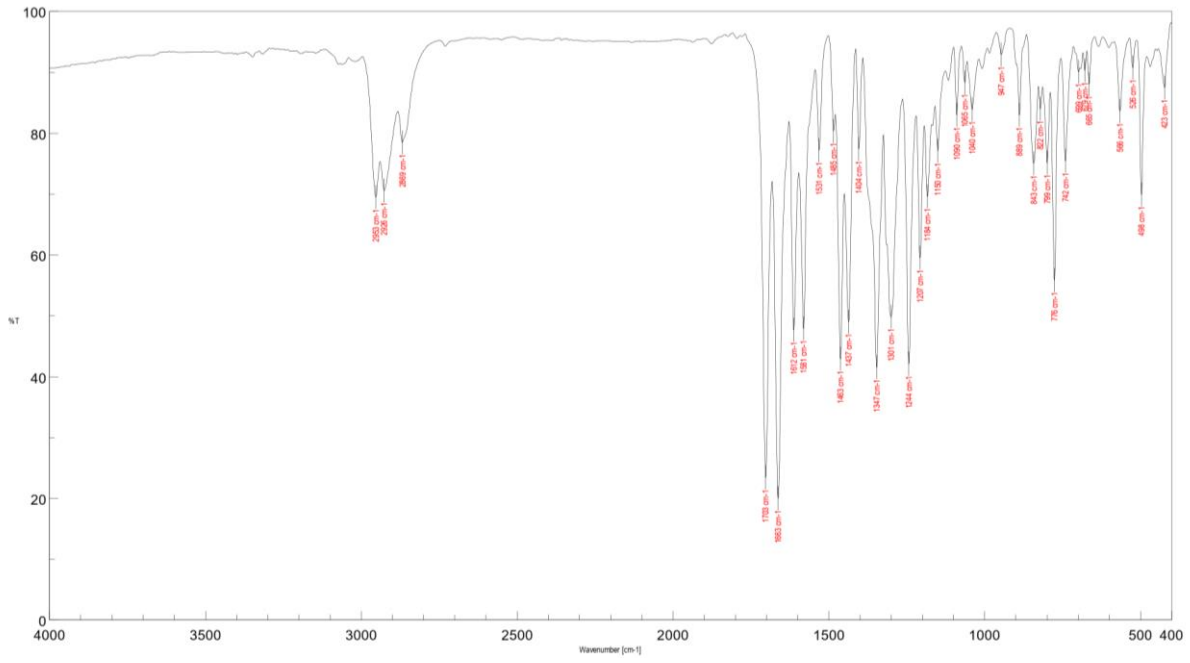


**Figure 21.** IR spectrum of (**5**) in KBr.

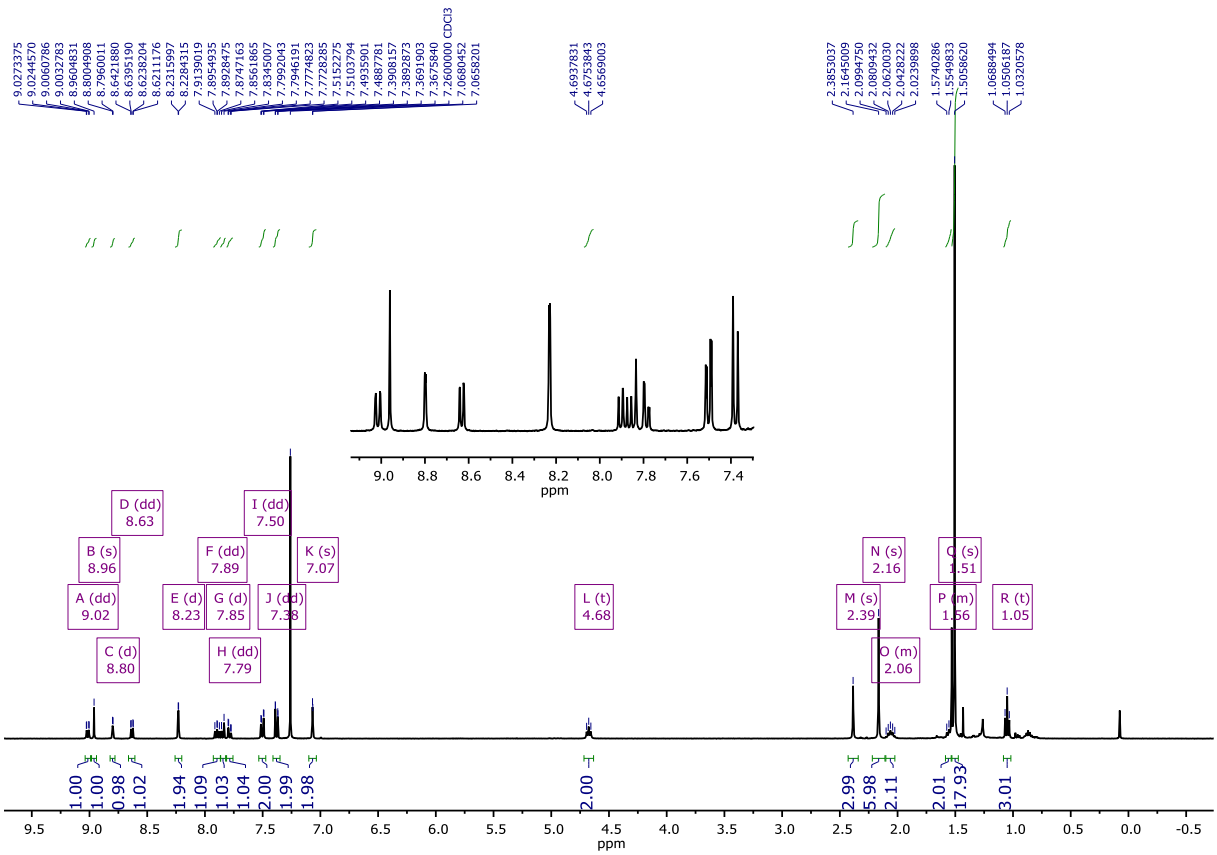


**Figure 22.** $^{1}$H NMR spectrum of (**6a**) (400 MHz, $CDCl_3$).

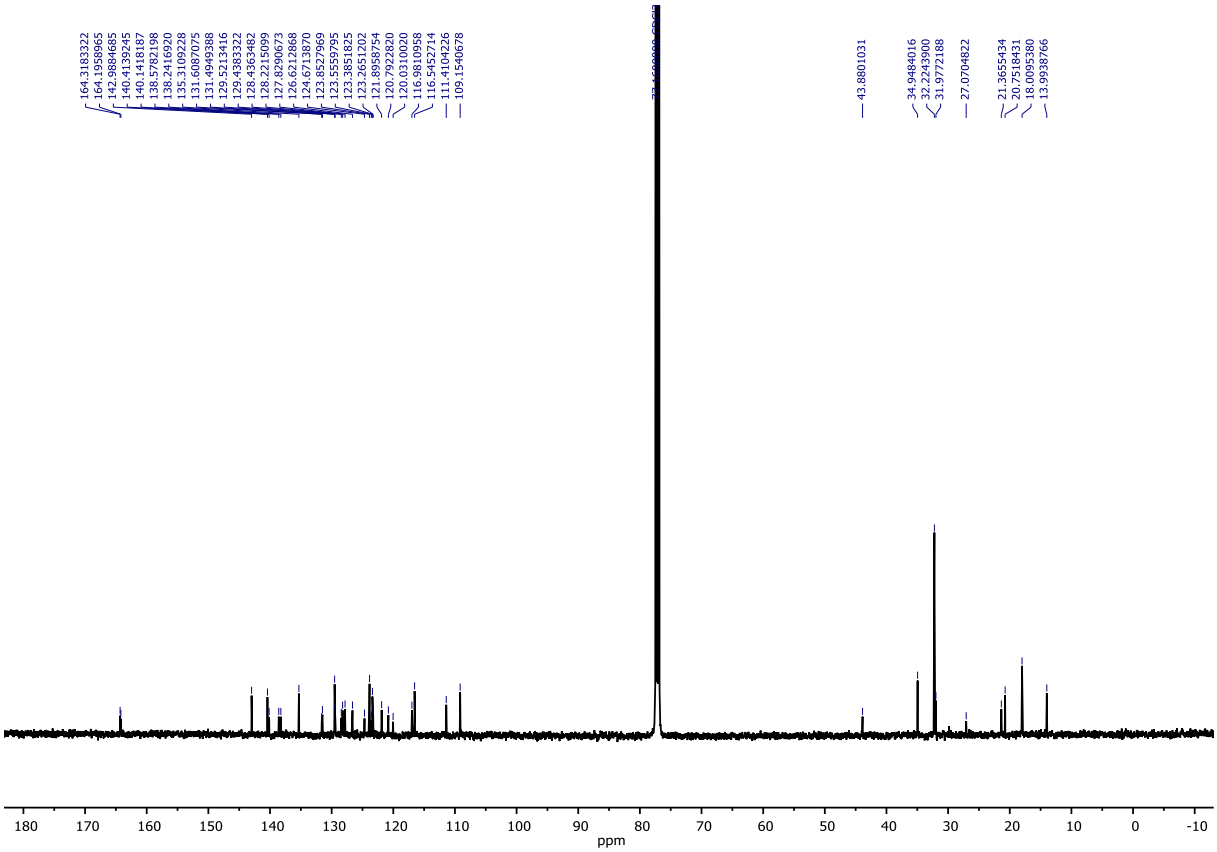


**Figure 23.** $^{13}$C NMR spectrum of (**6a**) (126 MHz, $CDCl_3$).

**Single Mass Analysis**
Tolerance = 20.0 PPM / DBE: min = -1.5, max = 80.0
Selected filters: None

Monoisotopic Mass, Odd and Even Electron Ions
9 formula(e) evaluated with 1 results within limits (up to 50 closest results for each mass)
Elements Used:
C: 0-100 H: 0-200 N: 3-3 O: 2-2

M. Grzelak AUTOSPEC
MMG0152_2-10b
z10B_mg1195h 210 (8.010) Cm (201:210) Voltage EI+ 110

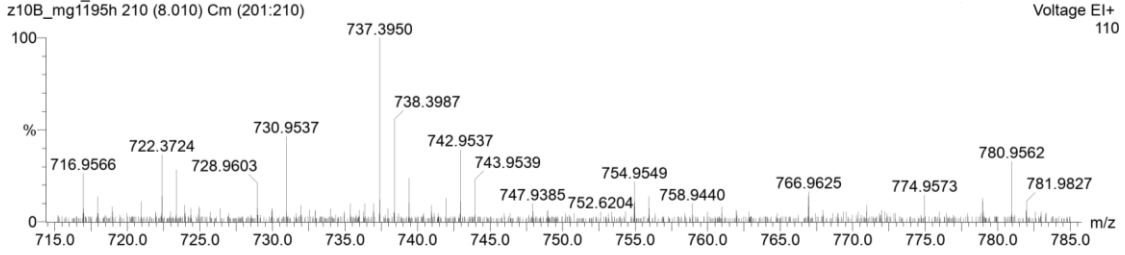


| | | | | | | |
|---|---|---|---|---|---|---|
| Minimum: | | | | -1.5 | | |
| Maximum: | | 5.0 | 20.0 | 80.0 | | |
| Mass | Calc. Mass | mDa | PPM | DBE | i-FIT | Formula |
| 737.3950 | 737.3981 | -3.1 | -4.2 | 28.0 | 1.0 | C51 H51 N3 O2 |

**Figure 24.** HRMS (EI) spectrum of (**6a**).

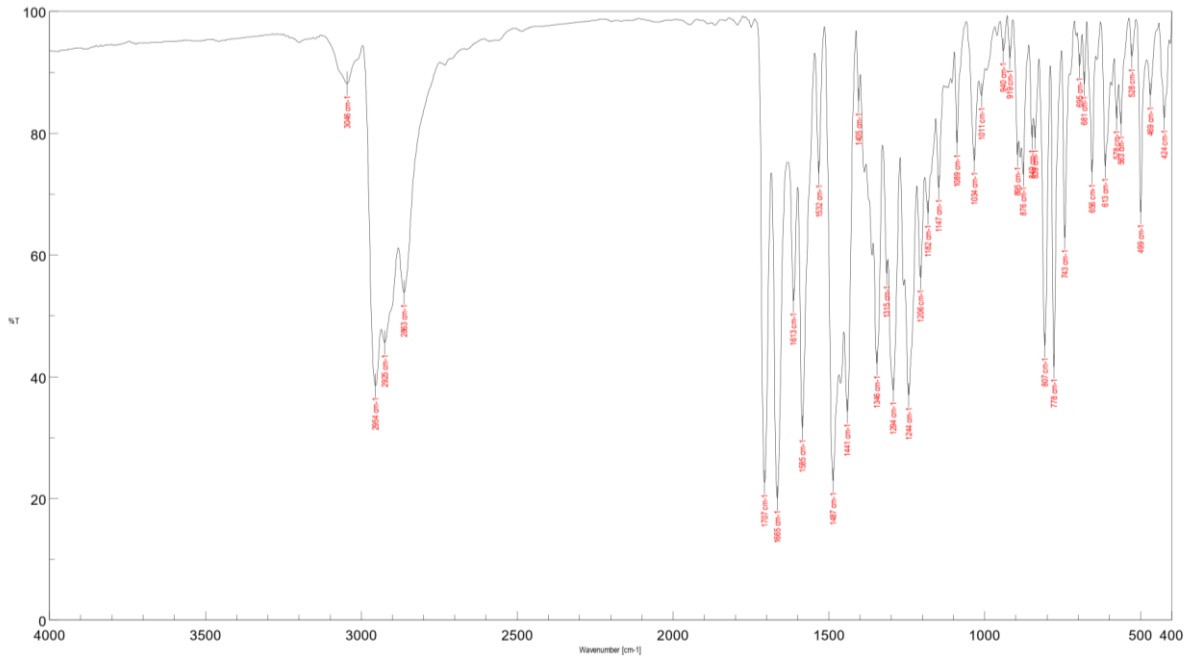


**Figure 25.** IR spectrum of (**6a**) in KBr.

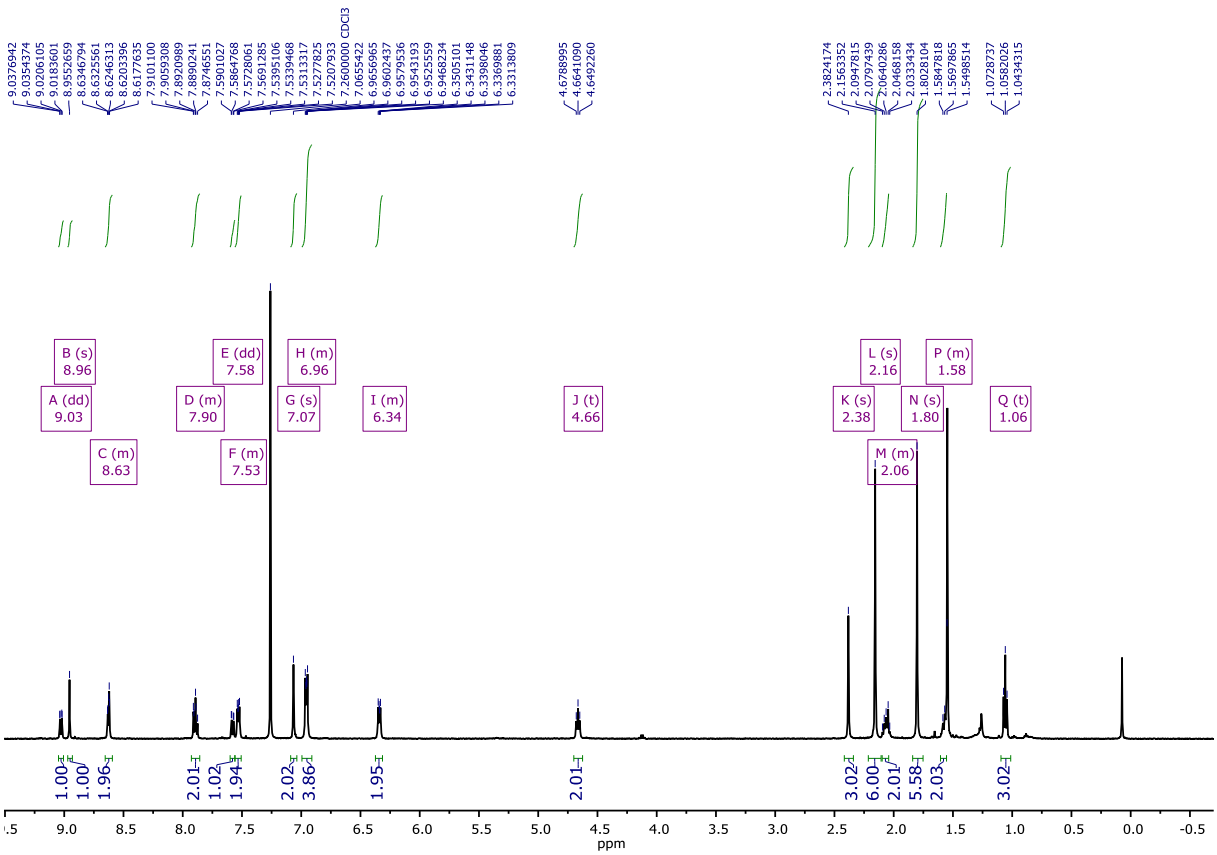


**Figure 26.** $^{1}$H NMR spectrum of (**6b**) (500 MHz, $CDCl_3$).

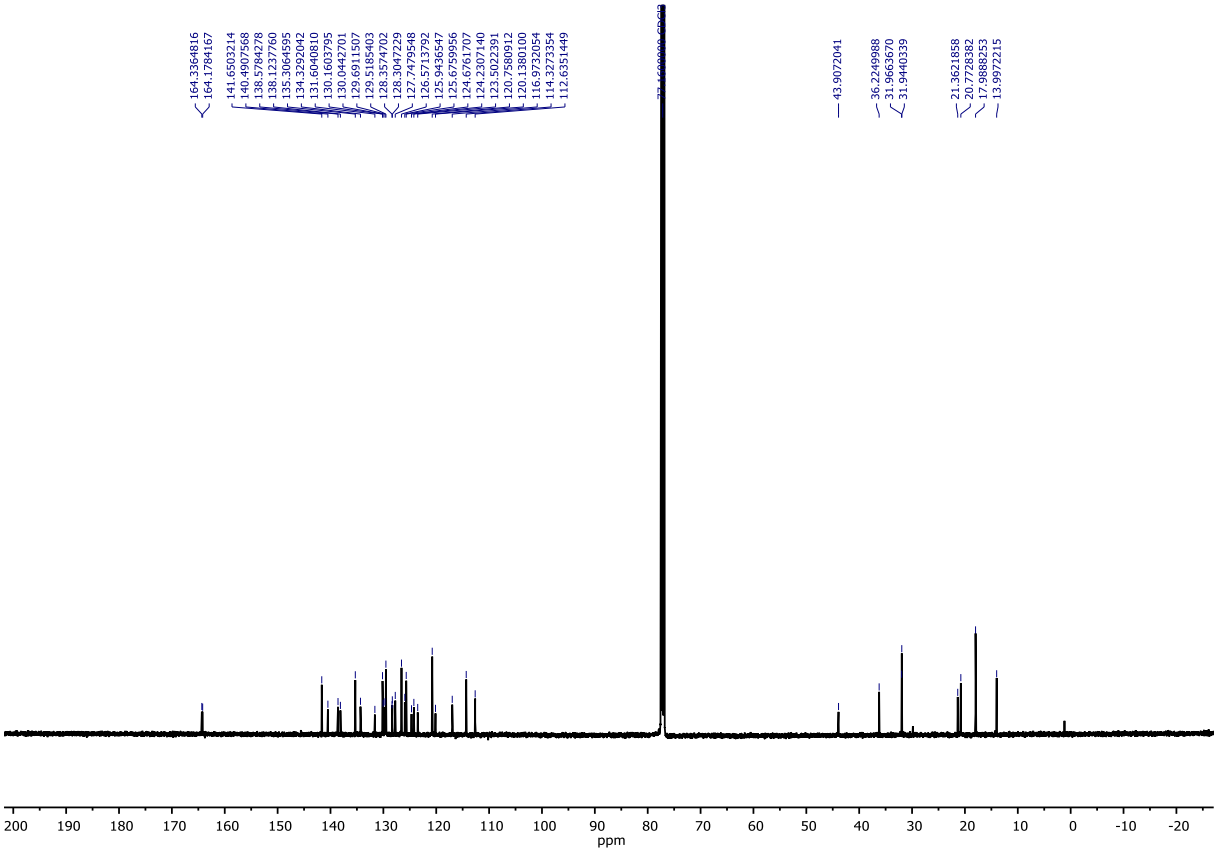


**Figure 27.** $^{13}$C NMR spectrum of (**6b**) (126 MHz, $CDCl_3$).

**Single Mass Analysis**
Tolerance = 20.0 PPM / DBE: min = -1.5, max = 80.0
Selected filters: None

Monoisotopic Mass, Odd and Even Electron Ions
8 formula(e) evaluated with 1 results within limits (up to 50 closest results for each mass)
Elements Used:
C: 0-100 H: 0-200 N: 3-3 O: 2-2

M. Grzelak AUTOSPEC
MMG0153-10b
z10B_mg1194h 159 (6.063) Cm (141:159) Voltage EI+ 441

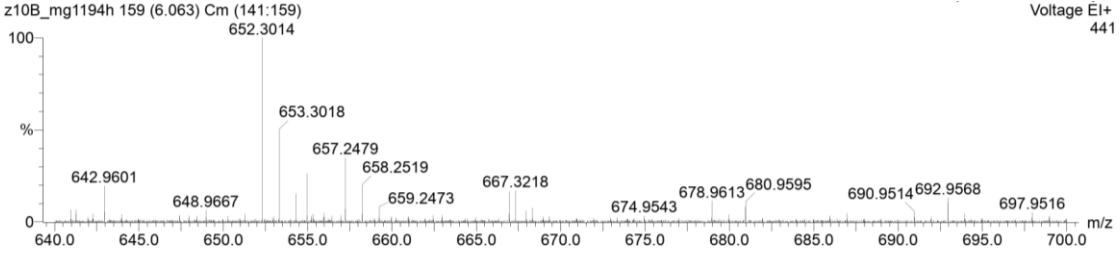


| | | | | | | |
|---|---|---|---|---|---|---|
| Minimum: | | | | -1.5 | | |
| Maximum: | | 5.0 | 20.0 | 80.0 | | |
| Mass | Calc. Mass | mDa | PPM | DBE | i-FIT | Formula |
| 667.3218 | 667.3199 | 1.9 | 2.8 | 28.0 | 0.8 | C46 H41 N3 O2 |

**Figure 28.** HRMS (EI) spectrum of (**6b**).

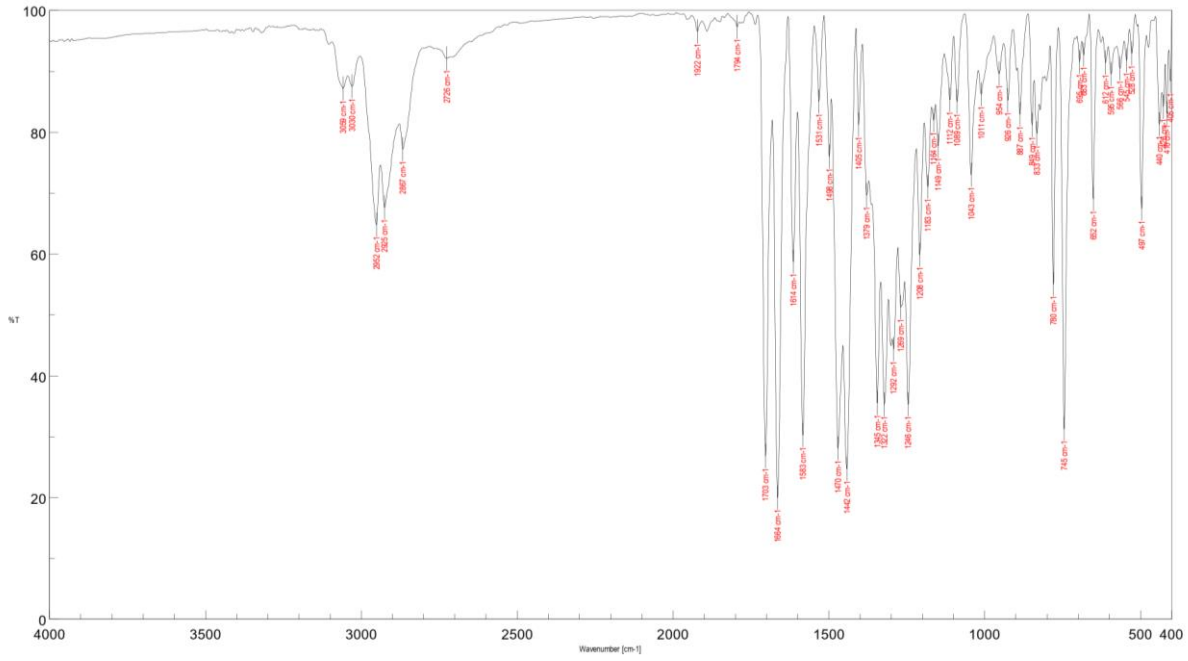


**Figure 29.** IR spectrum of (**6b**) in KBr.

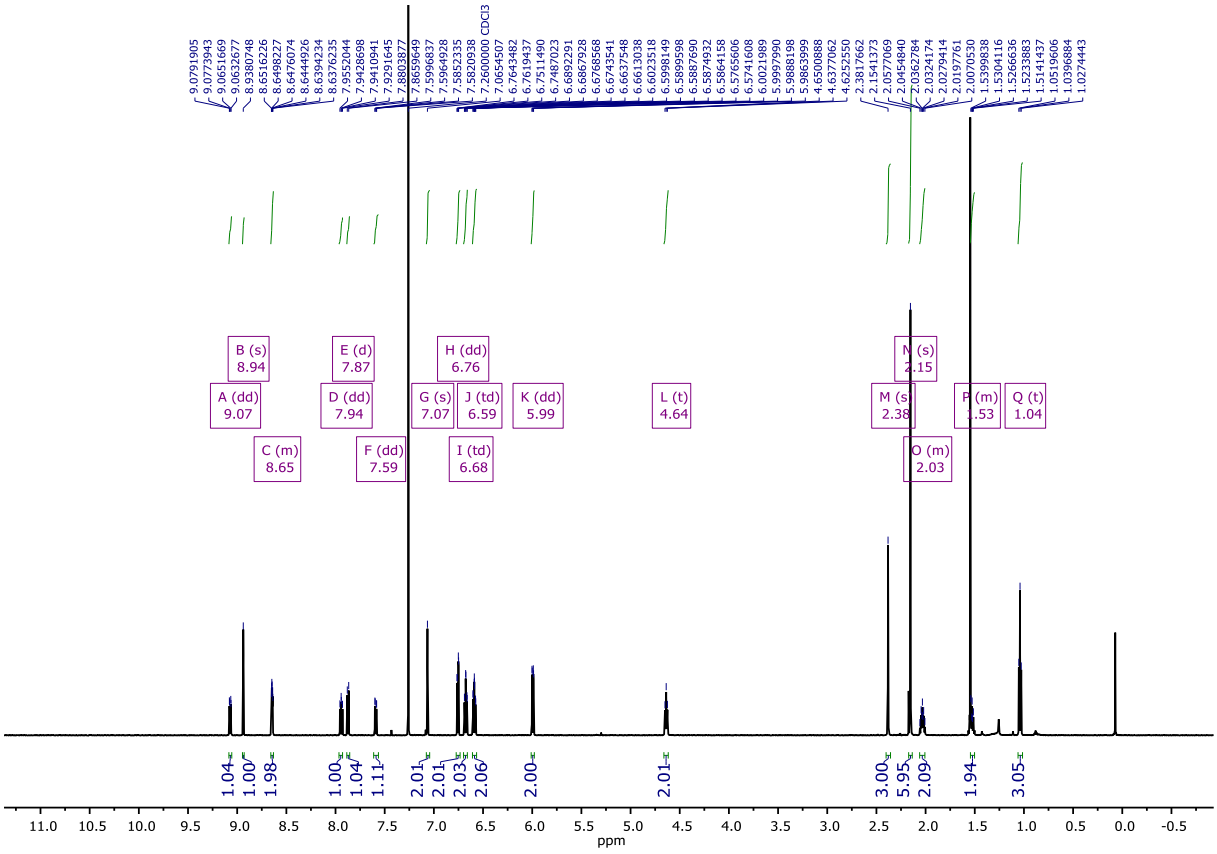


**Figure 30.** $^{1}$H NMR spectrum of (**6c**) (600 MHz, $CDCl_3$).

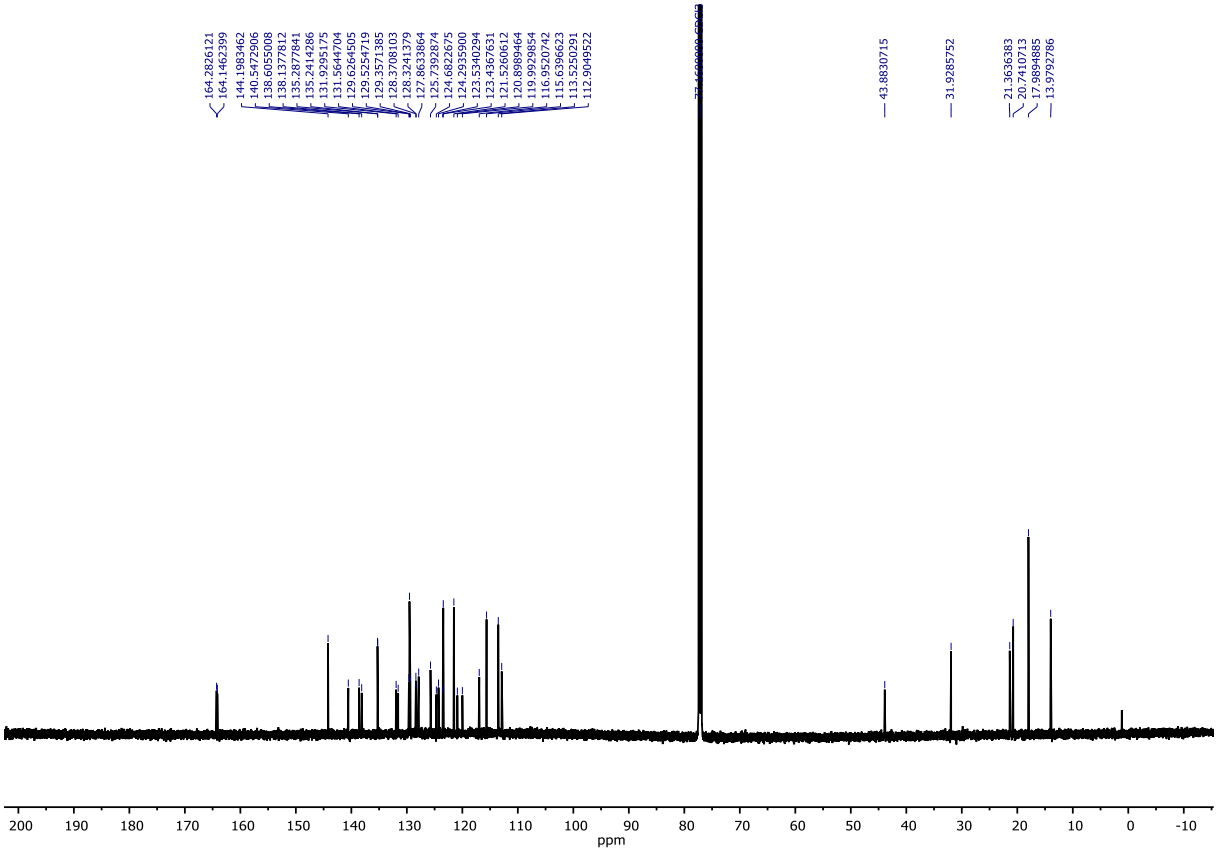


**Figure 31.** $^{13}$C NMR spectrum of (**6c**) (151 MHz, $CDCl3_3$).

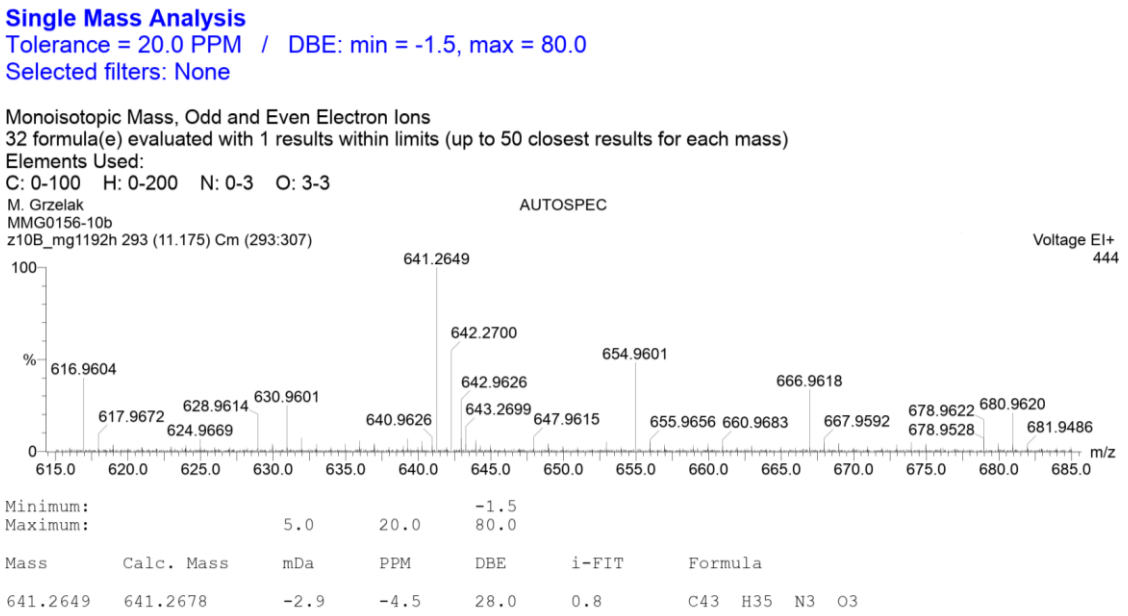


**Figure 32.** HRMS (EI) spectrum of (**6c**).

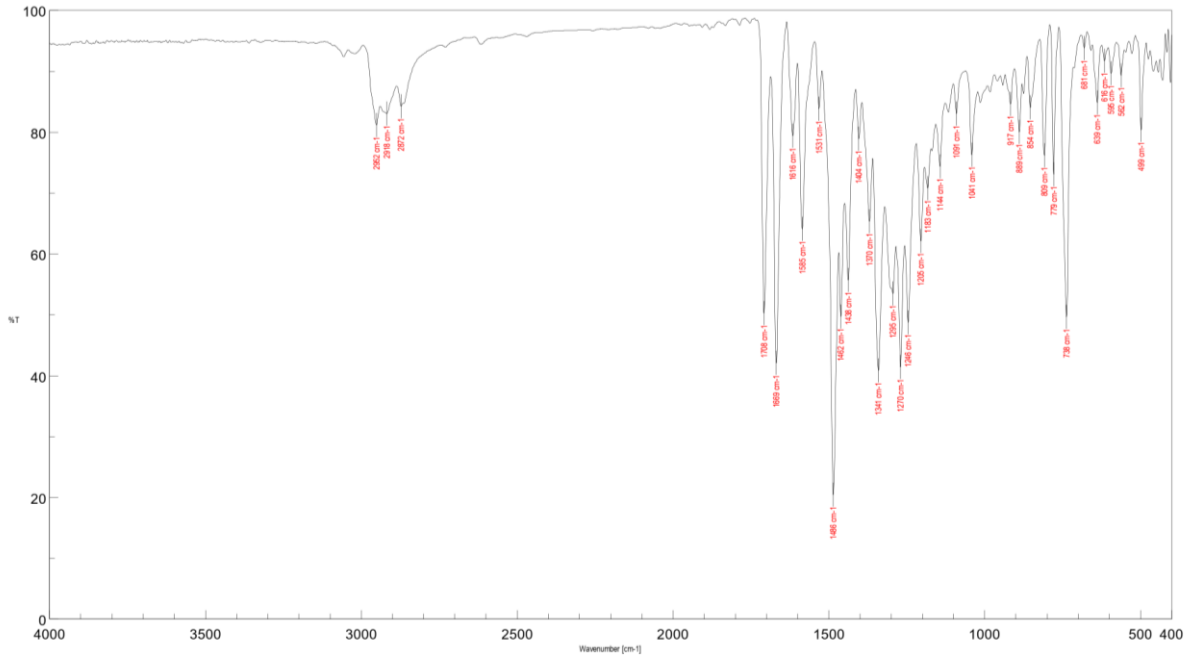


**Figure 33.** IR spectrum of (**6c**) in KBr.

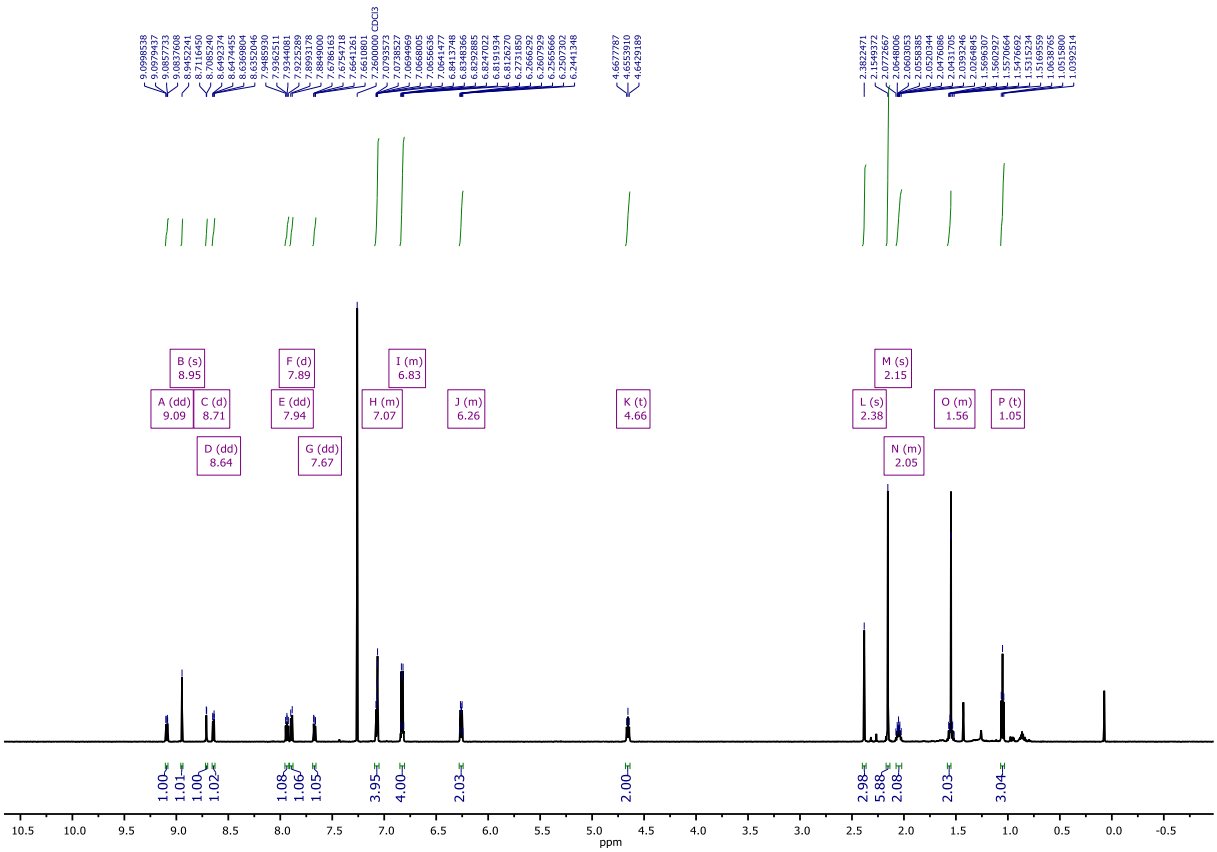


**Figure 34.** $^{1}$H NMR spectrum of (**6d**) (600 MHz, $CDCl_3$).

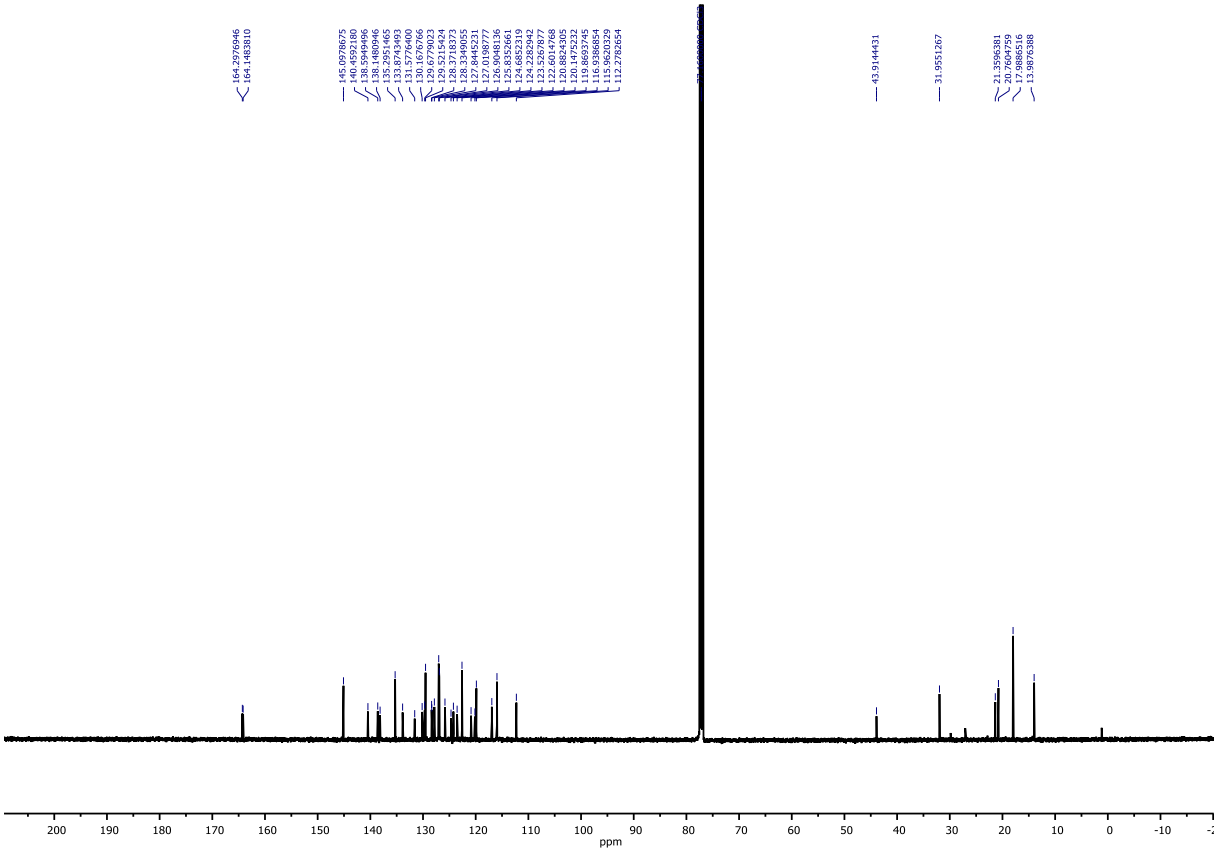


**Figure 35.** $^{13}$C NMR spectrum of (**6d**) (126 MHz, $CDCl_3$).

**Single Mass Analysis**
Tolerance = 20.0 PPM / DBE: min = -1.5, max = 80.0
Selected filters: None

Monoisotopic Mass, Odd and Even Electron Ions
8 formula(e) evaluated with 1 results within limits (up to 50 closest results for each mass)
Elements Used:
C: 0-100 H: 0-200 N: 3-3 O: 2-2 S: 1-1

M. Grzelak AUTOSPEC
MMG0157-10b
z10B_mg1193h 199 (7.590) Cm (199:212)
Voltage EI+
502

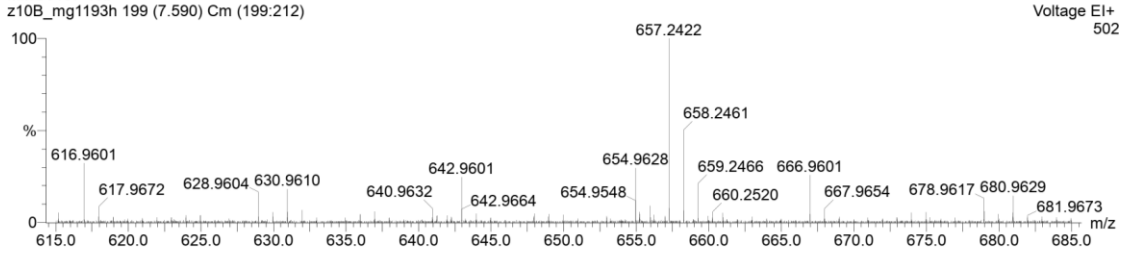


| | | | | | | |
|---|---|---|---|---|---|---|
| Minimum: | | | | -1.5 | | |
| Maximum: | | 5.0 | 20.0 | 80.0 | | |
| Mass | Calc. Mass | mDa | PPM | DBE | i-FIT | Formula |
| 657.2422 | 657.2450 | -2.8 | -4.3 | 28.0 | 1.6 | C43 H35 N3 O2 S |

**Figure 36.** HRMS (EI) spectrum of (**6d**).

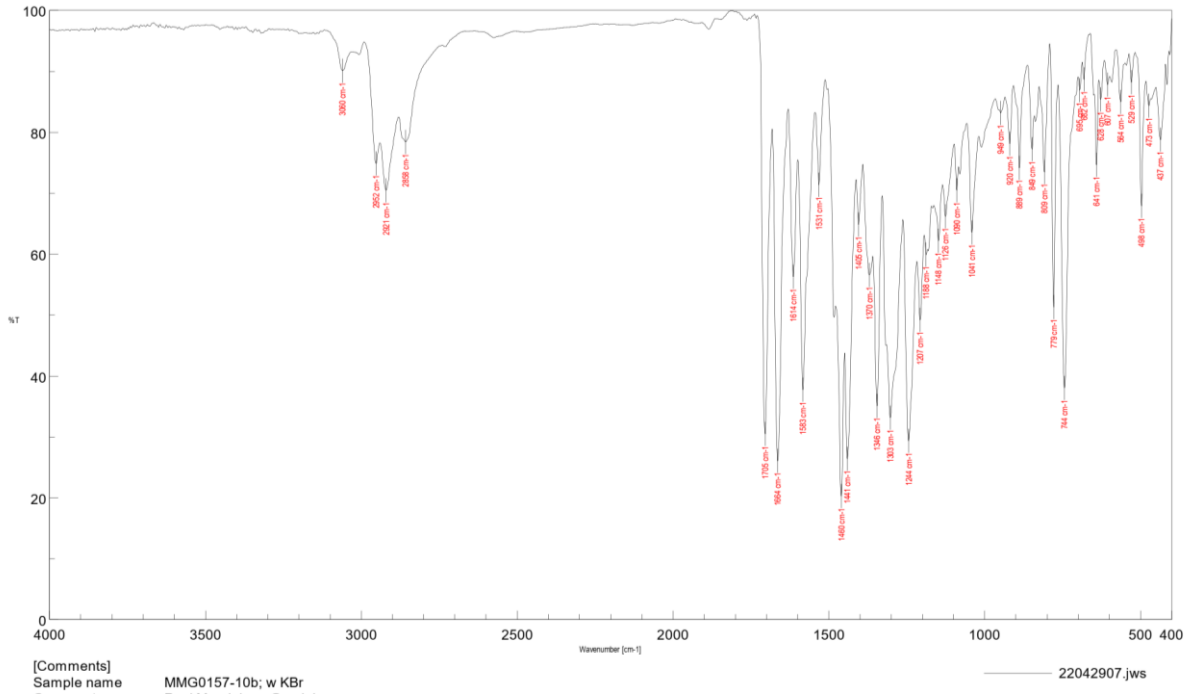


**Figure 37.** IR spectrum of (**6d**) in KBr.

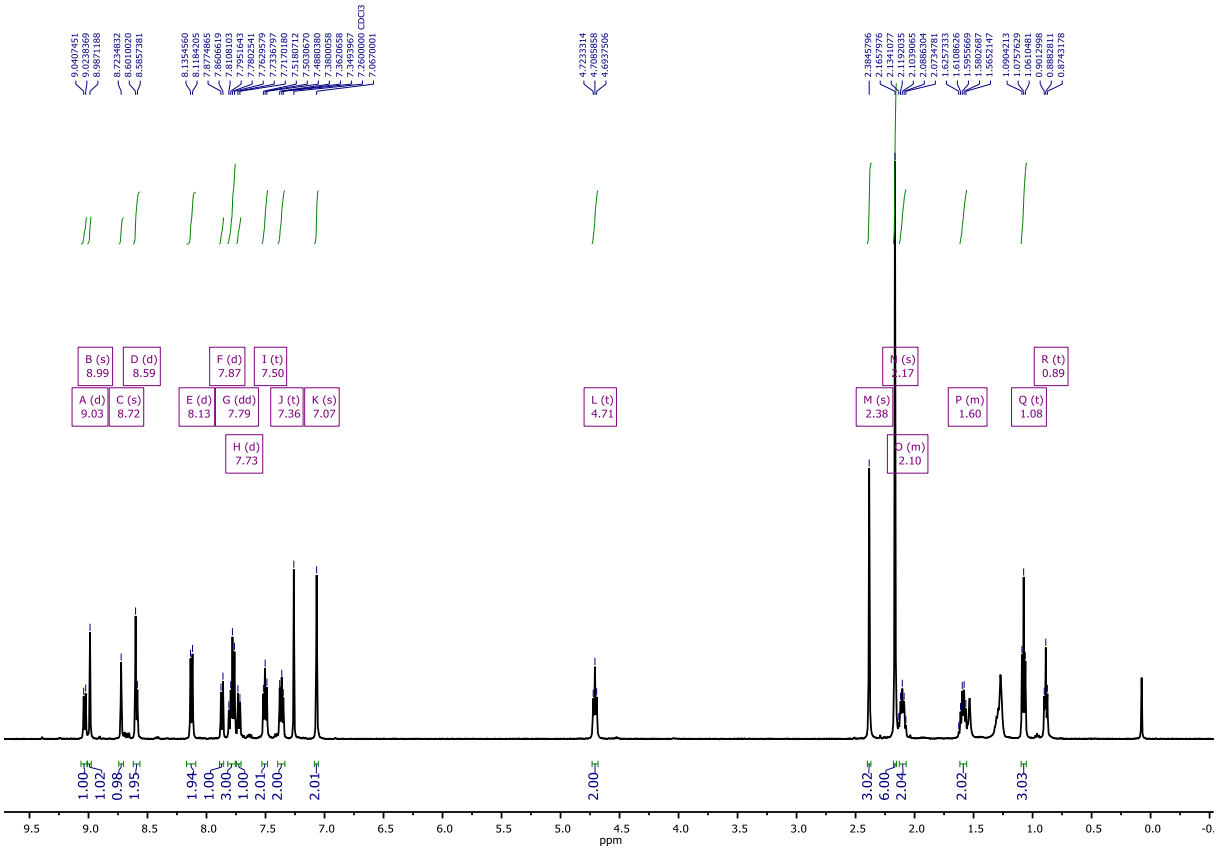


**Figure 38.** $^{1}$H NMR spectrum of (**7a**) (500 MHz, $CDCl_3$).

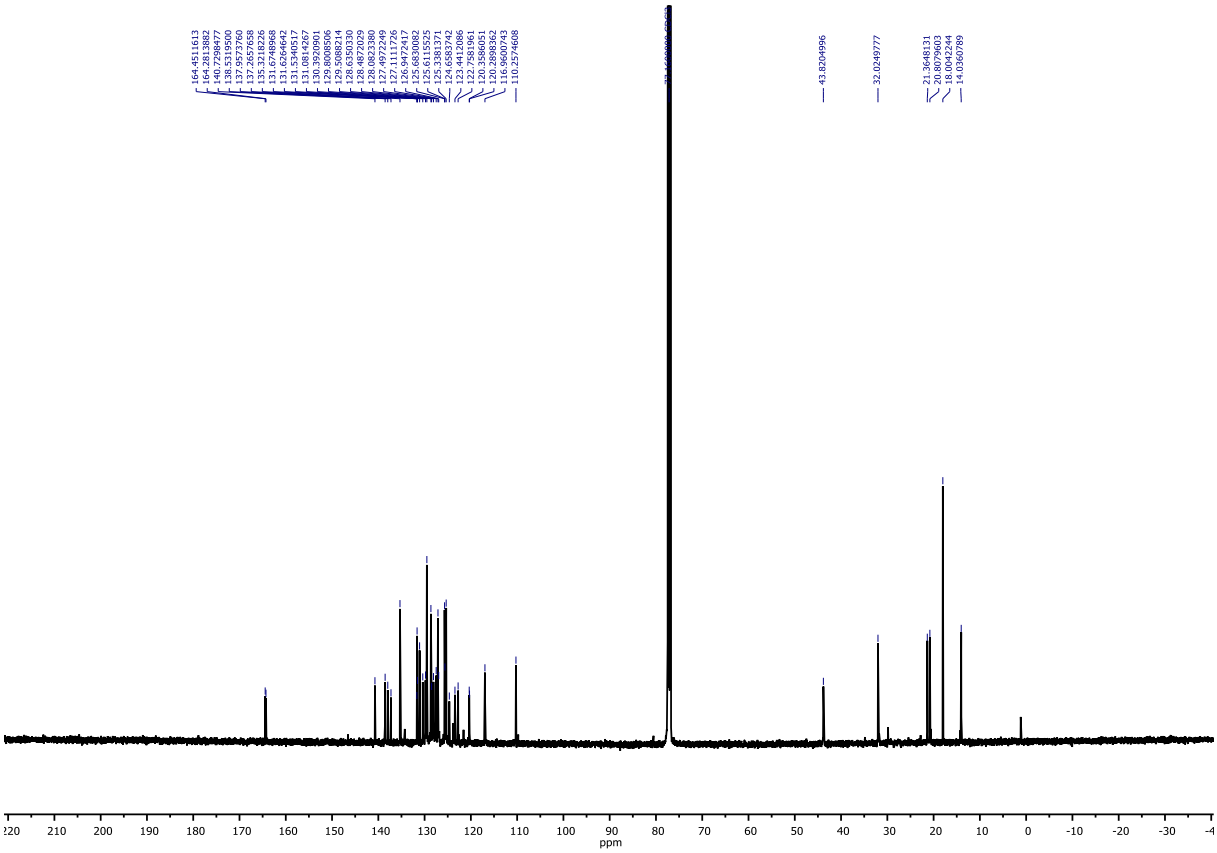


**Figure 39.** $^{13}$C NMR spectrum of (**7a**) (126 MHz, $CDCl_3$).

**Single Mass Analysis**
Tolerance = 20.0 PPM / DBE: min = -1.5, max = 150.0
Selected filters: None

Monoisotopic Mass, Odd and Even Electron Ions
73 formula(e) evaluated with 3 results within limits (up to 50 best isotopic matches for each mass)
Elements Used:
C: 0-100 H: 0-200 N: 0-2 O: 0-2

M. Grzelak
MMG0250-10b
z10B_mg0397h 60 (2.288) Cm (60:77)

AUTOSPEC

06-Mar-2023 17:32:59
Operator: Klara Nestorowicz
Voltage EI+
89

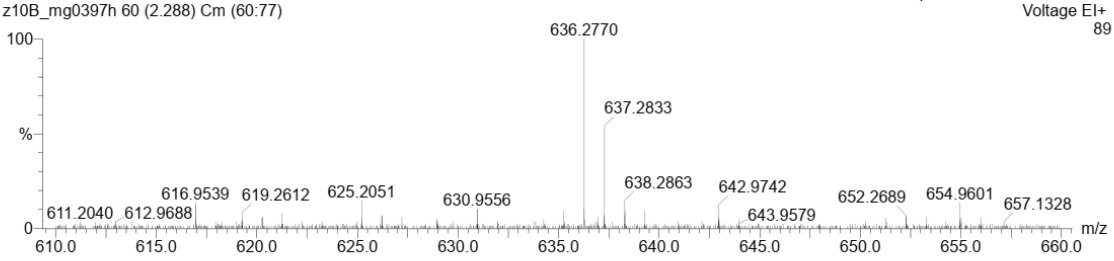


| | | | | | | |
|---|---|---|---|---|---|---|
| Minimum: | | | | -1.5 | | |
| Maximum: | | 5.0 | 20.0 | 150.0 | | |
| Mass | Calc. Mass | mDa | PPM | DBE | i-FIT | Formula |
| 636.2770 | 636.2777 | -0.7 | -1.1 | 29.0 | 0.1 | C45 H36 N2 O2 |

**Figure 40**. HRMS (EI) spectrum of **(7a)**.

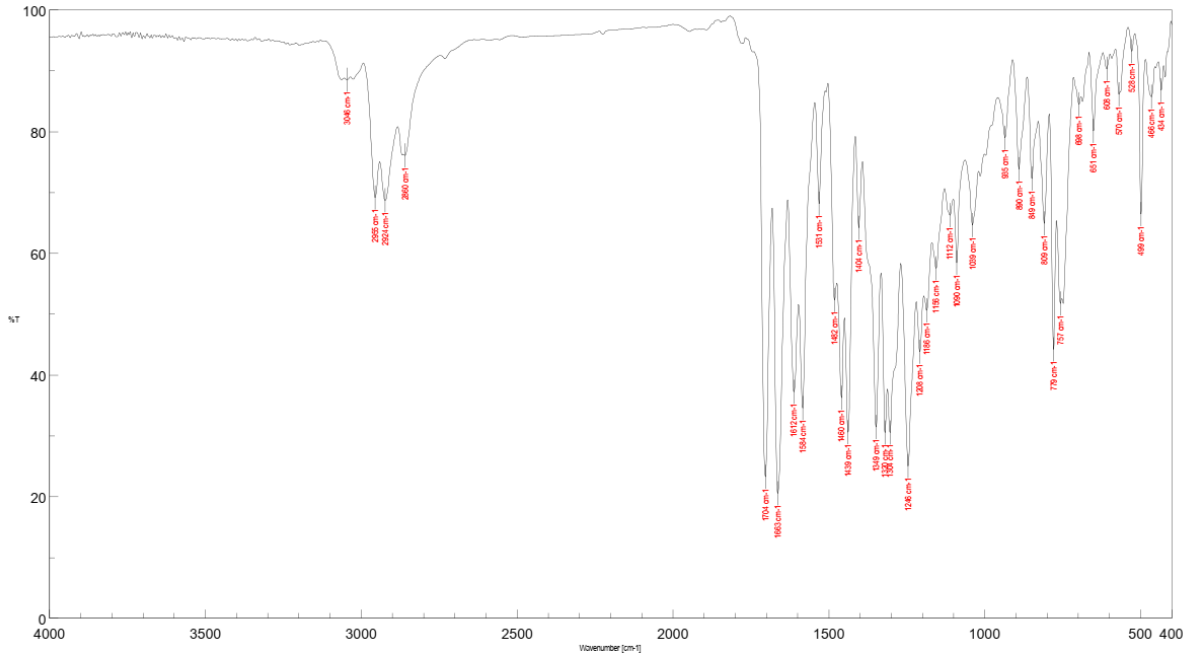


**Figure 41.** IR spectrum of (**7a**) in KBr.

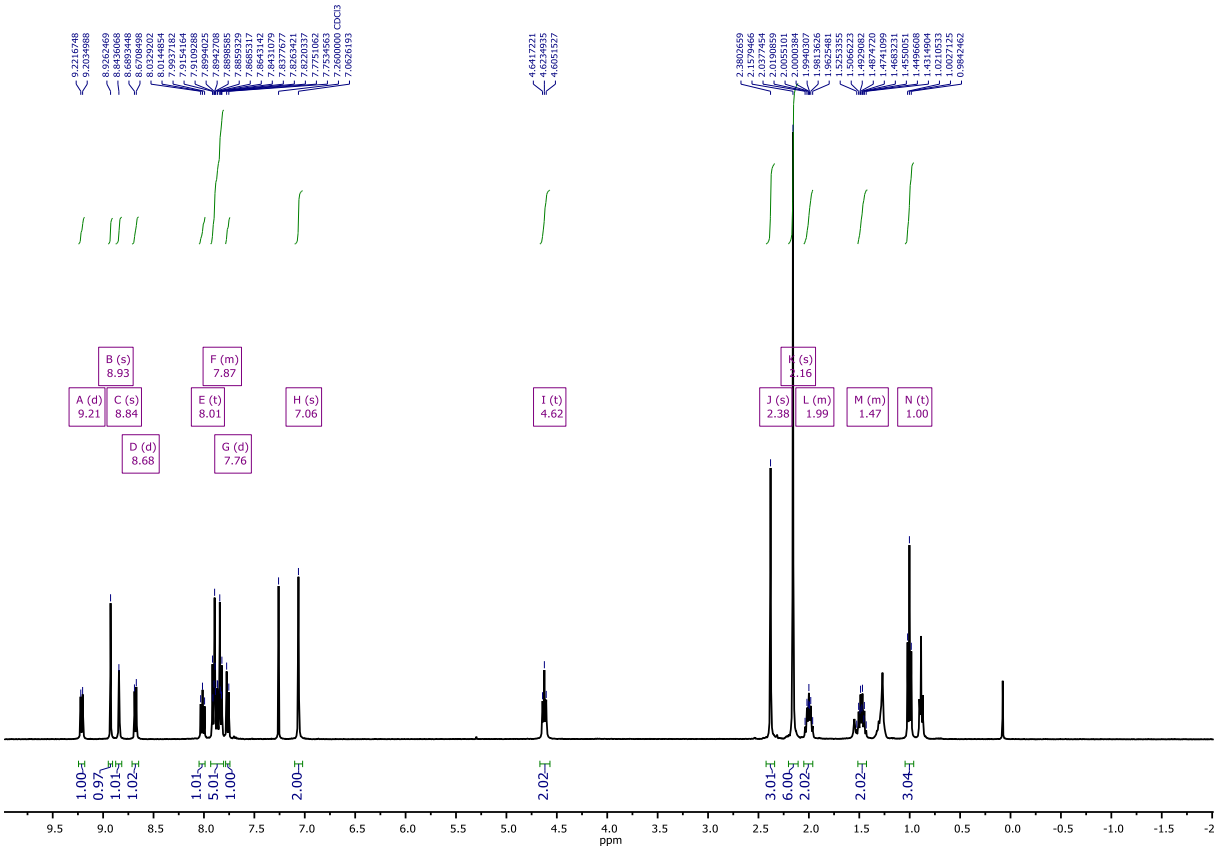


**Figure 42.** $^{1}$H NMR spectrum of (**7b**) (400 MHz, $CDCl_3$).

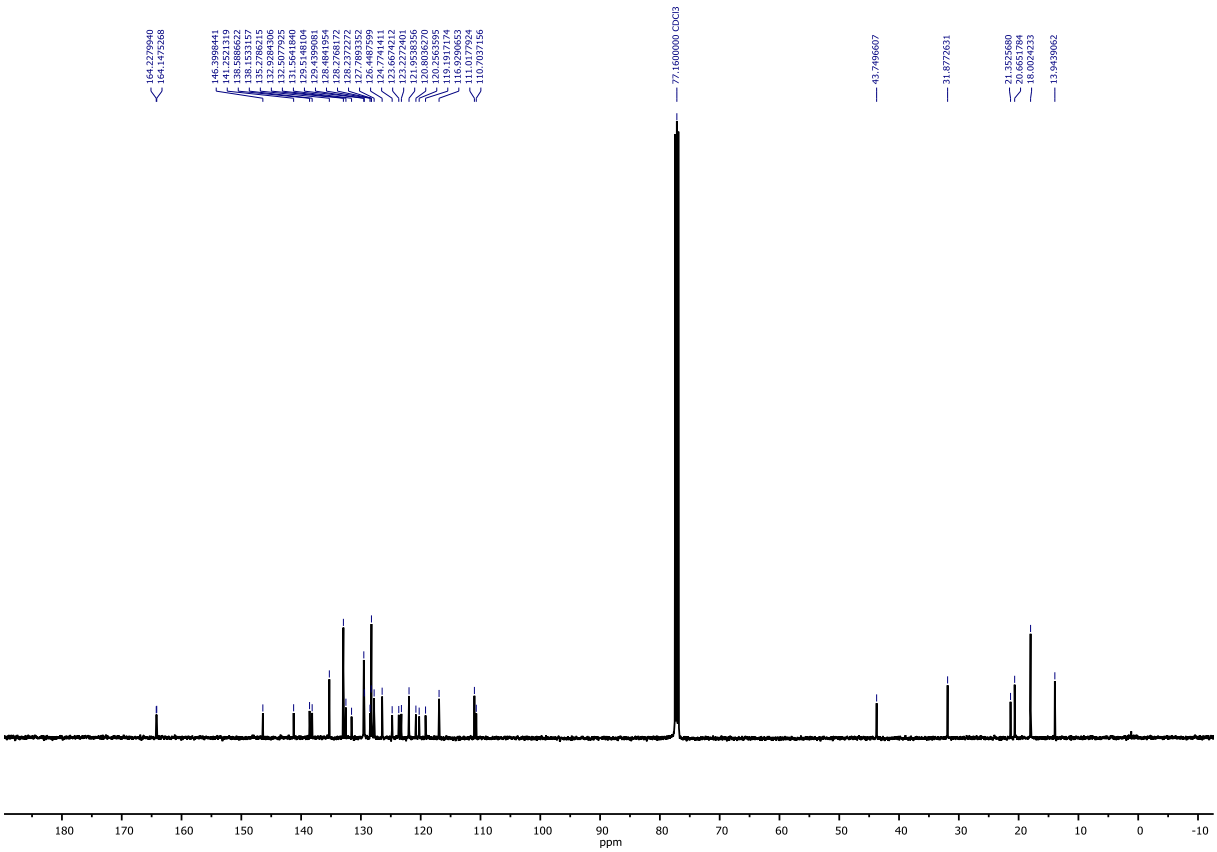


**Figure 43.** $^{13}$C NMR spectrum of (**7b**) (126 MHz, $CDCl_3$).

**Single Mass Analysis**
Tolerance = 20.0 PPM / DBE: min = -1.5, max = 150.0
Selected filters: None

Monoisotopic Mass, Odd and Even Electron Ions
49 formula(e) evaluated with 1 results within limits (up to 50 best isotopic matches for each mass)
Elements Used:
C: 0-100 H: 0-200 N: 3-3 O: 0-6

M. Grzelak
MMG0249-10b
z10B_mg0395h 90 (3.432) Cm (90:99)

AUTOSPEC

06-Mar-2023 17:11:51
Operator: Klara Nestorowicz
Voltage EI+
128

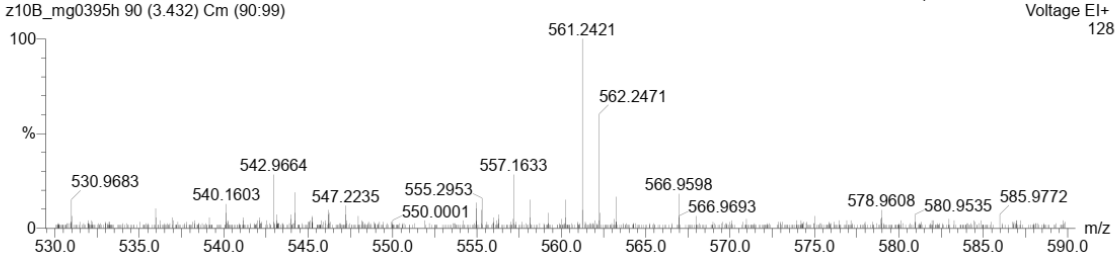


| | | | | | | |
|---|---|---|---|---|---|---|
| Minimum: | | | | -1.5 | | |
| Maximum: | | 5.0 | 20.0 | 150.0 | | |
| Mass | Calc. Mass | mDa | PPM | DBE | i-FIT | Formula |
| 561.2421 | 561.2416 | 0.5 | 0.9 | 25.0 | 3.4 | C38 H31 N3 O2 |

**Figure 44.** HRMS (EI) spectrum of **(7b)**.

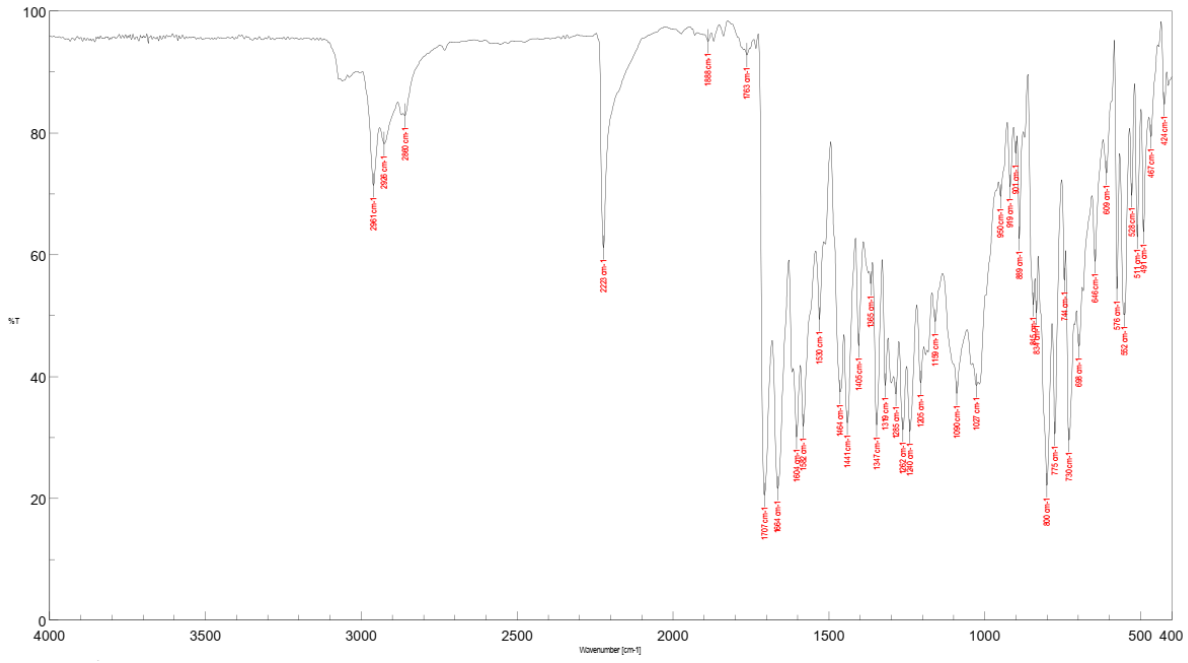


**Figure 45.** IR spectrum of (**7b**) in KBr.

## S4 Crystallography

**Table 1. Data collection and structure refinement parameters for6b, 5, 6c, 7a and 7b.**

| Compound number | 6b NMI-Ind-DMAc | 5 | 6c NMI-Ind-PXZ | 7a NMI-Ind-ANT | 7b NMI-Ind-PhCN |
|---|---|---|---|---|---|
| CCDC Number | | | | | |
| Chemical formula | $C_{50}H_{49}N_3O_4$ | $C_{63}H_{60}Br_2N_4O_7$ | $C_{44}H_{37}Cl_2N_3O_3$ | $C_{45}H_{36}N_2O_2$ | $C_{42}H_{42}N_3O_4$ |
| Formula weight | 755.92 g/mol | 1144.97 g/mol | 726.66 g/mol | 636.76 g/mol | 652.78 g/mol |
| Temperature | 296(2) K | 296(2) K | 100.01(10) | 296(2) K | 296(2) K |
| Wavelength | 1.54178 Å | 1.54178 Å | 1.54184 | 1.54178 Å | 1.54178 Å |
| Crystal size | 0.212 x 0.298 x 0.641 mm | 0.164 x 0.165 x 0.393 mm | 0.15 × 0.14 × 0.06 mm | 0.156 x 0.204 x 0.316 mm | 0.220 x 0.224 x 0.378 mm |
| Crystal habit | orange plate | yellow needle | light orange block | yellow prism | fluorescent yellow plate |
| Crystal system | monoclinic | triclinic | monoclinic | orthorhombic | triclinic |
| Space group | P1 21/c 1 | P -1 | P21/c | Pbca | P -1 |
| Unit cell dimensions | a = 16.6094(6) Å<br>α = 90°<br>b = 9.5173(3) Å<br>β = 104.757(2)°<br>c = 27.5112(9) Å<br>γ = 90° | a = 12.1492(17) Å<br>α = 84.599(11)°<br>b = 15.494(2) Å<br>β = 75.061(10)°<br>c = 15.744(3) Å<br>γ = 88.635(10)° | a = 23.9323(4) Å<br>α = 90°<br>b = 11.41330(17) Å<br>β = 97.5023(15) °<br>c = 13.3857(2) Å<br>γ = 90° | a = 11.4231(4) Å<br>α = 90°<br>b = 13.6228(4) Å<br>β = 90°<br>c = 44.3130(18) Å<br>γ = 90° | a = 11.2686(3) Å<br>α = 113.3290(10)°<br>b = 12.7274(3) Å<br>β = 94.2160(10)°<br>c = 13.7006(3) Å<br>γ = 104.5440(10)° |
| Volume | 4205.4(2) $Å^3$ | 2850.8(7) $Å^3$ | 3624.94(10) $Å^3$ | 6895.8(4) $Å^3$ | 1713.09(7) $Å^3$ |
| Z | 4 | 2 | 4 | 8 | 2 |
| Density (calculated) | 1.194 $g/cm^3$ | 1.334 $g/cm^3$ | 1.332 | 1.227 $g/cm^3$ | 1.266 $g/cm^3$ |
| Absorption coefficient | 0.596 $mm^{-1}$ | 2.254 $mm^{-1}$ | 1.974 $mm^{-1}$ | 0.583 $mm^{-1}$ | 0.647 $mm^{-1}$ |

| | | | | | |
|---|---|---|---|---|---|
| **F(000)** | 1608 | 1184 | 1520 | 2688 | 694 |
| **Theta range for data collection** | 2.75 to 68.73° | 2.87 to 62.11° | 3.726 to 73.201 | 1.99 to 52.14° | 3.58 to 68.35° |
| **Index ranges** | -18<=h<=20, -10<=k<=11, -30<=l<=33 | -12<=h<=12, -17<=k<=16, -17<=l<=15 | | -10<=h<=9, -12<=k<=11, -44<=l<=40 | -11<=h<=12, -15<=k<=15, -16<=l<=16 |
| **Reflections collected** | 32567 | 50181 | 21995 | 90340 | 50392 |
| **Independent reflections** | 7120 [R(int) = 0.0717] | 7096 [R(int) = 0.1396] | 7095 [R(int) = 0.0366] | 3357 [R(int) = 0.1769] | 6059 [R(int) = 0.0708] |
| **Goodness-of-fit on $F^2$** | 1.055 | 1.201 | 1.032 | 0.975 | 0.997 |
| **Final R indices** | 4320 data; I>2σ(I)<br>R1 = 0.0698, wR2 = 0.1741<br>all data<br>R1 = 0.1167, wR2 = 0.2002 | 2963 data; I>2σ(I)<br>R1 = 0.1315, wR2 = 0.3471<br>all data<br>R1 = 0.2850, wR2 = 0.4063 | 5724 data; I>2σ(I)<br>R1 = 0.0423, wR2 = 0.1097<br>all data<br>R1 = 0.0547, wR2 = 0.1179 | 1373 data; I>2σ(I)<br>R1 = 0.0731, wR2 = 0.1410<br>all data<br>R1 = 0.2581, wR2 = 0.2068 | 3205 data; I>2σ(I)<br>R1 = 0.0679, wR2 = 0.1836<br>all data<br>R1 = 0.1371, wR2 = 0.2253 |
| **Largest diff. peak and hole** | 0.794 and -0.347 eÅ$^{-3}$ | 1.048 and -0.834 eÅ$^{-3}$ | 0.305 and -0.645 eÅ$^{-3}$ | 0.261 and -0.279 eÅ$^{-3}$ | 0.536 and -0.260 eÅ$^{-3}$ |

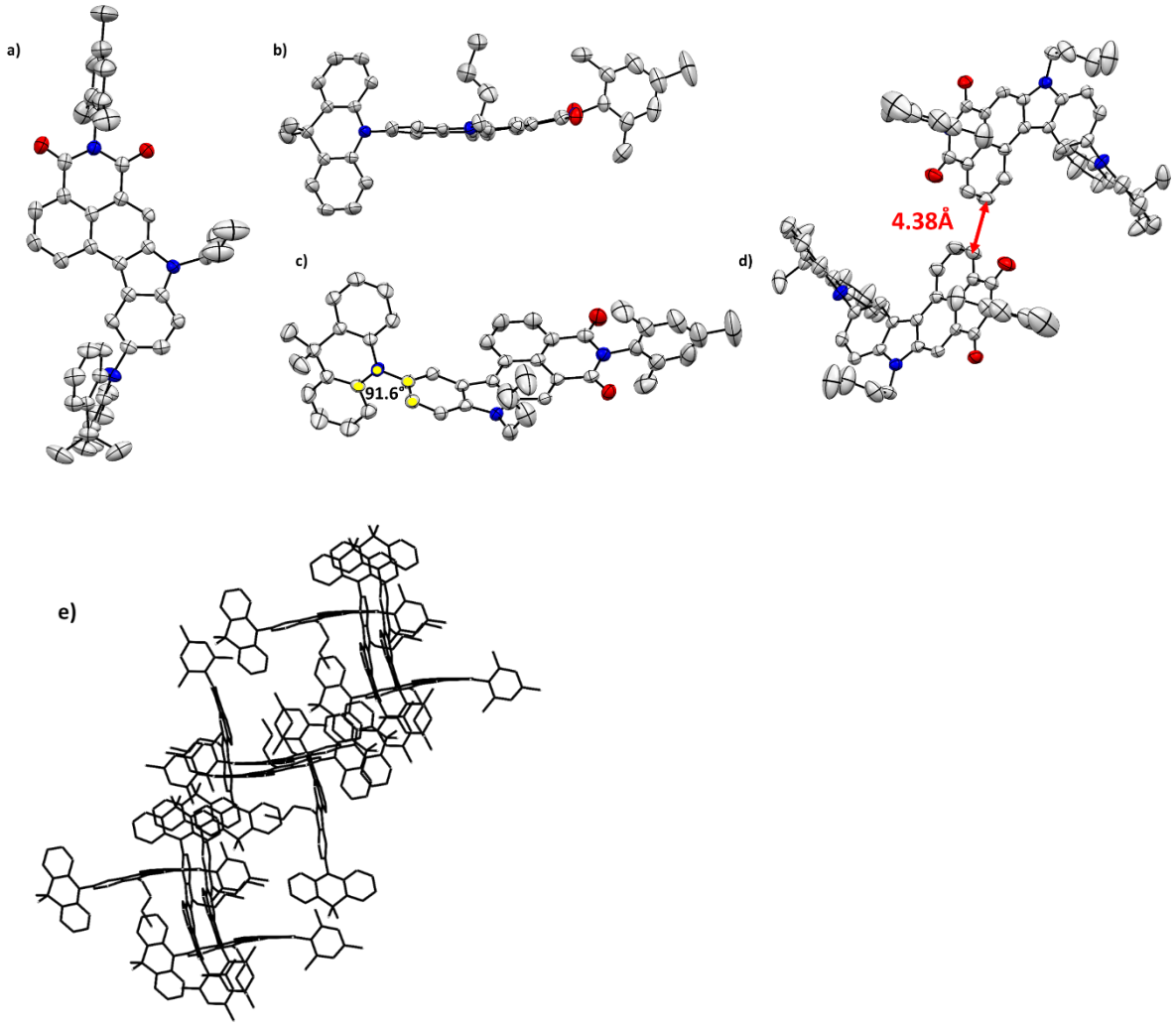


**Figure 46.** Crystallographic structure of 6b NMI-Ind-DMAc, a) Front view, b) side view, c) torsion angle, d) and e) space arrangement. Hydrogen atoms are omitted for the sake of clarity.

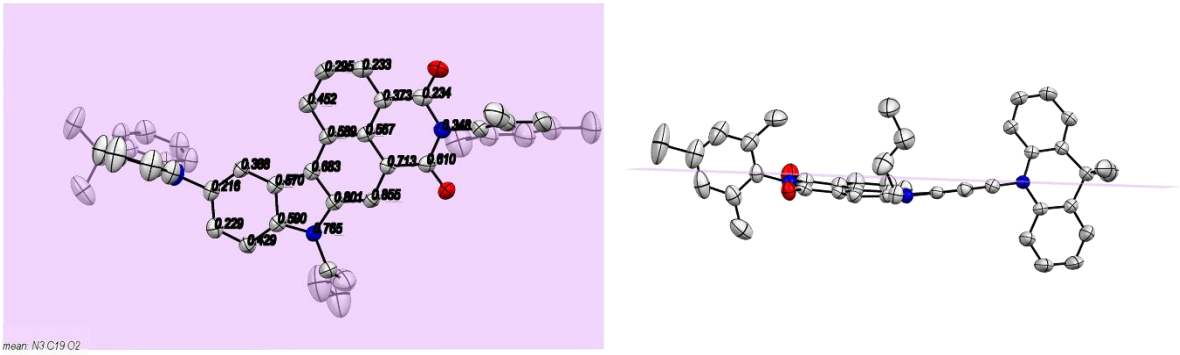


**Figure 47.** Closer view and all distances between atoms in 6b and plane (relative to N3, C19, O2).

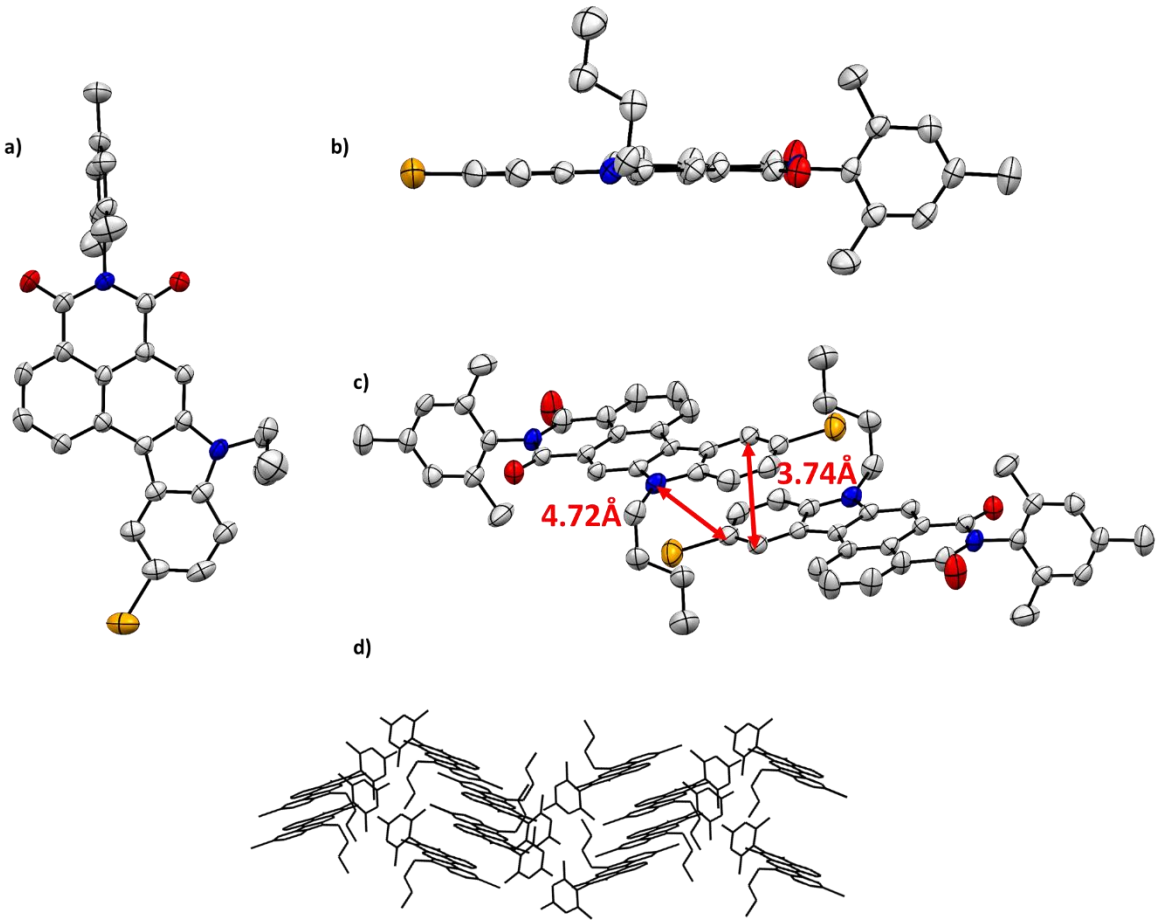


**Figure 48.** Crystallographic structure of 5, a) Front view, b) side view, c) and d) space arrangement. Hydrogen atoms are omitted for the sake of clarity.

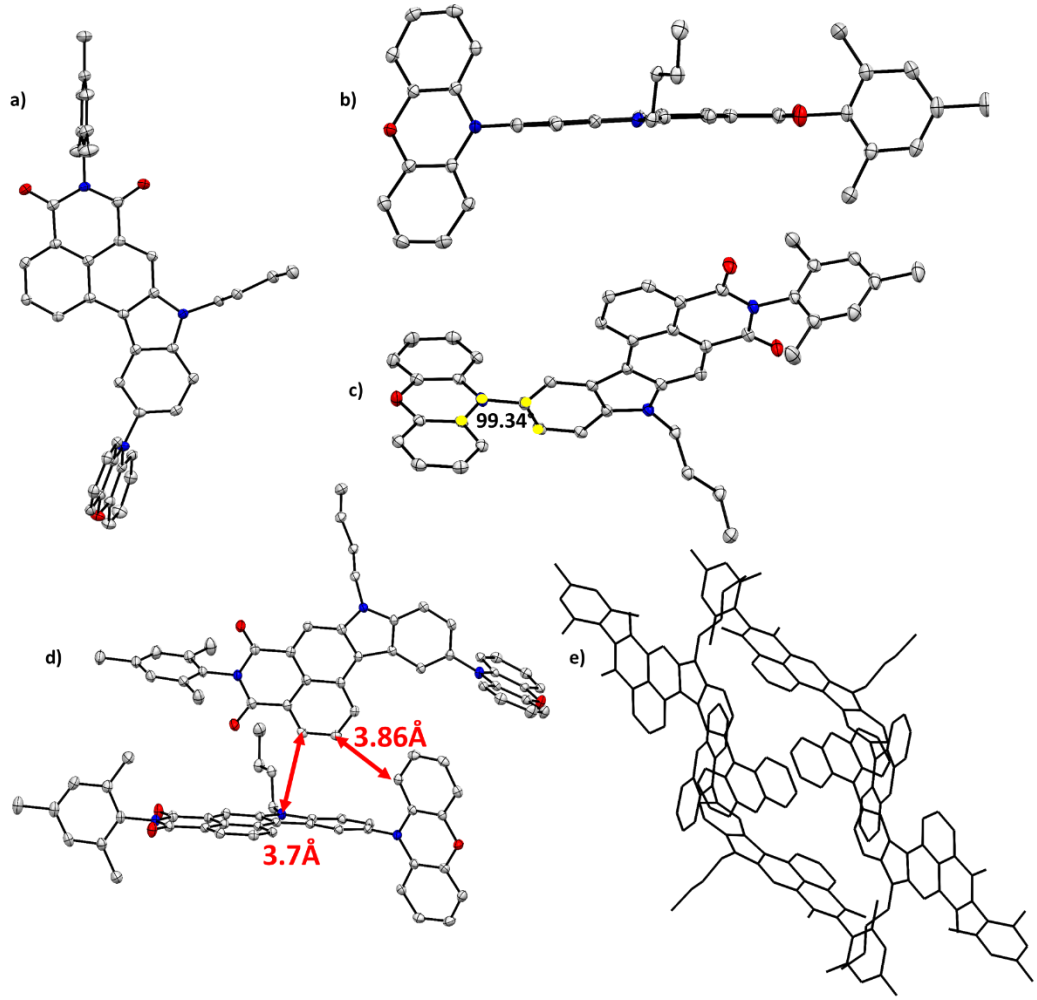


**Figure 49.** Crystallographic structure of 6c NMI-Ind-PXZ, a) Front view, b) side view, c) torsion angle, d) and e) space arrangement. Hydrogen atoms are omitted for the sake of clarity.

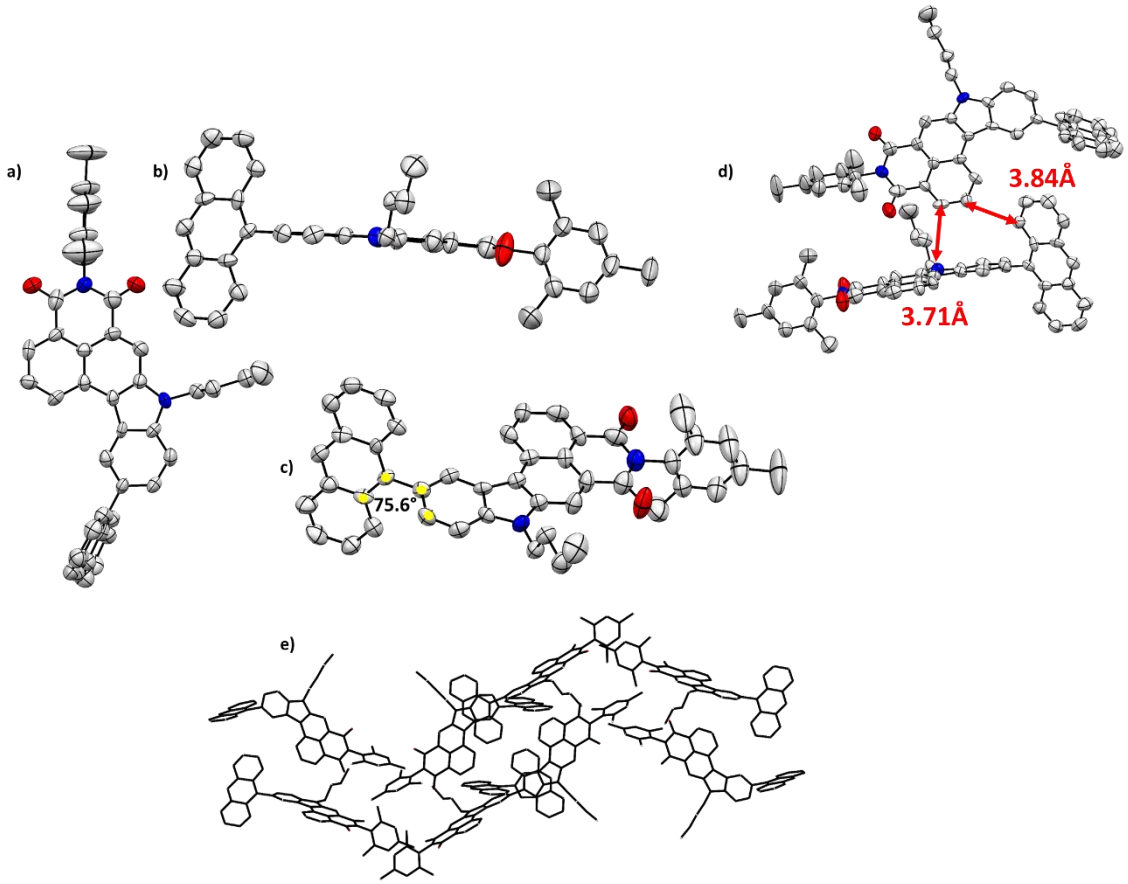


**Figure 50.** Crystallographic structure of 7a NMI-Ind-ANT, a) Front view, b) side view, c) torsion angle, d) and e) space arrangement. Hydrogen atoms are omitted for the sake of clarity.

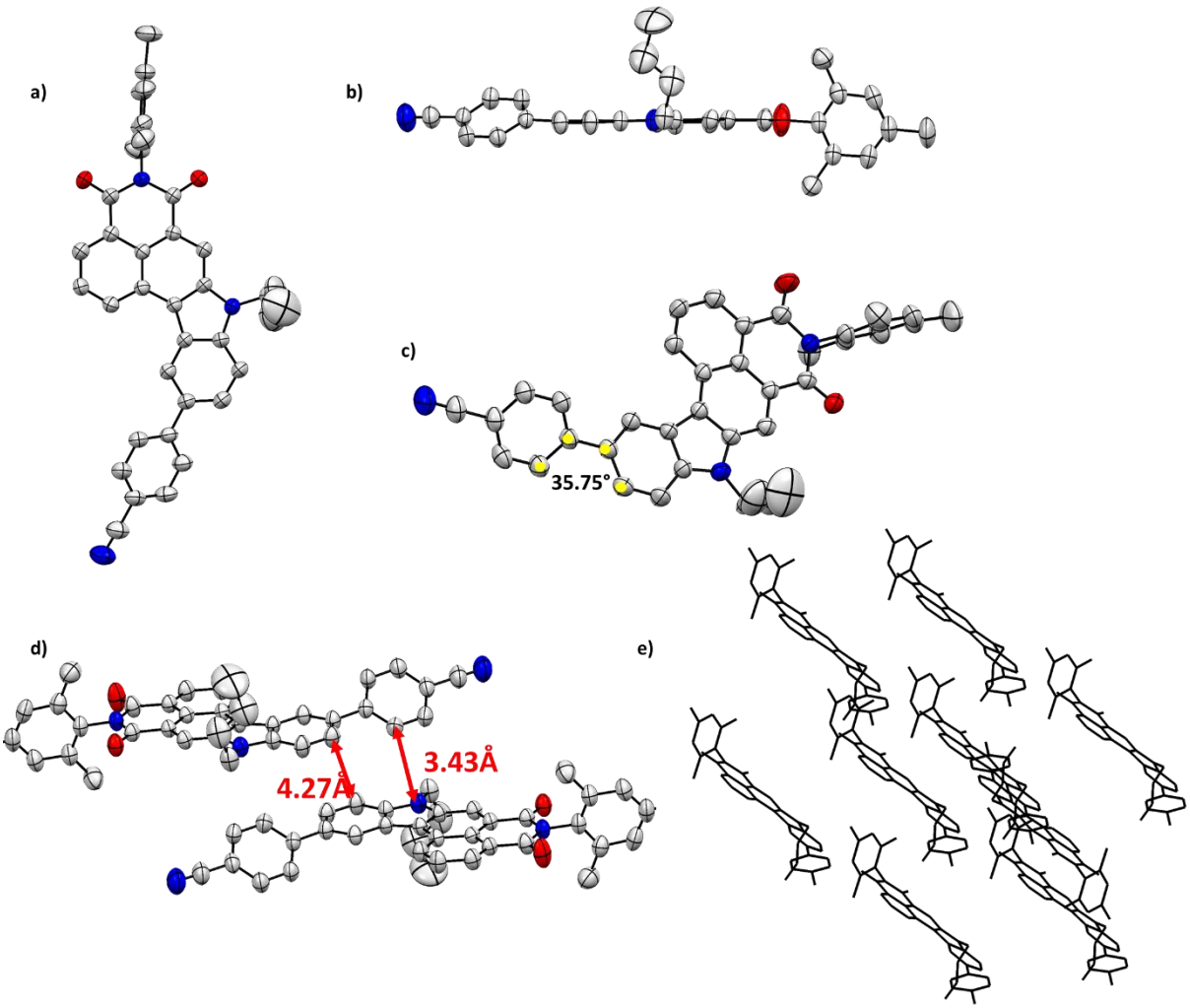


**Figure 51.** Crystallographic structure of **6b** NMI-Ind-PhCN, a) Front view, b) side view, c) torsion angle, d) and e) space arrangement. Hydrogen atoms are omitted for the sake of clarity.

**Table 2. Performance summary of OLEDs with emission peaks from 570 nm to 650 nm.**

| Emitter | Emmiter concentration [wt %] | λ [nm] | $V_{on}$[a] [V] | $EQE_{max}$[b] [%] | $EQE_{100}$[c] [%] | $EQE_{1000}$[d] [%] | $EQE_{10000}$[e] [%] | $L_{max}$ [cd/m²] |
|---|---|---|---|---|---|---|---|---|
| **BFDMAc-PhNAI**[1] | 1.5 | 590 | 3 | 19.8 | 10.6 | 10.4[f] | 4[f] | 2 671 |
| **BTDPAc-PhNAI**[1] | 3 | 601 | 3 | 18.7 | 10.5 | 10.5[f] | 4[f] | 2 537 |
| **BTDMAc-PhNA**[1] | 1.5 | 642 | 4 | 10.1 | 6.4 | 5.5[f] | -[g] | 680 |
| ***T*-DMAC-PPyM-1%**[2] | 1 | 578 | 3.3 | 18.6 | 14.7 | 9.3 | 5[f] | 14 265 |
| ***T*-DMAC-PPyM-3%**[2] | 3 | 586 | 3.3 | 14.4 | 12.6 | 8.4 | 4[f] | 13 553 |
| ***P*-DMAC-BPyM-1%**[2] | 1 | 579 | 3.2 | 26 | 21.7 | 18.3 | 3[f] | 15 754 |
| ***P*-DMAC-BPyM-3%**[2] | 3 | 593 | 3.3 | 21.2 | 20 | 16.2 | 2[f] | 15 505 |
| **PXZ-NA**[3] | 10 | 624 | 3.2 | 13 | 10.3[f] | 9.4[f] | -[g] | -[g] |
| **PTZ-NAI**[3] | 10 | 632 | 3.4 | 11.4 | 10.1[f] | 6[f] | -[g] | -[g] |
| **NAI-DMAC**[4] | 1.5 | 597 | 3 | 23.4 | 13.6 | 4.59 | -[g] | -[g] |
| **NAI-DPAC**[4] | 6 | 584 | 3 | 29.2 | 13 | 2.2 | -[g] | -[g] |
| **BTDMAc-NAI**[5] | 1.5 | 641 | 4 | 9.2 | 5[f] | -[g] | -[g] | 773 |
| **BFDMAc-NAI**[5] | 1.5 | 590 | 3 | 20.3 | 10[f] | 3.5[f] | -[g] | 2 350 |
| **6,7-DCNQx-DICz**[6] | 1 | 578 | -[g] | 23.9 | 23[f] | 22[f] | 15[f] | 10 000[f] |
| **5,8-DCNQx-DICz**[6] | 1 | 603 | -[g] | 12.5 | 12.4[f] | 10.2[f] | 6[f] | 9 000[f] |
| **PXZ-PQM**[7] | 5 | 592 | 3.4 | 20.4 | 17.5 | 11.3 | 4.9 | 21 900 |
| **DPXZ-PQM**[7] | 5 | 590 | 2.8 | 26 | 20.1 | 13.7 | 5 | 14 140 |
| **DPXZ-DPPM**[7] | 5 | 630 | 3.6 | 11.5 | 10.5 | 6.8 | -[g] | 6 017 |
| **poly(DOPAcNICz-TMP)**[8] | 9 | 624 | 3.4 | 4.1 | 2 | 1.9 | -[g] | 1 800 |
| **NMI-Ind-PXZ**[9] | 1 | 604 | 2.8 | 19.63 | 19.48 | 18.95 | 17.22 | 35 221 |
| **NMI-Ind-PTZ**[9] | 1 | 613 | 2.8 | 23.62 | 23.60 | 23.15 | 21.61 | 38 319 |

*[a] Turn-on voltage*
*[b] Maximum external quantum efficiency.*
*[c] Maximum EQE at 100 cd/m²*
*[d] Maximum EQE at 1000 cd/m²*
*[e] Maximum EQE at 10000 cd/m²*
*[f] Efficiency estimated from the chart given by the authors in the paper/ESI*
*[g] Data not given*


[1] T. Chen, C.-H. Lu, Z. Chen, X. Gong, C.-C. Wu, C. Yang, *Chem. Eur. J.* **2021**, 27, 3151.
[2] Y. Hu, Y. Zhang, W. Han, J. Li, X. Pu, D. Wu, Z. Bin, J. You, *Chem. Eng. J.* **2022**, 428, 131186.
[3] B. Wang, Y. Zheng, T. Wang, D. Ma, Q. Wang, *Org. Electron.* **2021**, 88, 106012.
[4] W. Zeng, H.-Y. Lai, W.-K. Lee, M. Jiao, Y.-J. Shiu, C. Zhong, S. Gong, T. Zhou, G. Xie, M. Sarma, K.-T. Wong, C.-C. Wu, C. Yang, *Adv. Mater.* **2018**, 30, 1704961.
[5] T. Chen, C.-H. Lu, C.-W. Huang, X. Zeng, J. Gao, Z. Chen, Y. Xiang, W. Zeng, Z. Huang, S. Gong, C.-C. Wu, C. Yang, *J. Mater. Chem. C*, **2019**, 7, 9087-9094.
[6] S. Kothavale, W. J. Chunga, J. Y. Lee, *J. Mater. Chem. C*, **2021**, 9, 528-536.
[7] J. Liang, C. Li, Y. Cui, Z. Li, J. Wang, Y. Wang, *J. Mater. Chem. C*, **2020**, 8, 1614-1622.
[8] S. Liu, Y. Tian, L. Yan, S. Wang, L. Zhao, H. Tian, J. Ding, L. Wang, *Macromolecules,* **2023**, 56, 3, 876–882.
[9] This work

## S5. Electrochemistry

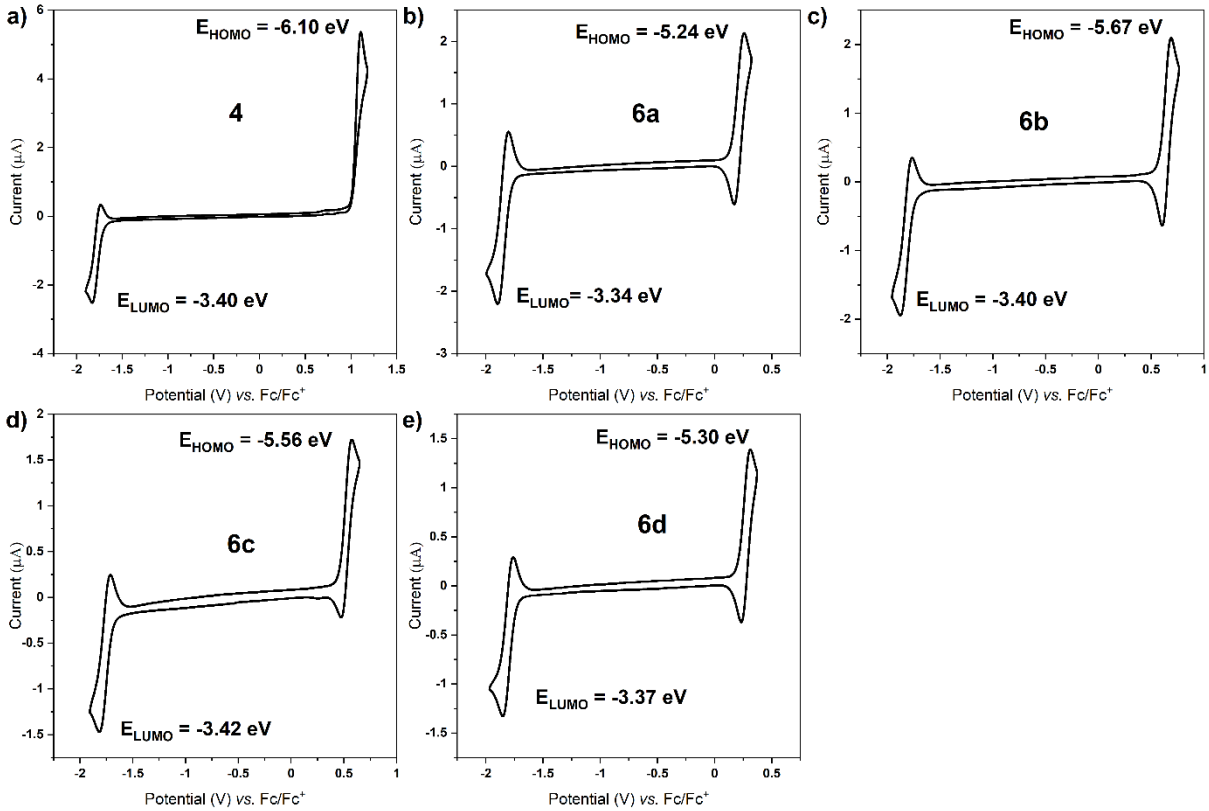


**Figure 52.** CV of 1 mM of compounds in 0.1 M $Bu_4NBF_4$ in DCM electrolyte at a scan rate of 50 mV/s.

Cyclic voltammograms (CV) of all compounds were recorded in 0.1 M $Bu_4NBF_4$ electrolyte solution of dichloromethane three electrodes arrangement being a working electrode (platinum disc), a reference electrode (silver wire) and a counter electrode (platinum wire). CV of all compounds were calibrated with ferrocene/ferrocenium ion ($Fc/Fc^+$) redox couple as the internal standard.

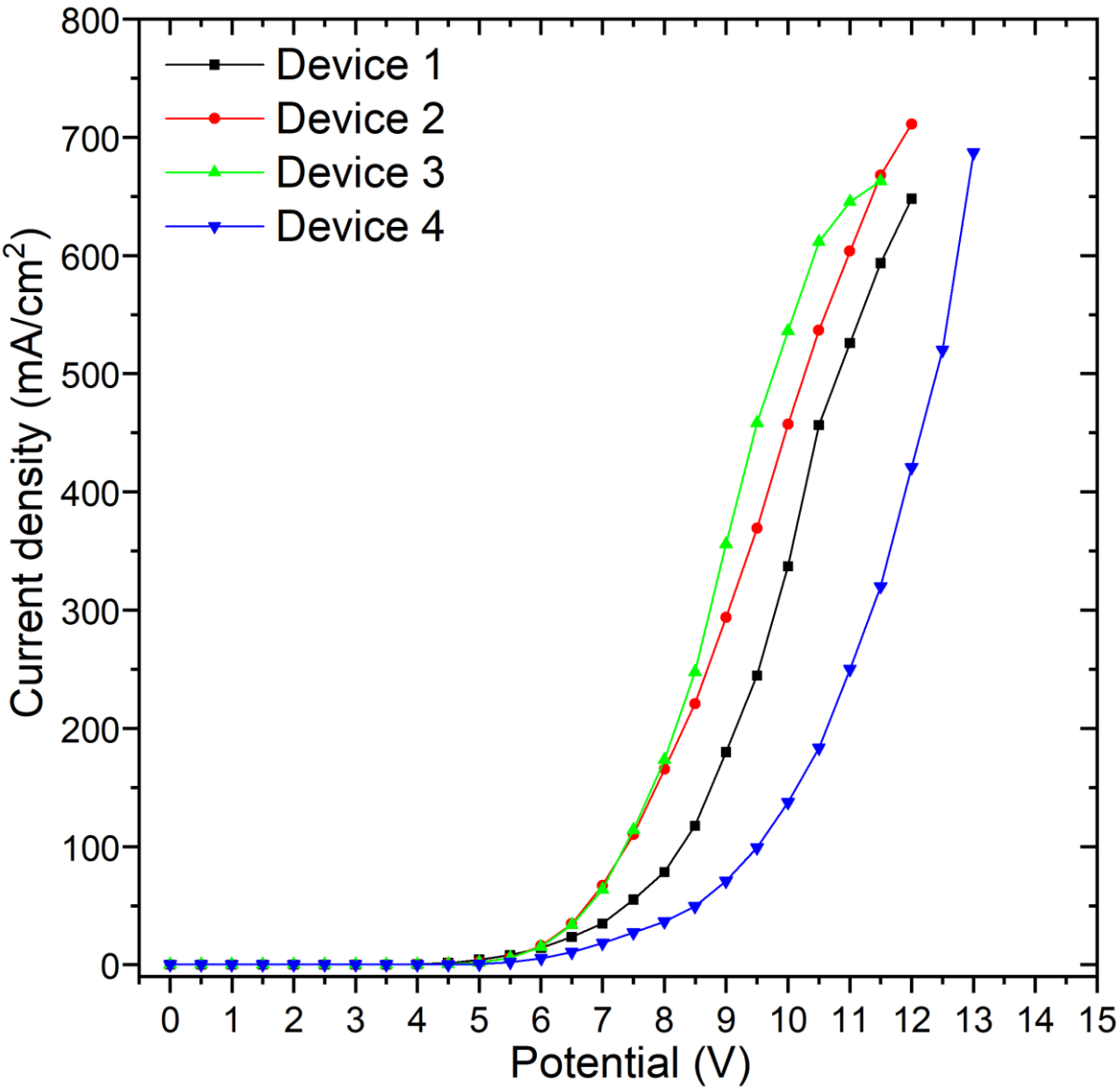


**Figure 53** The non-logarithmic chart of the current density-bias characteristics.

## S6 Computational Methods

**S6. 1** For the purpose of the calculations, compound **4** and each compound in the series **6a–6d** were represented by truncated model compounds in which the *n*-butyl groups were replaced with methyl groups, while the mesityl (2,4,6-trimethylphenyl) groups were replaced with hydrogen atoms. Lastly, the two *tert*-butyl groups of compounds **6a** were also replaced with hydrogen atoms. The deletion of the above-mentioned substituents is justified by the fact that they are not expected to play a significant role in the photophysics of compounds **4** and **6a–6d** as isolated molecules; their purpose is to reduce the tendency towards π-stacking in the condensed phase.

All calculations were performed for isolated molecules, which is to say, in vacuum. Except when noted otherwise, molecular symmetry was not used in the calculations.

S6.1.1 Conformation search

As a preliminary, the conformational preference of each model compound was investigated via geometry optimizations at the density functional theory (DFT) level of theory. The DFT calculations were performed in the computational chemistry software package Gaussian 16, Revision A.03.[1] The B3LYP exchange-correlation functional[2, 3] was employed in combination with the def2-SVP basis set.[4] In the course of the geometry optimizations, the energies and gradients were corrected for dispersion effects via the 'D3BJ' semiempirical correction scheme of Grimme and coworkers with Becke-Johnson damping.[5] All optimized geometries were confirmed to correspond to energy minima via the analytical calculation of vibrational modes.

S6. 1. 2 Optical properties

Having determined the conformational preference of the compounds under study, we proceeded to calculate their optical properties. At this stage, the ground electronic states of each compound was described with the use of the Møller-Plesset perturbation method of second order (MP2), while its excited electronic states were calculated with the use of the second-order algebraic diagrammatic construction (ADC(2)) method.[6, 7] The spin-opposite scaling [8, 9] (SOS) procedure was imposed at all times in both the MP2 and ADC(2) calculations. In order to avoid confusion with the conventional implementations of the MP2 and ADC(2) methods (i.e., without a rescaling of the same- and opposite-spin contributions to the correlation energy), these calculations are referred to by the acronyms SOS-MP2 and SOS-ADC(2).

The SOS-MP2 and SOS-ADC(2) calculations were performed with the program Turbomole, version 6.3.1.,[10] taking advantage of the frozen core and resolution of the identity[11-14] approximations. A restricted Hartree--Fock (RHF) reference determinant was used. The cc-pVDZ basis set [15] was employed in combination with the default auxiliary basis set. [16]

Before calculating the vertical excitation spectra of the compounds under study at the SOS-ADC(2)/cc-pVDZ level of theory, the ground-state equilibrium geometry of each conformer was reoptimized at the SOS-MP2/cc-pVDZ level of theory. This was done to ensure consistency between the method used for the optimization of the ground-state geometry, and the one employed in the subsequent calculation of the electronic excitation spectrum.

The structures of the excited electronic states were characterized by plotting electron density difference maps (EDDMs). An EDDM is defined simply as difference of the electron density of the excited state and that of the ground state at the same nuclear geometry. Thus, the EDDM shows the redistribution of electron density due to a vertical transition.

## S6. 2. Results and Discussion

### S6. 2.1. Conformational preference

We begin the discussion of the simulation results with the DFT-based conformation search. In compound **4** as well as in compounds **6a–6d**, the fused 1,8-naphthalimide-indole moiety is roughly planar. Compound **4** lacks an electron-donating group, and hence it exits in only a single conformation. As for the other four compounds, their conformers can be broadly classified into axial (*ax*) and equatorial (*eq*) geometries according to the internal conformation of the pendant electron-donating moiety (D).

The Gibbs free energies and mole fractions of the various conformers are listed in Table 3. Accompanying this data, their DFT-optimized equilibrium geometries are shown in Figure 53. The conformers of each compound are labeled with Roman numerals in order of increasing Gibbs free energy. The suffix -*ax* or -*eq* denotes the internal conformation of the D moiety.

Compound **6a** only has a single conformer, which is equatorial. Compounds **6b** and **6d** each have two equatorial conformers and a single axial conformer. For either compound, the equatorial conformers lie substantially lower energy than the axial conformer. This finding is consistent with the fact that in the molecular crystal phase, compound **6b** exists in an equatorial conformation.

Lastly, compound **6c** only has a single, equatorial, conformer. Again, this result is consistent with the crystallographic geometry of this compound. We have explicitly verified that, in the case of compound **6c,** an axial conformation does not correspond to a minimum on the ground-state potential energy surface (PES). An attempt to optimize an axial conformation leads to a first-order saddle point on the ground-state PES, as opposed to a minimum.

**Table 3:** Conformational preference of compounds **4** and **6a–6d** – calculated energies ($E$, including zero-point vibrational corrections), Gibbs free energies ($G$), and mole fractions ($x$) of the various conformers, as calculated at the B3LYP-D3BJ/def2-SVP level of theory. For each compound, the energy and the Gibbs energy of the most stable conformer (denoted conformer 1) are set to zero.

| Compound | Conformer | $E$, kJ/mol | $G$, kJ/mol | $x$ |
|---|---|---|---|---|
| **4** | 1 | 0 | 0 | 1 |
| **6a** | 1-*eq* | 0 | 0 | 1 |
| **6b** | 1-*eq* | 0 | 0 | 0.53 |
| | 2-*eq* | 0.0 | 0.3 | 0.47 |
| | 3-*ax* | 18.7 | 21.2 | $1\times10^{-4}$ |
| **6c** | 1-*eq* | 0 | 0 | 1 |

| | | | | |
|---|---|---|---|---|
| **6d** | 1-*eq* | 0 | 0 | 0.51 |
| | 2-*eq* | 0.1 | 0.1 | 0.48 |
| | 3-*ax* | 9.2 | 10.1 | 0.01 |

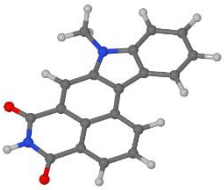

(a) compound **4**

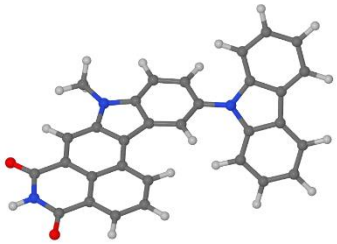

(b) compound **6a**, conformer 1-*eq*

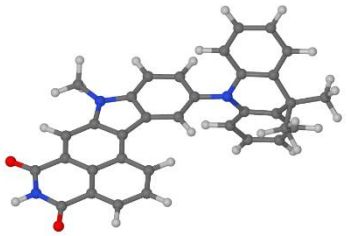

(c) compound **6b**, conformer 1-*eq*

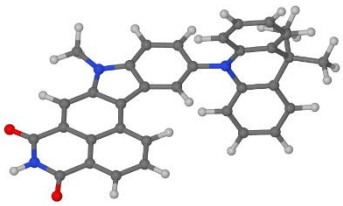

(d) compound **6b**, conformer 2-*eq*

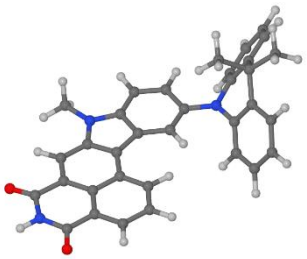

(e) compound **6b**, conformer 3-*ax*

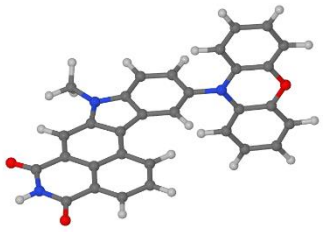

(f) compound **6c**, conformer 1-*eq*

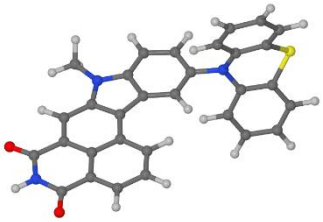

(g) compound **6d**, conformer 1-*eq*

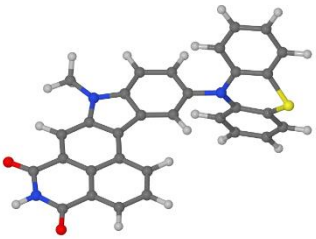

(h) compound **6d**, conformer 2-*eq*

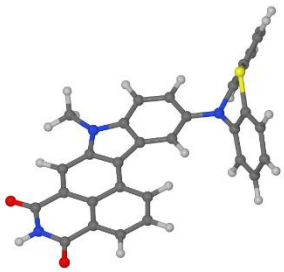

(i) compound **6d**, conformer 3-*ax*

**Figure 54:** Ground-state equilibrium geometries of compounds **4** and **6a–6d** as optimized at the B3LYP-D3BJ/def2-SVP level of theory.

S6 2.2. Optical Properties

The detailed discussion of the optical properties of the compounds under study can be found in the main body of the present paper. Accompanying this analysis, Table 4 provides an overview of the vertical excitation spectra of the predominant conformers.

Note that in the case of compound **6c**, there is a very slight inconsistency between the results of DFT and SOS-MP2 geometry optimizations – the former method predicts that the phenoxazine based electron-donating moiety is near-planar, whereas according to the latter method, it is somewhat non-planar with a visible butterfly-like deformation. As a consequence, at the SOS-MP2 level of theory, compound **6c** possesses two inequivalent equatorial conformers, which are denoted 1-*eq* and 2-*eq* in Table 4. The two conformers lie very close in energy, and their electronic excitation spectra are very similar.

**Table 4:** Electronic excitation spectra of compounds **4** and **6a–6d** as calculated at the SOS-ADC(2)/cc-pVDZ level of theory – vertical excitation energies ($\Delta E$) and associated oscillator strengths ($f$). $\mu$ is the orbital-unrelaxed electric dipole moment of the given state.

| Compound | Conformer | State | $\Delta E$, eV | $f$ | $\mu$, D |
|---|---|---|---|---|---|
| **4** | | $S_0$ | | | 5.9 |
| | | $S_1$ (dark NI ππ*) | 3.489 | 0.080 | 10.3 |
| | | $S_2$ (bright NI ππ*) | 3.849 | 0.455 | 11.5 |
| | | $S_3$ (NI ππ*) | 4.471 | 0.014 | 8.5 |
| | | $T_1$ (NI ππ*) | 2.759 | 0 | 7.7 |
| | | $T_2$ (NI ππ*) | 3.269 | 0 | 9.8 |
| | | $T_3$ (NI ππ*) | 3.731 | 0 | 7.0 |
| **6a** | 1-*eq* | $S_0$ | | | 4.7 |
| | | $S_1$ (dark NI ππ*) [a] | 3.455 | 0.061 | 10.3 |
| | | $S_2$ (bright NI ππ*) | 3.768 | 0.527 | 11.3 |
| | | $S_3$ (D ππ*) | 4.092 | 0.034 | 4.4 |
| | | $T_1$ (NI ππ*) | 2.773 | 0 | 5.9 |
| | | $T_2$ (NI ππ*) | 3.211 | 0 | 9.7 |
| | | $T_3$ (D ππ*) | 3.670 | 0 | 4.7 |
| **6b** | 1-*eq* | $S_0$ | | | 5.1 |
| | | $S_1$ (dark NI ππ*) | 3.478 | 0.085 | 9.3 |
| | | $S_2$ (bright NI ππ*) | 3.846 | 0.521 | 10.2 |
| | | $S_3$ (D→NI ICT) | 3.936 | $7\times10^{-4}$ | 28.8 |
| | | $T_1$ (NI ππ*) | 2.759 | 0 | 6.6 |
| | | $T_2$ (NI ππ*) | 3.260 | 0 | 8.9 |
| | | $T_3$ (NI ππ*) | 3.727 | 0 | 6.3 |
| **6b** | 2-*eq* | $S_0$ | | | 5.0 |
| | | $S_1$ (dark NI ππ*) | 3.512 | 0.079 | 9.1 |
| | | $S_2$ (bright NI ππ*) | 3.831 | 0.565 | 10.4 |

| | | | | | |
|---|---|---|---|---|---|
| | | $S_3$ (D→NI ICT) | 4.016 | $1\times10^{-4}$ | 30.1 |
| | | $T_1$ (NI ππ*) | 2.776 | 0 | 6.4 |
| | | $T_2$ (NI ππ*) | 3.281 | 0 | 9.0 |
| | | $T_3$ (NI ππ*) | 3.740 | 0 | 6.1 |
| **6b** | 3-*ax* | $S_0$ | | | 6.8 |
| | | $S_1$ (dark NI ππ*) | 3.160 | 0.094 | 17.4 |
| | | $S_2$ (bright NI ππ*) | 3.629 | 0.443 | 12.2 |
| | | $S_3$ (NI ππ*) | 4.189 | 0.097 | 10.9 |
| | | $T_1$ (NI ππ*) | 2.734 | 0 | 9.3 |
| | | $T_2$ (NI ππ*) | 2.893 | 0 | 14.6 |
| | | $T_3$ (NI ππ*) | 3.671 | 0 | 8.5 |
| **6c** | 1-*eq* | $S_0$ | | | 5.0 |
| | | $S_1$ (bright NI ππ*) | 3.520 | 0.080 | 8.6 |
| | | $S_2$ (D→NI ICT) | 3.802 | 0.001 | 28.4 |
| | | $S_3$ (bright NI ππ*) | 3.848 | 0.558 | 10.0 |
| | | $T_1$ (NI ππ*) | 2.779 | 0 | 6.0 |
| | | $T_2$ (NI ππ*) | 3.289 | 0 | 8.7 |
| | | $T_3$ (D ππ*) | 3.548 | 0 | 6.7 |
| **6c** | 2-*eq* | $S_0$ | | | 4.0 |
| | | $S_1$ (dark NI ππ*) | 3.492 | 0.083 | 7.9 |
| | | $S_2$ (D→NI ICT) | 3.724 | 0.001 | 26.9 |
| | | $S_3$ (bright NI ππ*) | 3.857 | 0.511 | 8.7 |
| | | $T_1$ (NI ππ*) | 2.764 | 0 | 5.2 |
| | | $T_2$ (NI ππ*) | 3.272 | 0 | 7.6 |
| | | $T_3$ (D ππ*) | 3.543 | 0 | 6.8 |
| **6d** | 1-*eq* | $S_0$ | | | 3.5 |
| | | $S_1$ (dark NI ππ*) | 3.487 | 0.084 | 7.5 |
| | | $S_2$ (bright NI ππ*) | 3.847 | 0.520 | 8.4 |
| | | $S_3$ (D→NI ICT) | 3.954 | $5\times10^{-6}$ | 25.0 |
| | | $T_1$ (NI ππ*) | 2.765 | 0 | 4.8 |
| | | $T_2$ (NI ππ*) | 3.264 | 0 | 7.2 |
| | | $T_3$ (NI ππ*) | 3.731 | 0 | 5.3 |
| **6d** | 2-*eq* | $S_0$ | | | 5.5 |
| | | $S_1$ (dark NI ππ*) | 3.515 | 0.081 | 9.1 |
| | | $S_2$ (bright NI ππ*) | 3.857 | 0.550 | 10.4 |
| | | $S_3$ (D→NI ICT) | 4.053 | $2\times10^{-4}$ | 26.8 |
| | | $T_1$ (NI ππ*) | 2.781 | 0 | 6.6 |
| | | $T_2$ (NI ππ*) | 3.289 | 0 | 9.1 |
| | | $T_3$ (NI ππ*) | 3.743 | 0 | 5.1 |
| **6d** | 3-*ax* | $S_0$ | | | 7.2 |

| | | | |
|---|---|---|---|
| $S_1$ (dark NI ππ*) | 3.275 | 0.084 | 6.1 |
| $S_2$ (bright NI ππ*) | 3.664 | 0.483 | 5.1 |
| $S_3$ (NI ππ*) | 4.253 | 0.050 | 4.2 |
| $T_1$ (NI ππ*) | 2.741 | 0 | 8.7 |
| $T_2$ (NI ππ*) | 2.999 | 0 | 14.2 |
| $T_3$ (NI ππ*) | 3.699 | 0 | 8.2 |

[a] In state labels, the fused 1,8-naphthalimide-indole moiety is denoted NI, and the donor moiety is denoted D.

**Figure 55** Canonical Hartree-Fock orbitals of conformers of compounds in the series **6a–6b**, plotted in the form of isosurfaces with isovalues of ±0.025 $a_0^{-3/2}$. The orbitals were calculated at ground-state equilibrium geometries as optimized at the SOS-MP2/cc-pVDZ level of theory.

(a) compound **6a**, conformer 1-*eq*

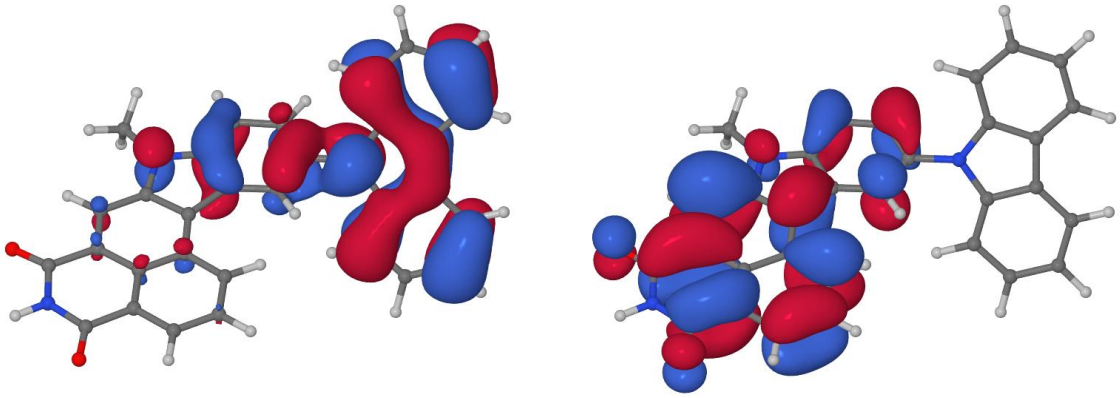

HOMO LUMO

(b) compound **6b**, conformer 1-*eq*

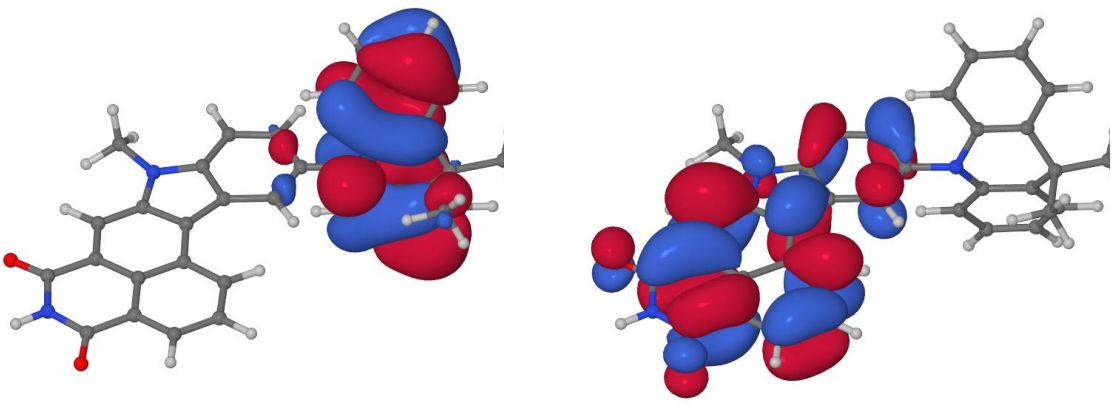

HOMO LUMO

(c) compound **6b**, conformer 2-*eq*

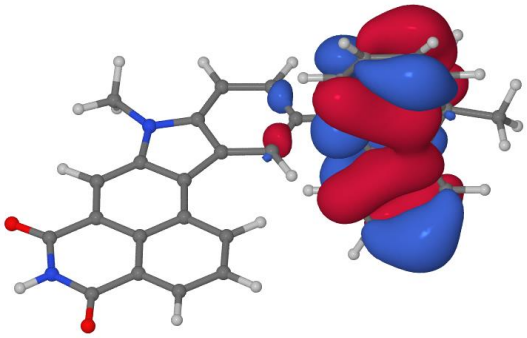

HOMO

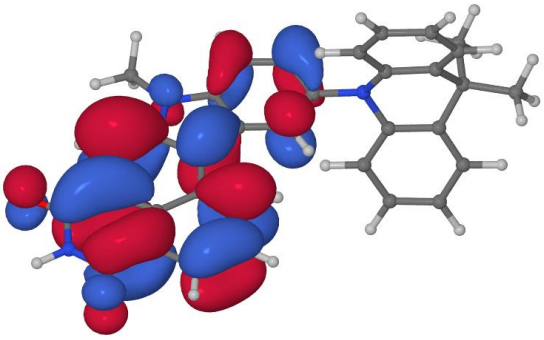

LUMO

(d) compound **6b**, conformer 3-*ax*

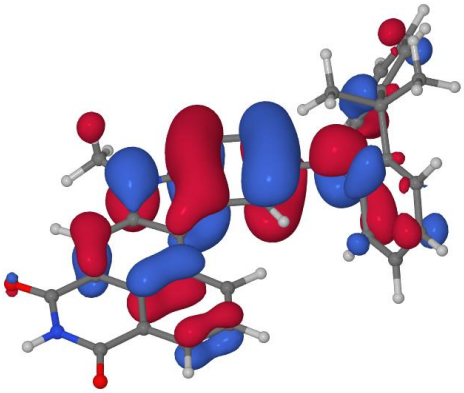

HOMO

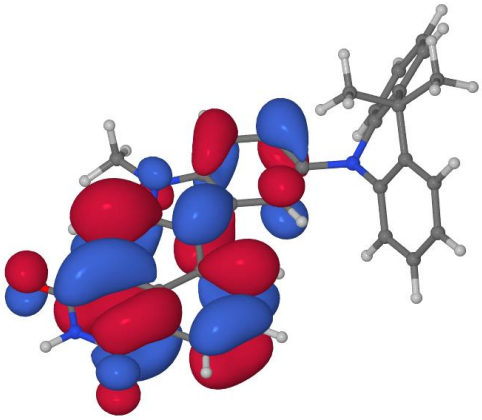

LUMO

(e) compound **6c**, conformer 1-*eq*

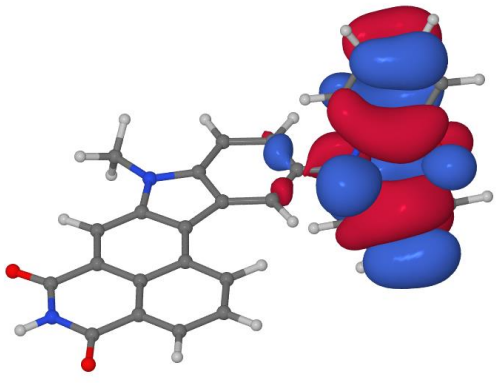

HOMO

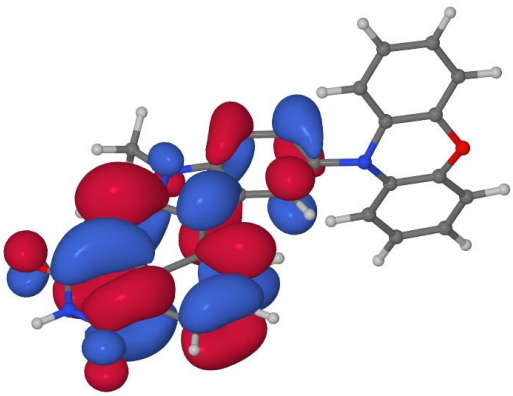

LUMO

(f) compound **6c**, conformer 2-*eq*

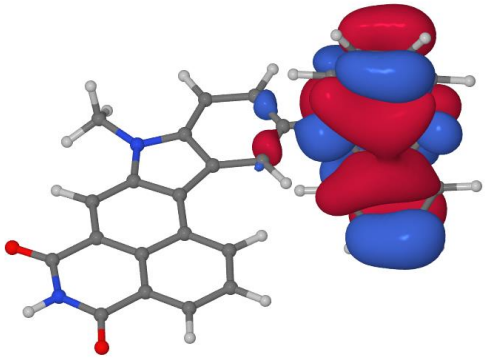

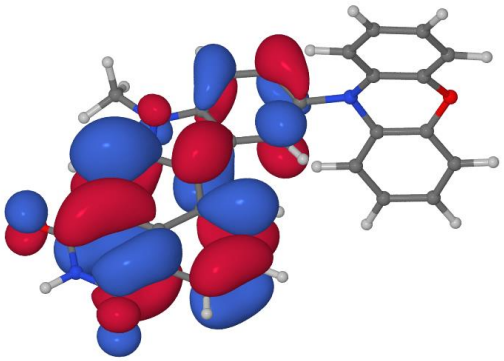

HOMO LUMO

(g) compound **6d**, conformer 1-*eq*

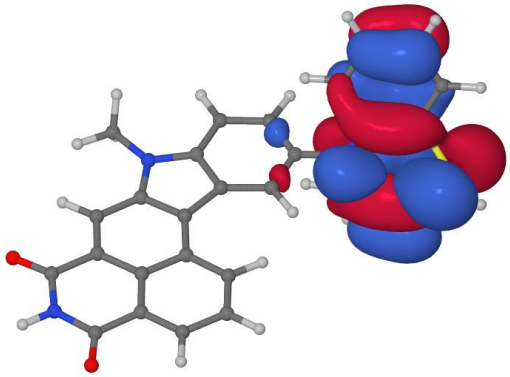

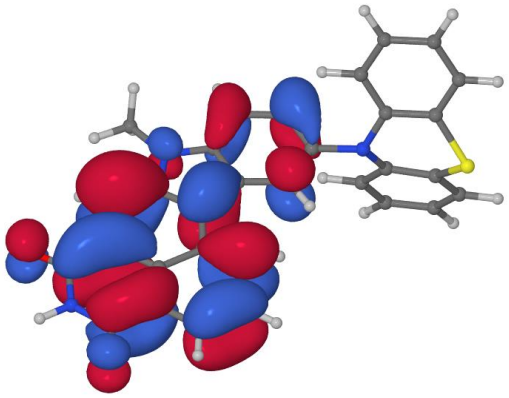

HOMO LUMO

(h) compound **6d**, conformer 2-*eq*

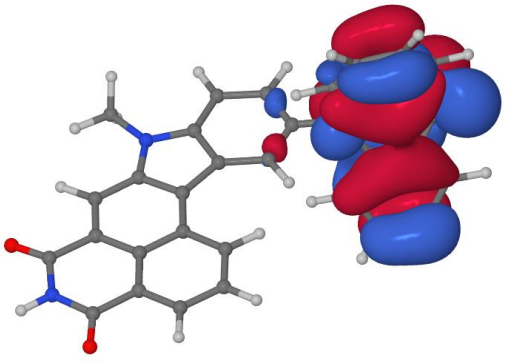

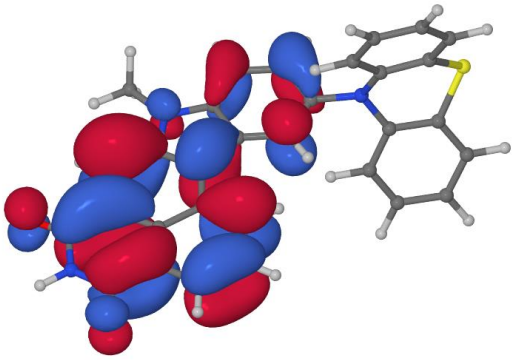

HOMO LUMO

(i) compound **6d**, conformer 3-*ax*

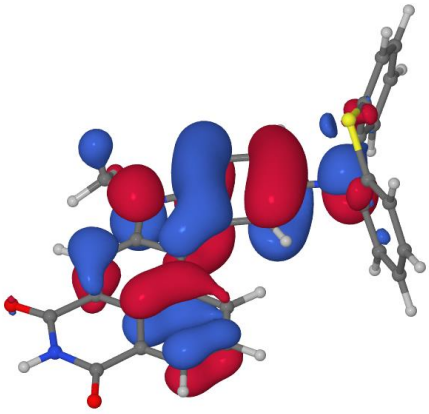

HOMO

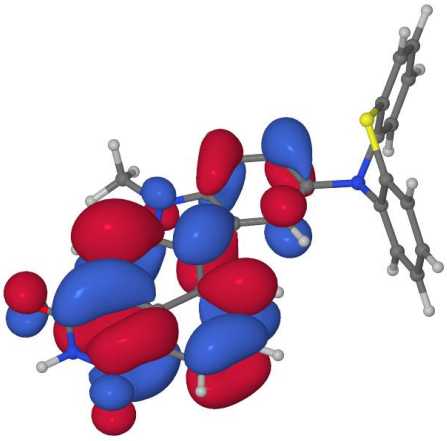

LUMO

**References**

[1] Gaussian 16, Revision A.03, Frisch, M. J.; Trucks, G. W.; Schlegel, H. B.; Scuseria, G. E.; Robb, M. A.; Cheeseman, J. R.; Scalmani, G.; Barone, V.; Petersson, G. A.; Nakatsuji, H.; Li, X.; Caricato, M.; Marenich, A. V.; Bloino, J.; Janesko, B. G.; Gomperts, R.; Mennucci, B.; Hratchian, H. P.; Ortiz, J. V.; Izmaylov, A. F.; Sonnenberg, J. L.; Williams-Young, D.; Ding, F.; Lipparini, F.; Egidi, F.; Goings, J.; Peng, B.; Petrone, A.; Henderson, T.; Ranasinghe, D.; Zakrzewski, V. G.; Gao, J.; Rega, N.; Zheng, G.; Liang, W.; Hada, M.; Ehara, M.; Toyota, K.; Fukuda, R.; Hasegawa, J.; Ishida, M.; Nakajima, T.; Honda, Y.; Kitao, O.; Nakai, H.; Vreven, T.; Throssell, K.; Montgomery, J. A., Jr.; Peralta, J. E.; Ogliaro, F.; Bearpark, M. J.; Heyd, J. J.; Brothers, E. N.; Kudin, K. N.; Staroverov, V. N.; Keith, T. A.; Kobayashi, R.; Normand, J.; Raghavachari, K.; Rendell, A. P.; Burant, J. C.; Iyengar, S. S.; Tomasi, J.; Cossi, M.; Millam, J. M.; Klene, M.; Adamo, C.; Cammi, R.; Ochterski, J. W.; Martin, R. L.; Morokuma, K.; Farkas, O.; Foresman, J. B.; Fox, D. J. Gaussian, Inc., Wallingford CT, 2016.

[2] Becke, A. D. Density-Functional Thermochemistry. III. The Role of Exact Exchange. *J. Chem. Phys.* **1993**, *98,* 5648–5652. DOI: 10.1063/1.464913

[3] Stephens, P. J.; Devlin, F. J.; Chabalowski, C. F.; Frisch, M. J. *J. Phys. Chem.* **1994**, *98*, 11623–11627. DOI: 10.1021/j100096a001

[4] Weigend, F.; Ahlrichs, R. Balanced Basis Sets of Split Valence, Triple Zeta Valence and Quadruple Zeta Valence Quality for H to Rn: Design and Assessment of Accuracy. *Phys. Chem. Chem. Phys.* **2005**, *7*, 3297–3305 . DOI: 10.1039/b508541a

[5] Grimme, S.; Ehrlich, S.; Goerigk, L. Effect of the damping function in dispersion corrected density functional theory. *J. Comp. Chem.* **2011**, *32*, 1456–1465. DOI: 10.1002/jcc.21759

[6] Trofimov, A. B.; Schirmer, J. An Efficient Polarization Propagator Approach to Valence Electron Excitation Spectra. *J. Phys. B: At., Mol. Opt. Phys.* **1995**, *28*, 2299–2324. DOI: 10.1088/0953-4075/28/12/003

[7] Hättig, C. Structure Optimizations for Excited States with Correlated Second-Order Methods: CC2 and ADC(2). In Advances in Quantum Chemistry; Jensen, H. J. Å., Ed.; Academic Press: New York, 2005; Vol. 50, pp 37–60.

[8] Jung, Y.; Lochan, R. C.; Dutoi, A. D.; Head-Gordon, M. Scaled Opposite-Spin Second Order Møller-Plesset Correlation Energy: An Economical Electronic Structure Method. *J. Chem. Phys.* **2004**, *121*, 9793–9802. DOI: 10.1063/1.1809602

[9] Winter, N. O. C.; Hättig, C. Scaled Opposite-Spin CC2 for Ground and Excited States with Fourth Order Scaling Computational Costs. *J. Chem. Phys.* **2011**, *134*, No. 184101. DOI: 10.1063/1.3584177

[10] TURBOMOLE V6.3.1 2011, a development of University of Karlsruhe and Forschungszentrum Karlsruhe GmbH (1989-2007), and TURBOMOLE GmbH (since 2007). Available from: http://www.turbomole.com

[11] Haase, F.; Ahlrichs, R. Semi-direct MP2 Gradient Evaluation on Workstation Computers: The MPGRAD Program. *J. Comput. Chem.* **1993**, *14*, 907–912. DOI: 10.1002/jcc.540140805

[12] Weigend, F.; Häser, M. RI-MP2: First Derivatives and Global Consistency. *Theor. Chem. Acc.* **1997**, *97*, 331–340. DOI: 10.1007/s002140050269

[13] Hättig, C.; Weigend, F. CC2 Excitation Energy Calculations on Large Molecules Using the Resolution of the Identity Approximation. *J. Chem. Phys*. **2000**, *113*, 5154–5161. DOI: 10.1063/1.1290013

[14] Köhn, A.; Hättig, C. Analytic Gradients for Excited States in the Coupled-Cluster Model CC2 Employing the Resolution-of-the-Identity Approximation. *J. Chem. Phys.* **2003**, *119*, 5021–5036. DOI: 10.1063/1.1597635

[15] Dunning, T. H., Jr. Gaussian Basis Sets for Use in Correlated Molecular Calculations. I. The Atoms Boron Through Neon and Hydrogen. *J. Chem. Phys.* **1989**, *90*, 1007–1023. DOI: 10.1063/1.456153

[16] Weigend, F.; Köhn, A.; Hättig, C. Efficient Use of the Correlation Consistent Basis Sets in Resolution of the Identity MP2 Calculations. *J. Chem. Phys.* **2002**, *116*, 3175–3183. DOI: 10.1063/1.1445115